

AD-A099 512 MISSION RESEARCH CORP SANTA BARBARA CA F/G 17/2.
OPTIMAL/ADAPTIVE DEMODULATION FOR M-ARY FSK IN FAST FADING.(U)
MAR 81 M J BARRETT F29601-78-C-0033

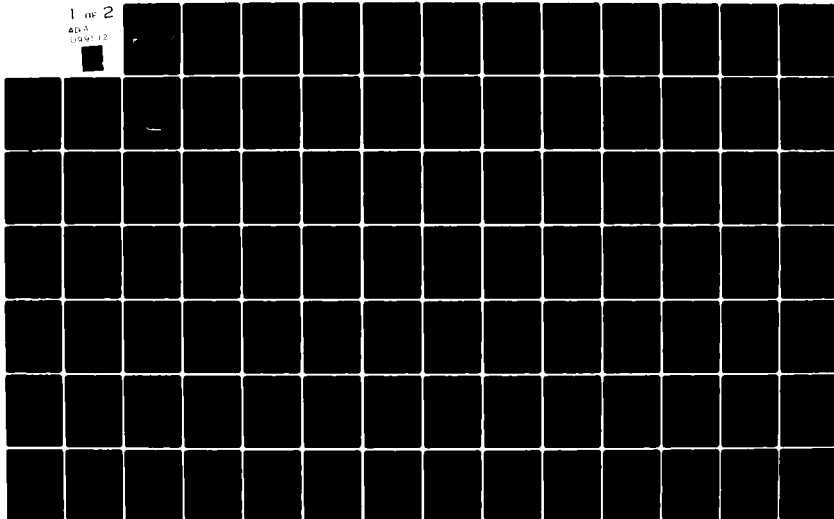
UNCLASSIFIED MRC-R-453

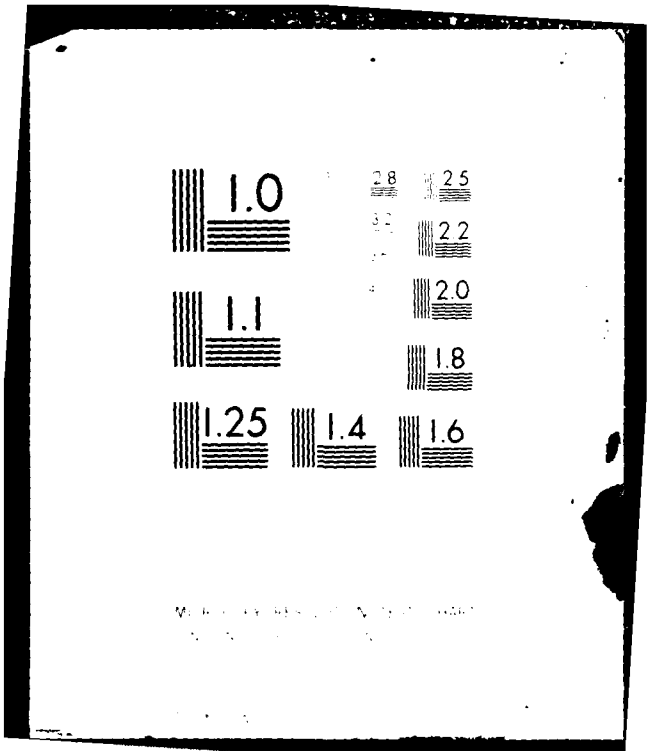
AFWL-TR-80-69

N/1

1 of 2

AD-A
099 512





MILITARY RESOLUTION TEST CHART
1950-A

AD-5200714

② LEVEL III

AFWL-TR-80-69

AFWL-TR-80-69

AD A099512

OPTIMAL/ADAPTIVE DEMODULATION FOR M-ARY FSK IN FAST FADING

M. J. Barrett

Mission Research Corporation
735 State Street
Santa Barbara, CA 93102

March 1981

Final Report

DTIC
ELECTE
JUN 1 1981
S D
B



Approved for public release; distribution unlimited.

DTIC FILE COPY

AIR FORCE WEAPONS LABORATORY
Air Force Systems Command
Kirtland Air Force Base, NM 87117

81 5 11 088

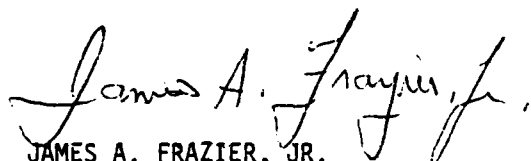
This final report was prepared by the Mission Research Corporation, Santa Barbara, California, under Contract F29601-78-C-0033, Job Order 46950403 with the Air Force Weapons Laboratory, Kirtland Air Force Base, New Mexico. Lieutenant James A. Frazier, Jr. (NTYC) was the Laboratory Project Officer-in-Charge.

When US Government drawings, specifications, or other data are used for any purpose other than a definitely related Government procurement operation, the Government thereby incurs no responsibility nor any obligation whatsoever, and the fact that the Government may have formulated, furnished, or in any way supplied the said drawings, specifications, or other data, is not to be regarded by implication or otherwise, as in any manner licensing the holder or any other person or corporation, or conveying any rights or permission to manufacture, use, or sell any patented invention that may in any way be related thereto.

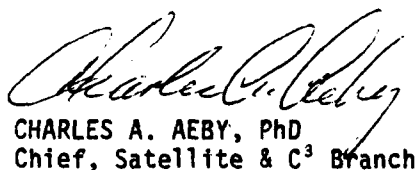
This report has been authored by a contractor of the United States Government. Accordingly, the United States Government retains a nonexclusive, royalty-free license to publish or reproduce the material contained herein, or allow others to do so, for the United States Government purposes.

This report has been reviewed by the Public Affairs Office and is releasable to the National Technical Information Service (NTIS). At NTIS, it will be available to the general public, including foreign nations.

This technical report has been reviewed and is approved for publication.

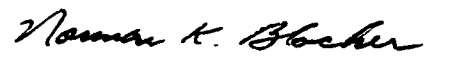


JAMES A. FRAZIER, JR.
1st Lt, USAF
Project Officer



CHARLES A. AEBY, PhD
Chief, Satellite & C³ Branch

FOR THE COMMANDER



NORMAN K. BLOCKER
Colonel, USAF
Chief, Applied Physics Division

UNCLASSIFIED

SECURITY CLASSIFICATION OF THIS PAGE (When Data Entered)

REPORT DOCUMENTATION PAGE		READ INSTRUCTIONS BEFORE COMPLETING FORM
1. REPORT NUMBER AFWL-TR-80-69	2. GOVT ACCESSION NO. AD-A099572	3. RECIPIENT'S CATALOG NUMBER
4. TITLE (and Subtitle) OPTIMAL/ADAPTIVE DEMODULATION FOR M-ARY FSK IN FAST FADING		5. TYPE OF REPORT & PERIOD COVERED Final Report
		6. PERFORMING ORG. REPORT NUMBER MRC-R-453
7. AUTHOR(s) M. J. Barrett		8. CONTRACT OR GRANT NUMBER(s) F29601-78-C-0033
9. PERFORMING ORGANIZATION NAME AND ADDRESS Mission Research Corporation 735 State Street Santa Barbara, CA 93102		10. PROGRAM ELEMENT, PROJECT, TASK AREA & WORK UNIT NUMBERS 64711F/46950403
11. CONTROLLING OFFICE NAME AND ADDRESS Air Force Weapons Laboratory (NTYC) Kirtland Air Force Base, NM 87117		12. REPORT DATE March 1981
		13. NUMBER OF PAGES 130
14. MONITORING AGENCY NAME & ADDRESS (if different from Controlling Office)		15. SECURITY CLASS. (of this report) Unclassified
		15a. DECLASSIFICATION DOWNGRADING SCHEDULE
16. DISTRIBUTION STATEMENT (of this Report) Approved for public release; distribution unlimited.		
17. DISTRIBUTION STATEMENT (of the abstract entered in Block 20, if different from Report)		
18. SUPPLEMENTARY NOTES		
19. KEY WORDS (Continue on reverse side if necessary and identify by block number) Frequency Shift Keying Maximum Likelihood Signal Scintillation Composite Hypothesis Test Signal Parameter Estimation Adaptive Signal Processing		
20. ABSTRACT (Continue on reverse side if necessary and identify by block number) This work extends the analysis developed in a preceding report, of optimal demodulation for M-ary FSK waveforms that are corrupted by rapid signal scintillation fading and noise. The research documented here extends the original analysis to incorporate estimation algorithms for signal spectral spreading. This new receiver design adapts to channel conditions and is called the optimal/adaptive demodulator. The optimal/adaptive demodulator operates like the optimal receiver previously documented except that it also forms the (Over)		

DD FORM 1473
1 JAN 73

UNCLASSIFIED

SECURITY CLASSIFICATION OF THIS PAGE (When Data Entered)

UNCLASSIFIED

SECURITY CLASSIFICATION OF THIS PAGE(When Data Entered)

20. ABSTRACT (Continued)

necessary spectral estimates of the received signal plus noise. The new design remains optimal, in the sense of minimum probability of error, in steady signal and slow fading conditions while providing successful performance in much faster fading conditions than possible with conventional receivers. The mathematical development, design and performance of the new optimal/adaptive demodulator are documented in this work.

UNCLASSIFIED

SECURITY CLASSIFICATION OF THIS PAGE(When Data Entered)

CONTENTS

	PAGE
ILLUSTRATIONS	3
SECTION	
I INTRODUCTION	5
STATEMENT OF THE PROBLEM	5
THE PHYSICAL CHANNEL	10
GAUSSIAN SIGNAL IN GAUSSIAN NOISE RECEIVERS	12
II THE OPTIMAL RECEIVER FOR GAUSSIAN SIGNALS IN AWGN	17
BACKGROUND	17
RECEIVER DERIVATION	19
PERFORMANCE ANALYSIS	19
RECEIVER PERFORMANCE - NUMERICAL METHODS	28
BASEBAND AUTOCORRELATION FUNCTIONS AND S ² /N	28
SAMPLE AUTOCORRELATION AND DFT COVARIANCE MATRIX	33
MONTE CARLO PROCEDURE	36
III ESTIMATION	37
ESTIMATION COST FUNCTION	38
CRITERION OF OPTIMALITY	41
THE STATISTIC \bar{z}	48
IV THE ADAPTIVE M-ARY FSK RECEIVER	50
ESTIMATING FILTERS	50
V DATA REDUCTION	55
REPARAMETERIZATION OF THE SPECTRAL ESTIMATE	56
OPTIMIZATION CRITERION	60
PROJECTION OPERATOR	64
SPECTRAL EIGENVECTOR ALGORITHM	67
VI EXPERIMENTAL RESULTS	70
CONVENTIONAL AND OPTIMAL RECEIVERS	70
ADAPTIVE RECEIVERS	77
CONCLUSIONS	84

	PAGE
REFERENCES	90
APPENDIX A - PROPERTIES OF THE IN-PHASE AND QUADRATURE COMPONENTS OF A NARROWBAND GAUSSIAN PROCESS	95
APPENDIX B - THE PROBABILITY DISTRIBUTION OF THE DFT OF A SAMPLED COMPLEX GAUSSIAN PROCESS	99
APPENDIX C - COMPUTATION OF THE COVARIANCE MATRICES L_j FROM THE SIGNAL AUTOCORRELATION FUNCTION AND WHITE NOISE DENSITY	107
APPENDIX D - THE GENERATION OF COMPLEX RANDOM VARIATES WITH THE CORRELATION MATRIX L	111
APPENDIX E - PROPERTIES OF THE COVARIANCE MATRIX WHICH ARE USEFUL IN OBTAINING INVERSES AND SQUARE ROOTS	113
APPENDIX F - ALGORITHM FOR THE ADAPTIVE RECEIVER WITH DATA REDUCTION	116
APPENDIX G - PRINCIPAL COMPONENTS AND THE REDUCED DIMENSION SPECTRAL ESTIMATE	122

Accession For	
NTIS GRA&I	<input checked="" type="checkbox"/>
DTIC TAB	<input type="checkbox"/>
Unannounced	<input type="checkbox"/>
Justification	
By	
Distribution/	
Availability Codes	
Avail and/or	
Dist	Special
A	

ILLUSTRATIONS

FIGURE		PAGE
1.	Combined multiplicative and additive noise.	5
2.	The physical channel.	11
3.	Baseband block diagram.	29
4.	Alternative block diagram.	30
5.	Magnitude transfer functions for $\mathcal{B}(f)$ and $\mathcal{B}(f+f_c)$.	31
6.	Mapping from \bar{z}^{-1} to $F(\bar{z}^{-1})$ to cost functions at the extremes of the confidence interval.	46
7.	Mapping from (\bar{z}^{-1}) to $F(\bar{z}^{-1})$ to cost functions at the extremes of the confidence interval for symmetric, translating cost functions.	47
8.	Block diagram of an adaptive receiver.	51
9.	Gaussian signal power spectral density - various decorrelation times, normalized signal power, $\Delta f = 1/T$ Hz.	72
10.	Cubic roll-off power spectral density - various decorrelation times, normalized signal power, $\Delta f = 1/T$ Hz.	73
11.	8-ary frequency shift keying performance in fast Rayleigh fading channel (Gaussian signal spectrum).	75
12.	8-ary frequency shift keying performance in fast Rayleigh fading channel (cubic roll-off signal spectrum).	76
13.	Signal bit energy-to-noise density required to achieve binary error rate P_b at various decorrelation times.	78
14.	8-ary FSK receiver performance. Adaptive vs. optimal and conventional receivers.	80
15.	Normalized basis vectors for four-parameter SEV and BLSS data reduction algorithms.	82

FIGURE		PAGE
16.	8-ary frequency shift keying performance in fast Rayleigh fading channel (cubic roll-off signal spectrum). Four-parameter SEV receiver vs. four-parameter BLSS receiver at $\tau_0 = 3.2$ ms.	83
17.	8-ary frequency shift keying performance in fast Rayleigh fading channel (cubic roll-off signal spectrum). Four-parameter SEV receiver vs. five-parameter BLSS receiver at $\tau_0 = 3.2$ ms.	85
18.	8-ary FSK frequency shift keying performance in fast Rayleigh fading channel (cubic roll-off signal spectrum). Four-parameter SEV receiver vs. five-parameter BLSS receiver at $\tau_0 = 4.90$ ms.	86
19.	8-ary FSK frequency shift keying performance in fast Rayleigh fading channel (cubic roll-off signal spectrum). Four-parameter SEV receiver vs. five-parameter BLSS receiver at $\tau_0 = 9.10$ ms.	87
20.	Comparative performance of BLSS algorithm at long and short prior integrating times.	88
F-1.	Block diagram of an adaptive receiver with data reduction.	117

I. INTRODUCTION

STATEMENT OF THE PROBLEM

This final report is concerned with the problem of demodulating multiple frequency-shift-keyed (FSK) signals corrupted by a combination of multiplicative and additive noise. The multiplicative noisy operator $\mathcal{N}(\Theta)$, which is illustrated in Figure 1, is of such a nature that transmitted sinusoidal signals $s_i(t)$, $i = 1, \dots, M$, are converted to zero mean Gaussian random processes $\mu_i(t)$, with peak spectral densities at the transmitted frequencies. The received signal $r_i(t)$ is the sum of $\mu_i(t)$ and independent white Gaussian noise $n(t)$. In terms of hypothesis testing the alternatives are:

$$\mathcal{H}_i : r_i(t) = s_i(t, \underline{\theta}_s) + n(t, \underline{\theta}_n) \quad , \quad 0 < t < T, \quad i = 1, \dots, M \quad (1)$$

where $n(t)$ is an additive white noise process and $\mu_i(t)$ is a segment of a zero mean stationary Gaussian random process. A decision must be made by analysis of $r(t)$, as to which \mathcal{H}_i is correct in a given observation interval $[0, T]$. The parameters $\underline{\theta}_s$ and $\underline{\theta}_n$ are the unknown statistics of the random processes $\mu_i(t)$ and $n(t)$, respectively.

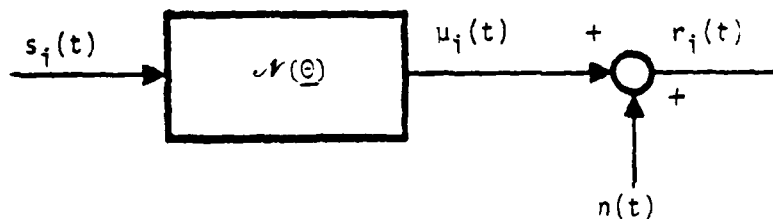


Figure 1. Combined multiplicative and additive noise.

For purposes of mathematical modeling, these parameters are considered to be fixed. In fact, they will change slowly enough with respect to hundreds of observation intervals T , that they may be modeled as constant.

In statistical terms, this problem is called "multiple alternative composite hypothesis testing."¹ The term composite refers to the condition that each hypothesis $\mathcal{H}_i(\theta)$ is actually a family of hypotheses over the range of (θ_s, θ_n) . Given knowledge of θ , it is possible to partition the space Ω of observed processes $r_i(t)$, $0 \leq t \leq T$ into decision regions, \mathcal{D}_i , each associated with an hypothesis \mathcal{H}_i , in a manner which leads to the minimum probability of misclassification. Without prior knowledge of θ , there are several alternative approaches all of which attempt to obtain the best partitioning on the average by incorporating the available knowledge about θ .

In some cases, the optimal partitioning of the space Ω , which is the union of decision regions \mathcal{D}_i , is independent of θ entirely, or at least independent of some degree of the dimension of θ . In these cases, there is a "uniformly most powerful" test.² Unfortunately, this is not the case for the problem at hand.

When a probability distribution is postulated for θ (that is, if θ is considered to be a random variable of known distribution rather than an unknown constant), one may obtain the best partition of the space Ω on the average over that probability distribution. In this approach, which is known as "Bayesian," the a priori distribution $p(\theta)$ is updated by the incorporation of data obtained from $r(t)$ over prior signaling intervals through the repeated use of Bayes' rule.

A "Bayesian" approach is strictly not applicable to the case of an unknown but constant θ . To derive an adaptive receiver from the Bayesian point of view would require the assumption of a priori distributions for the

signal-to-noise ratio and frequency dispersion parameters of the channel. This is not consistent with the rational criteria for evaluating receivers. We are interested in obtaining the best possible performance at each $\underline{\theta}$ rather than the best performance over some distribution of $\underline{\theta}$.

A third approach, which is more consistent with the nonrandom $\underline{\theta}$ case, is to estimate the value of $\underline{\theta}$ and to treat that estimate $\hat{\underline{\theta}}$ as if it were, in fact, the actual unknown parameter. An example of this approach is to use the maximum likelihood estimate $\underline{\theta}_{ML}$ in place of $\underline{\theta}$.³ Maximum likelihood estimates require knowledge of the structure of the distribution of $r_i(t)$ and the corresponding sampling statistic, but do not require an a priori distribution for $\underline{\theta}$. The parameter may be considered to be a fixed but unknown value. However, the use of a maximum likelihood estimate does not provide any guarantee that it will yield the minimum probability of misclassification on the average. In that sense, it is merely a heuristic technique.

The emphasis here is to obtain an adaptive partitioning of Ω based on information from prior observation intervals through an estimate of the power spectrum of $r_i(t)$ optimized for receiver performance. The technique is similar to that using maximum likelihood estimates in that an estimate is used in place of an actual statistic in an algorithm derived for known statistics; but it is on more firm theoretical ground since the estimator is optimized with respect to the receiver performance (misclassification probability).

The criterion of optimality for the estimator of the power spectrum is derived by a method related to confidence intervals in the theory of non-random parameter estimation. The optimality of the adaptive receiver is limited in two ways. First, consideration is given only to a receiver structured after the optimal (known statistics) receiver with a spectral estimate

replacing the a priori known spectral statistic. Second, the probability of misclassification, as a function of the correct spectrum and an erroneous estimate, is assumed to reach its minimum at the true spectrum, to be a symmetric function about the true value of the spectrum, increasing as a function of the error, and to approximately translate as a function of the true spectral value. For reasons that will later become evident, the symmetry and translation properties are for estimation costs as a function of the inverse of the spectrum.

An additional objective is to achieve near optimal (known Θ) performance with as small a collection of prior observations as possible. The degree and nature of the nonstationarity of the multiplicative noisy operator is unknown except that it may be assumed to change slowly with respect to hundreds of modulation intervals. Thus, the objective of a short prior memory is to permit the estimation of the time varying parameter and parenthetically to obtain the most rapid convergence consistent with near-optimal performance by having the wide tracking bandwidth which is made possible by a short prior observation interval. These objectives are not incorporated in the optimization criterion, but appear as a constraint on the design of the estimator. The estimator is arbitrarily constrained to operate on a single pole filtered version of the prior (raw) spectra and the time constraint is manipulated informally to achieve the desired trade-off between accuracy and tracking bandwidth.

In a more rigorous but less practically realizable approach one would have to characterize the nonstationarity beyond noting that it is slow with respect to many observation intervals T , assign and evaluate the cost associated with the length of the prior observation interval, and design the dynamics of the estimator accordingly. The approach taken here is considerably "freer" with regard to knowledge about the evolution of the parameter Θ . For estimator design purposes, the parameter is assumed to be constant within the "window" of the estimator, and no formal consideration is given to the nonstationarity of the channel disturbance.

The estimator of the power spectrum of the received signal $r_i(t)$, referred to above, is not an estimator of (analog) power spectral density (PSD) but of the magnitude-squared discrete Fourier transform of the process with N samples taken over an observation interval of T seconds coincident with the transmitted signal. This is referred to loosely here as the "estimate of the power spectrum" to avoid any confusion between continuous spectra and finite spectra.

Since the full dimensional estimator is computationally unwieldy, techniques of parametric spectral estimation are investigated which allow the spectrum to be estimated with the use of a small number of storage registers and associated arithmetic operations. The parametric spectral estimators are designed to produce reduced dimensional estimates with the least possible degradation in receiver performance.

Novel aspects of this study are in its nonBayesian approach to the adaptive demodulation problem and in the area of linear data reduction with negligible loss in receiver performance. Additionally, a detailed analysis of the misclassification error in the M -ary zero mean Gaussian frequency shift keying (FSK) case is presented which does not appear elsewhere.

In the remainder of this section, the physical channel to which the adaptive demodulation technique is directed is described; the history of the "Gaussian signal" (known statistics) problem and of the adaptive receiver problem is outlined. Section II deals with the optimum known statistics receiver and with a closely related efficient suboptimal (known statistics) receiver. In Section III the optimality of the spectral estimator is demonstrated and Section IV presents the adaptive receiver with the optimal estimator for the M -ary FSK Gaussian zero mean signal, in white Gaussian noise with no data reduction of the required spectrum estimate. Section V

introduces two techniques for reducing the dimension of the spectral estimate with negligible loss in the receiver performance. Section VI gives simulation results for the receivers.

THE PHYSICAL CHANNEL

The physical channels are wideband satellite uplinks and downlinks for data communications in the UHF band. Problems of severe fading associated with undesirable random phase and amplitude modulation occur during conditions of unusually high levels of ionization in the ionosphere. These conditions occur naturally near the equatorial zones and at the North and South Poles, but may also be caused by man in any region of the Earth by the introduction of radioactive materials in the atmosphere.

Figure 2 illustrates the problem. The ionized cloud acts as a kind of random lens, focusing and defocusing the downlink signal from the satellite. If satellite, cloud, and ground station were stationary with respect to each other, then the signal received on the ground would be steady but attenuated according to the geometry of the ionized cloud. Relative motion of the satellite, cloud, or receiver brings about the undesired modulation.

The signal path is not direct from the source to the receiver, but is made up of many reflection paths which add infinitesimal contributions at the receiving antenna. This type of propagation problem was studied originally by an analytic technique for a single phase screen by J. A. Ratcliffe.⁴ Subsequent work by Tatarskii,⁵ and Knepp and Valley,⁶ have dealt with the physical assumptions necessary to derive signal statistics, and current practice in this area is to estimate the signal spatial autocorrelation via a multiple phase screen (MPS) calculation through the computationally efficient two-dimensional Fast Fourier Transform (FFT). MPS

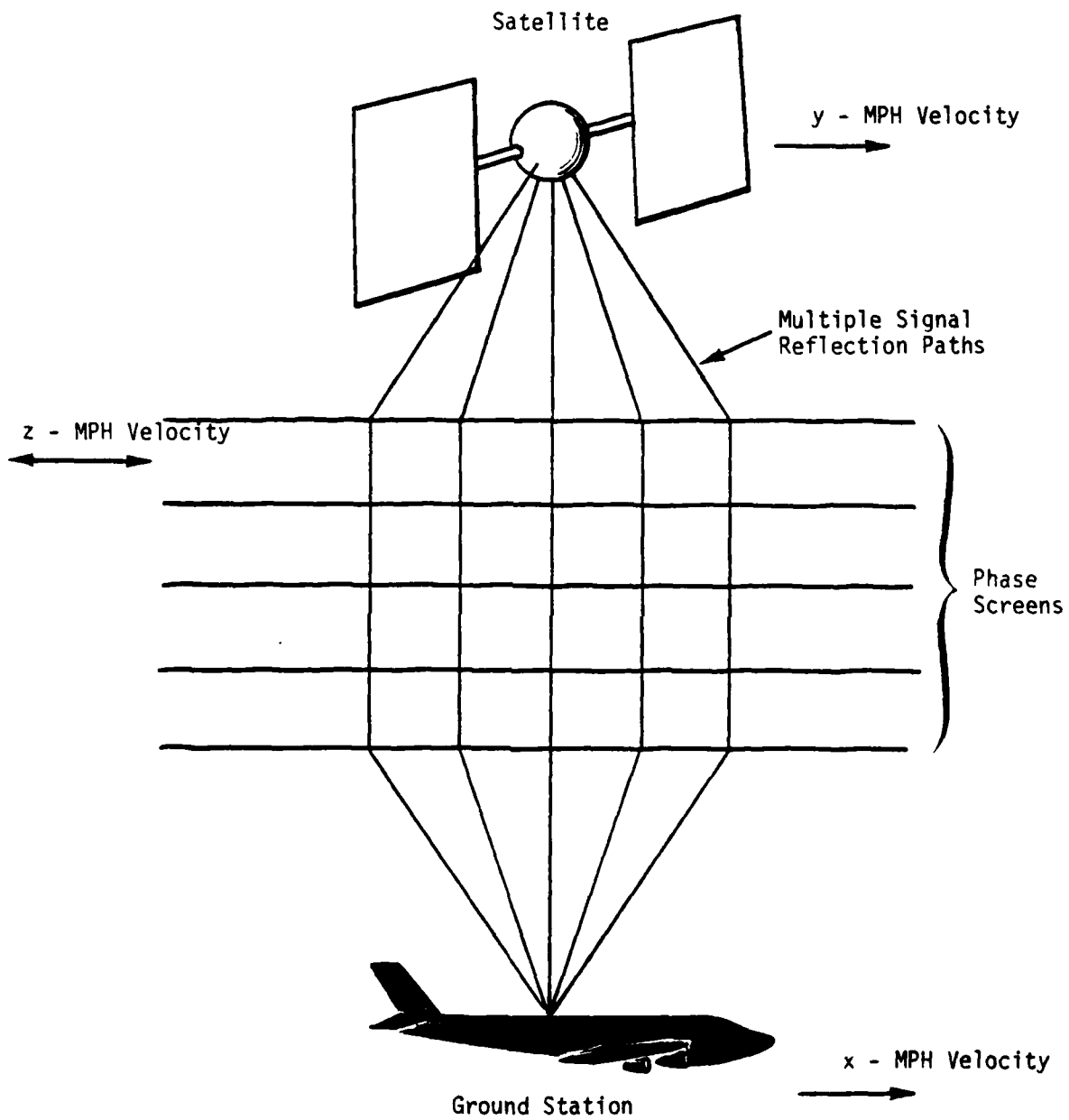


Figure 2. The physical channel.

routines allow the computation of signal amplitude and phase realizations at the receiver for several phase screens in tandem. A considerable amount of experimentation has been done with these routines and computational results have evolved over the last few years to the specification of two extreme conditions for the statistical structure of the received signal $\mu_i(t)$. At the two extremes are a Gaussian signal autocorrelation at the receiver, and a cubic roll-off spectrum.⁷ In either case the first order statistic is Gaussian. Results are given in Section VI for the performance of the optimal and conventional receivers with each of these conditions at various signal-to-noise ratios. The adaptive receivers are all evaluated for the cubic roll-off spectrum only, since it is a worst case of the two alternatives.

Either of these power spectral densities for $\mu_i(t)$ may be categorized by one parameter which is typically given in the time domain as the e^{-1} point on the autocorrelation function. This parameter is τ_0 , the signal decorrelation time. Only one other parameter enters the specification of the power spectral density of $r_i(t)$: the noise power spectral density. Due to an invariance property of the receivers under study to overall rescaling of the received signal $r_i(t) = \mu_i(t) + n(t)$, only the signal-to-noise ratio will be used as an indicator of this second parameter. The signal-to-noise ratio is given by the ratio of the autocorrelation of $\mu_i(t)$ at $t = 0$, to the power spectral density of $n(t)$ in watts per Hz.

GAUSSIAN SIGNAL IN GAUSSIAN NOISE RECEIVERS

The study of optimal receivers for the demodulation or detection of Gaussian signals corrupted by additive Gaussian noise has been carried out for over twenty years. Early discussions were given by Price^{8,9} and Middleton;¹⁰ and the problem was later revived by Kailath,¹¹ Stratonovich and Sosulin,¹² and Schweppe.¹³ Kennedy¹⁴ produced a small volume on the subject.

These treatments all deal with cases of known statistical structure of the signal and noise processes. The algorithms process the continuous-valued time waveform $r_i(t)$, or a sampled version of it, rather than operate upon a frequency domain representation as considered here in Section II, but the distinction is of little consequence. In either case the optimal (known statistics) receiver yields the same demodulation decision on a given sample of $r_i(t)$. Discrete Fourier transform (DFT) coefficients of a sampled $r_i(t)$ are used here rather than time samples as a computational convenience.

Several communication texts have discussions of the "noise in noise" demodulation and detection problem. Pertinent chapters and sections can be found in Van Trees⁵, Helstrom⁶, Whalen⁷ and Hancock and Wintz⁸. The latter text includes material on adaptive hypothesis testing from the Bayesian point of view.

The optimal receiver of Price and Kailath was interpreted by them and several succeeding authors as an extension of the classical matched filter for deterministic signals. In a matched filter demodulator the received waveform is crosscorrelated with local replicas of the several possible transmitted signals, and the most highly correlated of these is selected as the demodulation decision. Kailath¹¹ showed that the optimal receiver for detecting a Gaussian random process could be interpreted as a matched filter where the local replicas are given by minimum variance estimates of the same incoming waveform. These estimates are done under the assumption of different hypotheses for the spectrum of the received signal, so that only on the correct hypothesis is a minimum variance estimate actually obtained. This interpretation of the optimal receiver has led to its designation as the "estimator-correlator" receiver, and from this point of view the study of the receiver has been extended with particular emphasis to the nature of the estimator under wider classes of signal statistics.

Esposito^{19,20} showed that the estimator, in an on-off detection problem, is minimum variance only if the signal is Gaussian, and proceeded to give general expressions which show the type of estimate that is required in the non-Gaussian case. His expressions, which were based on the general likelihood ratio formula of Kailath²¹ involving Ito stochastic integrals, apply to random signals of arbitrary distribution in additive Gaussian noise. The class of signal statistics was specialized to the exponential family by Schwartz^{22,23} who was then able to use estimators based on sufficient statistics and give more explicit expressions for the estimator in the estimator-correlator receiver. This work has been extended to the incorporation of information from prior observation intervals using a Bayesian approach by Birdsall and Gobien,²⁴ Gobien,²⁵ and Lee, Nolte, and Hatsell.²⁶

More fundamental discussions of the Bayesian approach to parameter estimation are given by Keehn²⁷ and Spragins,²⁸ who include a table of reproducing densities. These apply where the sampling density for the unknown parameter has a sufficient statistic. Spragins proves that there is an appropriate choice of the form of the a priori density for the unknown parameter so that the a posteriori density (after updating by Bayes' rule) retains its functional form. The significance for Bayesian compound hypothesis testing is that it allows the sufficient statistic to be updated in a fixed algorithm. Otherwise the algorithm would tend to grow in complexity as more prior information is introduced. Chien and Fu²⁹ have interpreted the Bayesian updating procedure in terms of stochastic approximation algorithms and have proven the convergence of such algorithms in mean square and with probability one.

A problem with parameter estimation from prior observation intervals is that the detector or demodulator will have necessarily made some errors in classifying the prior samples. These errors in turn cause errors in estimating the required signal parameters. One may choose to ignore this problem, live with the errors, and derive the properties of the estimator under the

assumption that the priors are correctly classified. This is the approach taken here with a successful result. The data of Section VI indicate that there was very little effect on receiver performance from misclassified priors. A rigorous treatment of the problem of misclassified priors can be found in a monograph by Patrick and Costello³⁰ with a review of the literature in the area.

A quite different approach to hypothesis testing of Gaussian random processes was suggested by Miller and Rochwager.^{31,32,33,34} This diverges from the Price-Kailath algorithm in that no knowledge of the signal spectrum is required. The center frequency of the spectrum of $\mu_1(t)$ is estimated through the proportional relationship of the first moment of the power spectral density about the origin and the derivative of the corresponding autocorrelation at its origin—a property of the Fourier transform. The autocorrelation is estimated from products of uncorrelated pairs of samples of $r_i(t)$, and a separate noise level estimate is required to remove the effects of $n(t)$ from the computation. If the power spectral density of the received signal is known, the technique is clearly suboptimal; and where good estimates are available it is likely to perform poorly in comparison to a receiver with an estimator. However, there are situations where spectral estimation is impossible. For instance, if frequency band hopping techniques are used and the signal fading characteristics are significantly different among bands, there may be no other rational method to demodulate the signal other than that suggested by Miller and Rochwager.

Adaptive techniques for the filtering of signals without specific reference to applications in hypothesis testing have an interesting parallel development to adaptive communication systems. The fundamental problem is very much the same. Optimal minimum mean square estimators have been derived for known signal and noise statistics but these must often be estimated in practice. There are two stages of estimation involved. An

auxiliary estimator is applied to the unknown statistics and the resulting estimate is used in the primary filtering operation. Heuristic techniques were first introduced without consideration of the quality of the combined process. Weaver³⁵ gives several such examples for adaptive Wiener filtering. Later authors, Balkrishnan³⁶ and Davisson,³⁷ dealt with estimates of the estimation error and the problems of convergence. In the area of adaptive Kalman filtering, Mehra³⁸ introduced an adaptive algorithm which also has guarantees of convergence. Magill³⁹ improved upon the consideration of the quality of the estimator by restricting the unknown parameters to a finite set. His algorithm is optimal in the transient period as well as convergent to the correct statistics. A similar technique was used by Lainiotis⁴⁰ in the context of adaptive pattern recognition. Like Magill he postulated a finite collection of possible values for the unknown statistics with given a priori probabilities. These approaches are both Bayesian in the sense that they assign a priori probabilities to the unknown statistics.

Fundamental to this problem is the fact that the estimation cost is a function of the true value of the unknown parameter and is therefore itself an uncertain value. The Bayesian methods assume a probability distribution for the unknown parameter and average over it therefore making the criterion a nonrandom average cost. Without a prior distribution one must deal with an ensemble of cost functions to reflect the uncertainty in the true value of the unknown parameter. The approach taken here is to limit this ensemble to a confidence region for the parameter and to require that the estimator minimize the worst case over that ensemble of cost functions.

II. THE OPTIMAL RECEIVER FOR GAUSSIAN SIGNALS IN AWGN

BACKGROUND

The receiver derived here is an obvious extension of the development in the communications literature, complicated somewhat by the use of the DFT rather than analog signal processing. It differs from the receiver introduced by Kaliath¹¹ in that the DFT coefficients of the received process $r_i(t)$, rather than time samples, are used as the raw data. In this section, the joint probability density of the DFT coefficients of the received signal-plus-noise $r_i(t)$ is used in the derivation of a maximum a posteriori probability (MAP) receiver, rather than the corresponding density of time samples as done by Kaliath. The performance is demonstrably identical whether time samples or DFT coefficients are used, but efficient suboptimal techniques are expected to be more closely related to the receiver operating on DFT coefficients than upon time samples.

A few comments on terminology are necessary. The term AWGN stands for additive white Gaussian noise. The term optimal MPE refers to that receiver which yields a minimum probability of error for equally alternative signals. The MPE criterion reduces to the MAP criterion¹ which is used to derive the receiver. In the derivation of the MAP receiver, the joint probability density of the received DFT coefficients is viewed as a function of the index of which signal was transmitted, for a given sample \underline{z} of received data. \underline{z} is an N-dimensional block of complex numbers which corresponds to the DFT of a sample of $r_i(t)$ over the demodulation observation interval T . The index which maximizes the a posteriori probability

is selected as the receiver's decision. Thus, the optimal MPE receiver must have prior knowledge of the joint density of \underline{z} under each hypothesis of transmitted signal. This means that the signal dispersion and noise level are precisely known in advance; where these quantities are estimated, the receiver is no longer optimal MPE.

RECEIVER DERIVATION

A concise development of the optimal MPE M-ary receiver for Gaussian signals in Gaussian noise is presented here. The preliminaries appear in Appendices A and B where it is demonstrated that the DFT coefficients of the received signal-plus-noise are jointly distributed according to*

$$p_i(\underline{z}|i) = \pi^{-N} |\underline{L}_i|^{-1} e^{-\underline{z}^T \underline{L}_i^{-1} \underline{z}^*}, \quad \underline{z} \in C^N \quad (2)$$

where \underline{z} is the vector of DFT coefficients defined by Equation B.3 and the matrix \underline{L}_i is given by†

$$[\underline{L}_i]_{k,\ell} = E\{z_k z_\ell^*\} \text{ on the } i^{\text{th}} \text{ hypothesis} \quad (3)$$

It is convenient to deal with the log-likelihood function:

$$\ln p(\underline{z}|i) = -N \ln(\pi) - \ln |\underline{L}_i| - \underline{z}^T \underline{L}_i^{-1} \underline{z}^* \quad (4)$$

The first term of the log-likelihood function may be discarded in maximizing Equation 4 since it is neither a function of the data \underline{z} nor the index i . The second term is a function of the index i but not of the data. Its practical function is to impart a bias in favor of those signals which are received with a reduced signal power; a situation which may be expected to occur in the extreme channels of deviation frequency. In this analysis the term is not used since its effects have proven to be insignificant

* The notation $\underline{z} \in C^N$ means " \underline{z} is an N-dimensional complex valued vector."

† The notation $[\underline{L}_i]_{k,\ell}$ should read "the k,ℓ^{th} element of the matrix \underline{L}_i ."

for many performance cases of interest. The third term is a quadratic form in the data \underline{z} and inverse covariance matrix \underline{L}_i^{-1} . The receiver which uses this term only makes its decision according to

$$\text{decision} = p, \text{ where } \min_{k \in \mathcal{D}} \{ \underline{z}^T \underline{L}_k^{-1} \underline{z}^* \} = \underline{z}^T \underline{L}_p^{-1} \underline{z}^* \quad (5)$$

Note that \underline{L}_i is the covariance matrix of the signal-plus-noise DFT coefficients rather than that of the signal alone. An adaptive receiver must estimate the signal-to-noise ratio, unlike a conventional noncoherent FSK receiver which does not incorporate the signal-to-noise ratio and is nevertheless optimal (in an undisturbed channel) at each noise level.

PERFORMANCE ANALYSIS

An analytical solution to the probability of error for the optimal MPE receiver does not seem possible* since the integrals involved are not conveniently expressed in terms of known tabulated functions. When available, analytic expressions are advantageous as an efficient means to the evaluation of receiver performance, as the foundation for sensitivity studies, and as a convenient tool to optimize receiver parameters. A discussion of the analytical approach, to the extent that it may be carried out, is given here. Familiarity with the Jacobian method for transformation of multidimensional random variables is assumed.

A receiver performance evaluation typically proceeds from the joint density of the received signal-plus-noise to the joint density of the receiver statistics where the error probability may be formulated as an integral in a simplified form. The received data vector \underline{z} is shown in Appendix B to be distributed according to the complex normal distribution:

$$p(\underline{z}|i) = \pi^{-N} |\underline{L}_i|^{-1} e^{-\underline{z}^T \underline{L}_i^{-1} \underline{z}^*}, \quad \underline{z} \in \mathbb{C}^N \quad (6)$$

* Exponentially tight bounds were obtained for the nonoverlapping signal spectra case by Viterbi.¹⁷

and the receiver statistics are given by

$$q_k \triangleq \underline{z}^T \underline{L}_k^{-1*} \underline{z}^* \quad , \quad k \in \mathcal{D}_M \quad (7)$$

Let the index set of hypotheses be

$$\mathcal{D}_M \triangleq \{1, 2, \dots, M\} \quad (8)$$

and designate the joint distribution of statistics

$$\underline{q}_M = [q_1, q_2, \dots, q_M]^T \quad (9)$$

by $f_M(\underline{q}|i)$ on the i^{th} hypothesis. Then the probability of a correct modulation decision is

$$P_{c/i} = \int_0^\infty \int_{q_i}^\infty \int_{q_i}^\infty \dots \int_{q_i}^\infty f_M(\underline{q}_M|i) dq_1 dq_2 \dots dq_M dq_i \quad (10)$$

A correct decision is made when q_i is smaller than all of the other q_k 's.

The transformation from $p(\underline{z}|i)$ to $f_M(\underline{q}_M|i)$ is at least a twofold reduction in dimension. The data \underline{z} is an N -dimensional complex-valued vector where N is the number of complex samples per observation interval. Thus \underline{z} has $2N$ real numbers in its description whereas \underline{q} is M -dimensional and real-valued with

$$M \leq N \quad (11)$$

The number of transmitted frequencies is at most equal to the DFT dimension N for a conventional DFT-implemented M -ary FSK receiver. This change in dimension is significant to the application of a Jacobian technique. One must first transform the variables to a space of the same dimension and then integrate over the extra variables.

We start with Equation 6 and undertake several successive changes of variable. First, a representation of the distribution of \underline{z} in polar form is useful to avoid problems in differentiating the complex distribution. Define the vectors

$$\underline{r} \triangleq [r_0, r_1, \dots, r_{N-1}]^T \quad (12)$$

$$\underline{\theta} \triangleq [\theta_0, \theta_1, \dots, \theta_{N-1}]^T \quad (13)$$

where

$$z_k = r_k e^{j\theta_k}, \quad k=0, \dots, N-1$$

$$r_k \geq 0 \text{ for all } k \quad (14)$$

A transformation from the distribution in \underline{z} to the corresponding distribution in \underline{r} and $\underline{\theta}$ is most readily accomplished if \underline{z} is written in terms of its real and imaginary parts. Let

$$\text{Re } \underline{z} \triangleq [\text{Re}\{z_0\}, \text{Re}\{z_1\}, \dots, \text{Re}\{z_{N-1}\}]^T \quad (15)$$

$$\text{Im } \underline{z} \triangleq [\text{Im}\{z_0\}, \text{Im}\{z_1\}, \dots, \text{Im}\{z_{N-1}\}]^T \quad (16)$$

then the complex normal distribution may be rewritten in terms of $\text{Re } \underline{z}$, $\text{Im } \underline{z}$:

$$p(\text{Re}(\underline{z}) + j\text{Im}(\underline{z}) | i)$$

$$= \pi^{-N} |\underline{L}_i|^{-1} \exp(-\text{Re } \underline{z}^T \underline{L}_i^{-1*} \text{Re } \underline{z} + \text{Im } \underline{z}^T \underline{L}_i^{-1*} \text{Im } \underline{z})$$

(17)

and the corresponding distribution in terms of \underline{r} and $\underline{\theta}$ is

$$g(\underline{r}, \underline{\theta} | i) = \pi^{-N} |\underline{L}_i|^{-1} \prod_{k=0}^{N-1} (r_k) e^{-r^T \underline{\Omega}_i(\underline{\theta}) \underline{r}}, \quad r_i \geq 0 \quad (18)$$

where $[\underline{\Omega}_i(\underline{\theta})]_{k,\ell} \triangleq [\underline{L}_i^{-1*}]_{k,\ell} e^{j(\theta_k - \theta_\ell)}$ $\begin{matrix} k=0, \dots, N-1 \\ \ell=0, \dots, N-1 \end{matrix}$

the phase angles associated with \underline{z} are imbedded in the matrix of the quadratic form in the exponent. The substitution of \underline{r} , and $\underline{\Omega}_k(\underline{\theta})$ in the exponent of Equation 17 is straightforward. It remains only to show that the Jacobian of the transformation from $p(\underline{z} | i)$ to $g(\underline{r}, \underline{\theta} | i)$ is given by

$$|J_{[\underline{r}, \underline{\theta}]}(\text{Re } \underline{z}, \text{Im } \underline{z})| = \left[\prod_{k=0}^{N-1} (r_k) \right]^{-1} \quad (19)$$

It is convenient to approach this from the inverse transformation

$$|J_{[\text{Re } \underline{z}, \text{Im } \underline{z}]}(\underline{r}, \underline{\theta})| = \prod_{k=0}^{N-1} (r_k) \quad (20)$$

Using the relation

$$\begin{aligned} r_k \cos \theta_k &= \text{Re } \{z_k\} \\ r_k \sin \theta_k &= \text{Im } \{z_k\} \end{aligned} \quad k=0, \dots, N-1 \quad (21)$$

The nonzero elements of the $2N \times 2N$ Jacobian matrix are

$$\begin{aligned} [J_{[\text{Re } \underline{z}, \text{Im } \underline{z}]}(\underline{r}, \underline{\theta})]_{k, \ell+N} &= \frac{\partial \text{Re } z_k}{\partial r_\ell}, \quad \begin{matrix} k=0, \dots, N-1 \\ \ell=0, \dots, N-1 \end{matrix} \\ &= \cos \theta_k, \quad k=\ell \end{aligned} \quad (22)$$

$$\begin{aligned}
[J_{[\text{Re } \underline{z}, \text{Im } \underline{z}]}(\underline{r}, \underline{\theta})]_{k, \ell} &= \frac{\partial \text{Im} z_k}{\partial r_\ell} & k=0, \dots, N-1 \\
& & \ell=N, \dots, 2N-1 \\
&= \sin \theta_k & k = \ell & (23)
\end{aligned}$$

$$\begin{aligned}
[J_{[\text{Re } \underline{z}, \text{Im } \underline{z}]}(\underline{r}, \underline{\theta})]_{\ell+N, k} &= \frac{\partial \text{Re} z_k}{\partial \theta_\ell} & k=N, \dots, 2N-1 \\
& & \ell=0, \dots, N-1 \\
&= -r_k \sin \theta_k & k=\ell & (24)
\end{aligned}$$

$$\begin{aligned}
[J_{[\text{Re } \underline{z}, \text{Im } \underline{z}]}(\underline{r}, \underline{\theta})]_{k+N, \ell+N} &= \frac{\partial \text{Im} z_k}{\partial \theta_\ell} & k=N, \dots, 2N-1 \\
& & \ell=N, \dots, 2N-1 \\
&= r_k \cos \theta_k & k=\ell & (25)
\end{aligned}$$

It may be demonstrated that the determinant of the Jacobian is

$$|J_{[\text{Re } \underline{z}, \text{Im } \underline{z}]}(\underline{r}, \underline{\theta})| = \prod_{k=0}^{N-1} r_k (\cos^2 \theta_k + \sin^2 \theta_k) \quad (26)$$

which establishes Equation 19.

It is desired to transform the joint distribution $g(\underline{r}, \underline{\theta} | i)$ to a distribution of $2N$ statistics

$$\begin{aligned}
q_k(\underline{r}, \underline{\theta}) &= \underline{r}^T \Omega_k(\underline{\theta}) \underline{r} & k=0, 1, \dots, N-1 \\
\theta_k &= \theta_k & k=0, 1, \dots, N-1 & (27)
\end{aligned}$$

where the set of M hypotheses has been augmented by $N-M$ dummy variables and the N phase angles are retained in the new density to allow the use of

a Jacobian technique in the transformation. The new distribution is given by

$$p(\underline{q}_N, \underline{\vartheta}/i) = \begin{cases} g[Q^{-1}(\underline{q}_N, \underline{\vartheta})/i] / |J_{[\underline{q}_N, \underline{\vartheta}]}(\underline{r}, \underline{\vartheta})| & (28) \\ 0, \text{ where no inverse image exists} \end{cases}$$

where the transformation Q , defined by

$$Q : (\underline{r}, \underline{\vartheta}) \longrightarrow (\underline{q}_N, \underline{\vartheta})$$

is nonlinear but has a single-valued inverse for all but pathological choices of the set of $\underline{\Omega}_k(\underline{\vartheta})$. The new density is zero in the region where, for a given $(\underline{q}_N, \underline{\vartheta})$, no corresponding image $(\underline{r}, \underline{\vartheta})$ exists. Since the statistics are coupled through the covariance matrices of Equation 27 not all $(\underline{q}_N, \underline{\vartheta})$ are possible as images of $(\underline{r}, \underline{\vartheta})$ under the transformation Q .

At this stage, the analytic approach begins to break down. There is no convenient expression for the Jacobian of this transformation except that which follows from the definition of a determinant. The Jacobian matrix $J_{[\underline{q}_N, \underline{\vartheta}]}(\underline{r}, \underline{\vartheta})$ has the following elements:

$$\frac{\partial q_k}{\partial r_\ell} = 2 r_\ell [\Omega_k(\underline{\vartheta})]_{\ell, \ell} + \sum_{n \neq \ell} r_n [\Omega_k(\underline{\vartheta})]_{n \neq \ell} \quad (29)$$

$$k=0, \dots, N-1$$

$$, \quad \ell=0, \dots, N-1$$

$$\frac{\partial \theta_k}{\partial r_\ell} = 0$$

$$k=0, \dots, N-1$$

$$, \quad \ell=N, \dots, 2N-1$$

$$\frac{\partial q_k}{\partial \theta_\ell} = r_k \sum_{n \neq \ell} r_n \sin(\theta_\ell - \theta_n) [L_i^{-1}]_{n,\ell}$$

$$\frac{\partial \theta_k}{\partial \theta_\ell} = \delta_{k,\ell}$$

$$\begin{aligned} & k=N, \dots, 2N-1 \\ & \ell=0, \dots, N-1 \end{aligned} \quad (30)$$

$$\begin{aligned} & k=N, \dots, 2N-1 \\ & \ell=N, \dots, 2N-1 \end{aligned}$$

The determinant of the Jacobian matrix involves terms from only the first of these four expressions, due to the property of determinants⁴¹

$$\begin{vmatrix} \underline{A} & \underline{B} \\ \underline{C} & \underline{D} \end{vmatrix} = |\underline{A}| \cdot |\underline{D} - \underline{C} \underline{A}^{-1} \underline{B}| \quad (31)$$

which holds for square matrices with $|\underline{A}| \neq 0$. Since $\underline{B}=\underline{0}$ and $\underline{D}=\underline{1}$, the right hand side of Equation 31 reduces to $|\underline{A}|$. However, the remaining matrix has generally all nonzero terms which makes the expression in Equation 28 for the transformation not useful for an analytical evaluation of the channel performance.

There is a related integral which may be useful either as an approximation to the optimal channel performance, as an approximation to the performance of the suboptimal receiver introduced in Section III, or as a bounding integral for either of these. Without further reference to its ultimate use, let us just consider it a related integral which appears to be more tractable.

If the off-diagonal elements of L_i^{-1} are zero, the probability density of Equation 18 has no dependence on phase angles since they occur

only in off-diagonal elements. Then, upon integrating over the phase angles, the distribution of envelopes \underline{r} becomes

$$g(\underline{r}/i) = 2^N |\underline{L}_i|^{-1} \prod_{k=0}^{N-1} (r_k) e^{-\underline{r}^T \underline{L}_i^{-1} \underline{r}} \quad (32)$$

which is a joint Rayleigh density (that could be factored into independent marginal densities under the assumption that \underline{L}_i^{-1} is diagonal.) The Jacobian of the transformation from \underline{r} to \underline{q}_N involves elements from Equation 29 which under the simplifying assumption are

$$\frac{\partial q_k}{\partial r_\ell} = 2r_\ell [L_k^{-1}]_{\ell\ell} \quad , \quad \begin{array}{l} k=0, \dots, N-1 \\ \ell=0, \dots, N-1 \end{array} \quad (33)$$

A matrix may be formed from the diagonal elements of the N L_k^{-1} matrices, including the N -M dummy statistics introduced earlier:

$$[\Gamma]_{k,\ell} = [L_k]_{\ell\ell} \quad \begin{array}{l} k=0, \dots, N-1 \\ \ell=0, \dots, N-1 \end{array} \quad (34)$$

then the Jacobian of the transformation from \underline{r} to \underline{q}_N is

$$|J_{\underline{q}_N}(\underline{r})| = 2^N \prod_{k=0}^{N-1} (r_k) |\Gamma| \quad (35)$$

and the distribution of statistics becomes:

$$f_N(\underline{q}_N/i) = \begin{cases} |\underline{L}_i|^{-1} |\Gamma|^{-1} e^{-q_i} & , \quad q \in \mathcal{P} \\ 0 & , \quad q \notin \mathcal{P} \end{cases} \quad (36)$$

where

$$\mathcal{P} \triangleq \{ \underline{q}_N = \Gamma \underline{x} \mid x_i \geq 0, i=1, \dots, N \} \quad (37)$$

The χ_i 's correspond to $|z_i|^2$ or channel received power and are always positive. \mathcal{P} is the set of statistics which are images of some data vector \underline{z} and is limited to a region within the positive orthant of N -space by the positive matrix $\underline{\Gamma}$ acting on the vector of positive elements

$$\underline{\chi} \triangleq [|z_0|^2 |z_1|^2 \dots |z_{N-1}|^2]^T \quad (38)$$

Now the channel performance may be expressed, for the special case of diagonal covariance matrices:

$$P_{c/i} = \int \int \dots \int_{\substack{\underline{L}_i \\ \underline{q}_N \in \mathcal{P} \cap \mathcal{V}}} |\underline{L}_i|^{-1} |\underline{\Gamma}|^{-1} e^{-\underline{q}_i \underline{\Gamma} \underline{q}_i} dq_1 \dots dq_N \quad (39)$$

where $\mathcal{V}_i \triangleq \{ \underline{q} | q_k \leq q_k, k \in \mathcal{D} \}$ (40)

The matrix $\underline{\Gamma}$ completely describes the optimal receiver which is identical to the SPLOT receiver* for diagonal covariance matrices. The rows of $\underline{\Gamma}$ generate the statistics \underline{q}_N through the relationship

$$\underline{q}_N = \underline{\Gamma} \underline{\chi} \quad (41)$$

and $\underline{\Gamma}$ is perfectly matched to the diagonal covariance matrices via Equation 34. If an invertible matrix other than $\underline{\Gamma}$ is used in generating the statistics, say

$$\tilde{\underline{q}}_N = \tilde{\underline{\Gamma}} \underline{\chi} \quad (42)$$

* Stationary process-long observation time receiver.

the channel performance integral becomes

$$\bar{P}_{c/i} = \int \int \dots \int_{\mathcal{P} \cap \mathcal{V}_i} |\underline{L}_i|^{-1} |\underline{\tilde{\Gamma}}|^{-1} e^{-\underline{\Gamma}^i \underline{\tilde{\Gamma}}^{-1} \tilde{q}_i} d\tilde{q}_1 d\tilde{q}_2 \dots d\tilde{q}_N \quad (43)$$

where $\underline{\Gamma}^i$ is a row vector consisting of the i^{th} row of $\underline{\Gamma}$.

The performance integrals given by Equations 39 and 43 apply to the SPLOT approximation to the optimal (known statistics) receiver which is introduced in Section III. They are not tractable integrals and are used only in a formal manner in the sequel. Equation 37, for a correct receiver matrix $\underline{\Gamma}$, is evaluated by numerical methods explained in the remainder of this section.

RECEIVER PERFORMANCE - NUMERICAL METHODS

A Monte Carlo technique was developed to evaluate the performance of the optimal MPE 8-ary FSK receiver with Gaussian zero-mean signals in AWGN. A sampled-data receiver, employing an ideal (impulse) sampler was used in the analysis. The discussion here is divided into three parts. The first part deals with the incorporation of signal-to-noise ratio (SNR) including a derivation of the autocorrelation function of the continuous-time baseband waveform in terms of the radio-frequency signal spectrum and white noise level at the receiver. The second part treats the calculation of DFT covariance matrices based on sampled versions of the baseband autocorrelation functions, and the third part explains the use of these matrices in obtaining system performance.

BASEBAND AUTOCORRELATION FUNCTIONS AND SNR

The received signal power spectral density (PSD) will be represented by $\psi_r'(f)$, with the prime designating a waveform that exists prior

to any filtering at the receiver. $\psi_{r'}(f)$ is a two-sided spectrum with the units of watts/hertz (W/Hz). The corresponding white noise density will be designated $N_0/2$ W/Hz. The appropriate definition of signal-to-noise ratio, where the signal is a segment of a stationary Gaussian process, is given by

$$\text{SNR} = \frac{T \int_{-\infty}^{\infty} \psi_{r'}(f) df}{N_0/2} \quad (44)$$

where the numerator is the signal energy received during a modulation interval T , and the denominator is the white noise density. The first step is to evaluate the autocorrelation function of the baseband analog signal $x(t) + jy(t)$, defined below, in terms of $\psi_{r'}(f)$ and N_0 .

In considering the effect of the baseband filter on the received signal spectrum, it is convenient to manipulate the block diagram of the receiver to produce the effect of the baseband filter in front of the mixer. This artifice helps to avoid some notational complexity. Figure 3 shows the baseband block diagram for the transformation of the received signal-plus-noise $r'(t)$ to the complex-valued baseband waveform $x(t) + jy(t)$.

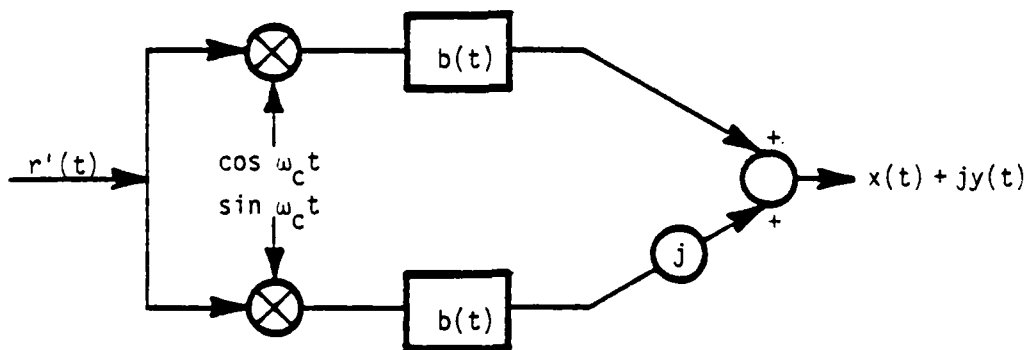


Figure 3. Baseband block diagram.

The two baseband analog filters are denoted by their identical impulse responses $b(t)$. This block diagram is expressed analytically by the convolution integral:

$$\begin{aligned} x(t) + jy(t) &= \int_0^{\infty} b(\tau) r'(t-\tau) [\cos\omega_c(t-\tau) + j\sin\omega_c(t-\tau)] d\tau \\ &= e^{j\omega_c t} \int_0^{\infty} b(\tau) e^{-j\omega_c \tau} r'(t-\tau) d\tau \end{aligned} \quad (45)$$

The rearrangement of the convolution integral given by Equation 45 suggests an alternative form for the block diagram with a filter in front of the mixer as shown in Figure 4.

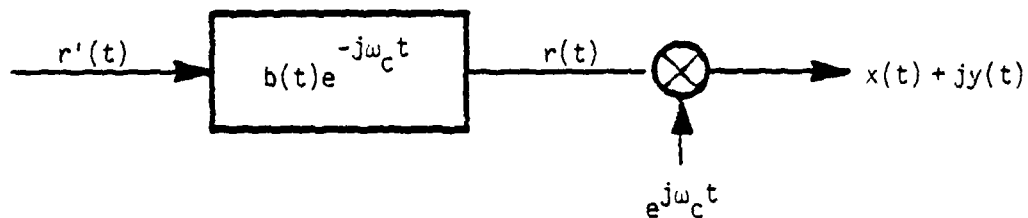


Figure 4. Alternative block diagram.

Here the post-filter received waveform is identified as

$$r(t) = \int_0^{\infty} b(\tau) e^{-j\omega_c \tau} r'(t-\tau) d\tau \quad (46)$$

The properties of the Fourier transform:

$$\begin{aligned} \mathcal{F}\{b(t)\} &= \int_{-\infty}^{\infty} b(t) e^{-j2\pi ft} dt \\ &\triangleq \mathcal{B}(f) \end{aligned} \quad (47)$$

give the the result that the transfer function of the filter in Figure 4 is

$$\mathcal{F}\{b(t)e^{-j\omega_c t}\} = \mathcal{B}(f+f_c) \quad (48)$$

where $\omega_c = 2\pi f_c$. In this report we consider an ideal filter with the magnitude transfer function:

$$|\mathcal{B}(f)| = \begin{cases} 1 & , -B < f < B \\ 0 & , \text{ otherwise} \end{cases} \quad (49)$$

so that $|\mathcal{B}(f+f_c)|$ becomes

$$|\mathcal{B}(f+f_c)| = \begin{cases} 1 & , -B - f_c < f < B - f_c \\ 0 & , \text{ otherwise} \end{cases} \quad (50)$$

The relationship of $|\mathcal{B}(f)|$ and $|\mathcal{B}(f+f_c)|$ is illustrated by Figure 5.

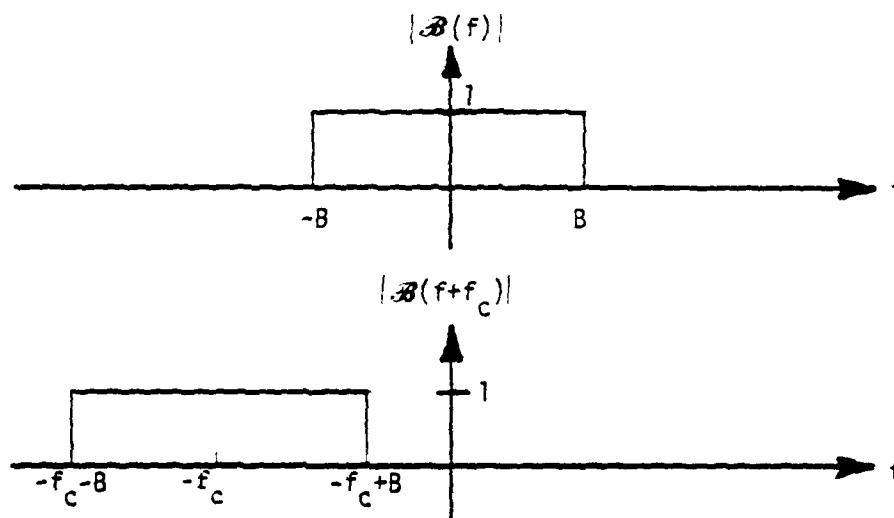


Figure 5. Magnitude transfer functions for $\mathcal{B}(f)$ and $\mathcal{B}(f+f_c)$.

Now the effect of the baseband filter is confined to the transfer function from $r'(t)$ to $r(t)$. Make the following definition for the statistics of the post-filter received signal-plus-noise $r(t)$:

$$r(t) = s(t) + n(t) \quad (51)$$

$$E\{r^*(t)r(t+\tau)\} \triangleq R_r(\tau) \quad (52)$$

$$E\{s^*(t)s(t+\tau)\} \triangleq R_s(\tau) \quad (53)$$

$$E\{n^*(t)n(t+\tau)\} \triangleq R_n(\tau) \quad (54)$$

where $s(t)$ and $n(t)$ are the signal and noise terms of $r(t)$. By the linearity of the expectation operator,

$$R_r(\tau) = R_s(\tau) + R_n(\tau) \quad (55)$$

where

$$R_s(\tau) = \int_{-\infty}^{\infty} \psi_r(f) |\mathcal{B}(f + f_c)|^2 e^{j2\pi f\tau} df \quad (56)$$

$$R_n(\tau) = \int_{-\infty}^{\infty} \frac{N_0}{2} |\mathcal{B}(f + f_c)|^2 e^{j2\pi f\tau} df \quad (57)$$

It remains only to "demodulate" these autocorrelation functions by the complex mixing operation illustrated in Figure 4 to obtain the corresponding signal and noise statistics for $x(t) + jy(t)$:

$$\begin{aligned} & E \left\{ s^*(t) e^{-j\omega_c t} s(t+\tau) e^{j\omega_c(t+\tau)} \right\} \\ &= R_s(\tau) e^{j\omega_c \tau} \\ &= \int_{-\infty}^{\infty} \psi_r(f) |\mathcal{B}(f + f_c)|^2 e^{j2\pi(f + f_c)\tau} df \\ &= \int_{-B}^B \psi_r'(f - f_c) e^{j2\pi f\tau} df \end{aligned} \quad (58)$$

and

$$\begin{aligned}
 & E \left\{ n^*(t) e^{-j\omega_c t} n(t+\tau) e^{j\omega_c (t+\tau)} \right\} \\
 & = R_n(\tau) e^{j\omega_c \tau} \\
 & = \int_{-B}^B \frac{N_0}{2} e^{j2\pi f \tau} df \quad (59)
 \end{aligned}$$

These are the required baseband statistics for the waveform prior to the sampler. In the next section the method of approximation to sample values of Equations 58 and 59 are discussed.

SAMPLE AUTOCORRELATION AND DFT COVARIANCE MATRIX

The details of the technique for calculating the DFT covariance matrix from the time sample autocorrelation function are discussed in Appendix C. Here the approximation used to obtain the time-sample autocorrelation function from the signal PSD $\psi_r(f)$ is treated.

The signal and noise terms (Equations 56 and 57) are handled separately for computational efficiency — for each signal PSD several noise levels are considered. In Appendix C it is indicated that $2N-1$ samples, evenly spaced in the interval $-T \leq \tau \leq T$ are required from the continuous, time autocorrelation function, where T is the modulation interval and N is the number of samples per modulation interval in the receiver. To approximate the integral of Equation 56 a DFT of much greater dimension than $2N$ is used and the result is undersampled to the desired $2N-1$ samples. The approximation to the integral is

$$\begin{aligned}
 & \int_{-B}^B \psi_r'(f - f_c) e^{j2\pi f \tau} df \\
 & \approx \frac{1}{2TP} \sum_{k=-2BTP}^{2BTP} \psi_r' \left[\frac{k}{2TP} - f_c \right] e^{j \frac{2\pi k \tau}{2TP}} \quad (60)
 \end{aligned}$$

where the PSD $\psi_r(f - f_c)$ is sampled at intervals of $1/(2TP)$ Hz and a rectangular approximation is used. The integral is evaluated for N' points of τ where $N' = 2TP/\Delta t$ is the dimension of the DFT used, resulting in the expression

$$R_{s, x + jy}(n) = \frac{1}{2TP} \sum_{k = -2 \text{ BTP}}^{2 \text{ BTP}} \psi_r \left[\frac{k}{2TP} - f_c \right] e^{j \frac{2\pi kn}{N'}} \quad (61)$$

where $R_{s, x + jy}(n)$ is used to denote the approximate time-sample autocorrelation function of the sample sequence $x(n\Delta t) + jy(n\Delta t)$. Equation 61 is a form of inverse DFT of dimension N' with elements of the sample sequence set to zero where they fall outside the bandwidth of the baseband filter. The use of the FFT algorithm will result in N' values of the autocorrelation function. Of these only $2N-1$ points are used where $N=N'/2P$ is the number of samples per observation interval T in the sampled-data receiver. These are the $2N-1$ points surrounding the origin.

The corresponding noise autocorrelation function (Equation 57) is approximated by

$$R_{n, x + jy}(n) = N_o B \delta(n) \quad (62)$$

where we have chosen to ignore the contribution of noise autocorrelation at values other than $n=0$. This approximation will be valid where the baseband filter cutoff is in the neighborhood of the folding frequency $N/2T$ Hz, which is the cutoff frequency used in this report.

The numerical method of obtaining signal-to-noise ratio normalization makes use of the fact that arbitrary rescaling of Equations 56 and 57

will not affect the resulting performance. The signal power is normalized by establishing the equality

$$\sum_{k=-\infty}^{\infty} \psi_T' \left[\frac{k}{2TP} - f_c \right] = 2TP \quad (63)$$

via a numerical technique and then setting the noise variance accordingly. The appropriate value of N_0 is obtained by solving Equation 44 for given values of SNR and T with the signal power set to one watt.

The signal autocorrelation function obtained by Equation 61 is arranged in a signal time-sample covariance matrix:

$$\underline{R}_S = \begin{bmatrix} R_S(0) & R_S(1) & \dots & R_S(N-1) \\ R_S(-1) & R_S(0) & & \\ \vdots & & \dots & \\ R_S(-N+1) & & \dots & R_S(0) \end{bmatrix} \quad (64)$$

As shown in Appendix C, the two dimensional DFT (with some rearrangements) of the array \underline{R}_S is the signal-term of the DFT covariance matrix:

$$E\{z_j z_l^*\} = \frac{1}{N^2} \sum_{n=0}^{N-1} \sum_{m=0}^{N-1} R_S(n-m) e^{-j \frac{2\pi kn}{N}} e^{j \frac{2\pi lm}{N}} + \frac{N_0 B}{N} \delta(k, l) \quad (65)$$

The noise term affects only the elements on the main diagonal of the DFT covariance matrix \underline{L}_i defined by

$$[\underline{L}_i]_{k, l} \triangleq E\{z_k z_l^*\} \quad (66)$$

The DFT covariance matrix on the i^{th} hypothesis of signal transmitted, is defined by having the element in row k and column l equal to the expected value of the product of coefficients z_k and z_l^* .

MONTE CARLO PROCEDURE

Using the method described above a set of M DFT covariance matrices is computed for each level of signal frequency dispersion and for each signal-to-noise ratio. The different DFT covariance matrices correspond to different transmitted deviation frequencies. It is assumed that the envelope of the received signal spectrum is the same for each transmitted frequency, that the spectra are symmetrical about the transmitted frequency, and that they have the detailed functional forms discussed in Section VI. The DFT covariance matrices are all that is necessary to determine system performance by the statistical sampling method.

In Appendices D and E the technique to obtain sample vectors \underline{z}_i distributed according to the complex normal distribution with covariance matrix \underline{L}_i is developed. The technique involves the computation of a square root matrix for each \underline{L}_i which is used to produce the appropriate degree of correlation by matrix-vector multiplication with an uncorrelated random complex normal vector. For each one of many trials a sample vector \underline{z}_i is obtained. The sample vector corresponds to a particular hypothesis i of signal transmitted, level of frequency dispersion, and white noise level.

The sample vectors are tested with decision rules for the conventional receiver equation, for the optimal MPE receiver equation, and for a particular suboptimal receiver which is described in Section III. The number of correct decisions obtained and total number of trials for each hypothesis are tallied and cumulative results are computed over an equal number of trials of all M hypotheses. Results are given in Section VI.

III. ESTIMATION

The previous section dealt with a known statistics optimal receiver quite similar to the one developed by Kailath. It differs only in that the DFT coefficients of $r_i(t)$ at a given sample rate over the observation interval $(0,T)$ are considered the raw data rather than time samples. As previously mentioned, the receiver's decision is identical in either formulation. The analysis of the misclassification error in Section II concludes with the derivation of an intractable integral—even for the simplified case where the off diagonal elements of the covariance matrix \underline{L}_i are set to zero. The receiver performance for rapid fading conditions is available only through numerical evaluations which are impractical for more than a small number of points due to the large dimension of the domain space of the integration (which is sixteen in the case of interest). This situation makes the derivation of an optimal spectral estimation keyed to the exact receiver performance impossible or at least impractical. In this section an optimal estimator is derived under some simplifying assumptions about the receiver performance integral.

The complete matrix \underline{L}_i will not have to be estimated but rather only the elements on the main diagonal. These points are mean values of magnitude-squared DFT coefficients whereas the off diagonal elements of \underline{L}_i are covariances between different DFT coefficients. The levels of frequency dispersion, length of the observation interval, and sample rate of the particular system under consideration are in a realm where an approximation of the matrix \underline{L}_i , in the receiver algorithm, by another matrix with the same main diagonal, but set to zero on the off-diagonal, yields approximately the same receiver performance.

This approximation to the optimal receiver is known as the stationary process long observation time (SPLOT) algorithm. In Section VI it is experimentally verified that the SPLOT algorithm yields a receiver performance indistinguishable by Monte Carlo integration from the optimal (known statistics) receiver in all cases of interest.

ESTIMATION COST FUNCTION

Two equations are given in Section II for the probability of a correct decision of the SPLOT algorithm as a function of the true statistics \underline{L}_i of the received signal and of the receiver matrix $\underline{\Gamma}$. Equation 39 pertains to the performance when a correct receiver matrix $\underline{\Gamma}$ is used and Equation 43 gives the performance when an erroneous matrix $\tilde{\underline{\Gamma}}$ is used. In either case the integrals describing the performance are not evidently tractable. The receiver matrix $\underline{\Gamma}$ is made up of rows which are the inverse of power spectrum values for the received signal $r_i(t)$. Actually, only one row of $\underline{\Gamma}$ needs to be estimated. The signal frequency dispersion is narrow enough, in the practical case of interest, and the sampling rate rapid enough that the M rows of $\underline{\Gamma}$ which are used in the receiver algorithm can be generated as rotational shifts of one row. Thus, to implement a SPLOT adaptive receiver one may consider the estimation of a centered power spectrum of N elements

$$\begin{aligned} \underline{\sigma}^{-2} &= [\sigma_0^{-2} \sigma_1^{-2} \dots \sigma_{N-1}^{-2}]^T \\ &= [(E\{|z_0|^2\})^{-1} (E\{|z_1|^2\})^{-1} \dots (E\{|z_{N-1}|^2\})^{-1}]^T \end{aligned} \quad (67)$$

where $E\{|z_0|^2\}$ is the power at the center of the spectrum of the received signal, and $E\{|z_1|^2\}$ and $E\{|z_{N-1}|^2\}$ are the two points on either side, etc. It is important to note that the receiver requires an estimate of the inverse of the mean-square magnitude of DFT coefficients rather than the mean of the inverse which would be quite a different problem.

The cost function for determining the quality of the estimate $\hat{\sigma}^{-2}$ is defined by the degradation in the probability of a correct decision on the average over M hypotheses

$$C(\underline{\sigma}^{-2}, \tilde{\underline{\sigma}}^{-2}) = \frac{1}{M} \sum_{i=1}^M [P_{c/i}(\underline{\Gamma}) - \tilde{P}_{c/i}(\underline{\Gamma}, \tilde{\underline{\Gamma}})] \quad (68)$$

where $P_{c/i}$ and $\tilde{P}_{c/i}$ are the probabilities of correct decisions, defined by Equations 39 and 43 of Section II, for the receivers incorporating correct statistics and erroneous statistics respectively.

Of course $C(\underline{\sigma}^{-2}, \tilde{\underline{\sigma}}^{-2})$ is not known since it cannot be practically evaluated. The objective here is to investigate what assumptions are necessary regarding this cost function that an optimal adaptive receiver may be obtained. From another point of view: If an estimator is specified for $\underline{\sigma}^{-2}$ what properties of $C(\underline{\sigma}^{-2}, \tilde{\underline{\sigma}}^{-2})$ must hold for it to be optimal? All that can be said about the cost function without evaluating it numerically is that it goes to zero when the correct spectrum is used and that it is positive for all other values—this statement derives from the optimality of the known statistics receiver. A primary question to ask is whether this property can be extended to the individual spectral elements σ_k^{-2} , $k=0, \dots, N-1$, since it will greatly simplify the analysis if the estimators of individual spectral elements can be considered separately.

In general it is not true that the cost function is minimized at the correct spectral value for an individual spectral estimate $\hat{\sigma}_k^{-2}$. If all of the other spectral estimates were simultaneously too large or too small the best estimate of σ_k^{-2} would be correspondingly above or below the true value. This is evident since the receiver decision is insensitive to overall rescaling of the received signal $r_i(t)$. If all of the estimates used in the receiver matrix $\underline{\Gamma}$ are off by the same factor, the receiver decision is still optimal. This fact derives from Equations 38 through 41

of Section II which show that the SPLOT receiver makes its decision by selecting the minimum element of the vector

$$q_N = \underline{\Gamma} \underline{\chi} \quad (69)$$

where $\underline{\chi}$ is the vector of magnitude-squared DFT coefficients computed for a particular observation interval. If either $\underline{\Gamma}$ or $\underline{\chi}$ is rescaled by a factor, the minimum element of q_N is unchanged.

It is, however, reasonable to assume that if the data used in estimating each element σ_k^{-2} are statistically independent, the estimation errors will be randomly scattered above and below the correct values so that the best estimate of a particular σ_k^{-2} will occur near its true value with a high probability. Therefore, the first ad hoc assumption regarding $C(\underline{\sigma}^{-2}, \tilde{\underline{\sigma}}^{-2})$ will be that the individual costs in estimating particular spectral values achieve a minimum at the true value. This allows us to consider these estimators independently but restricts the estimators to be based upon statistically independent data.

There is a slight correlation between DFT coefficients of different frequencies given by the off-diagonal elements of the \underline{L}_i matrix. These terms were neglected in making the SPLOT approximation to the optimal receiver since they had little effect on the receiver decision for the particular channel conditions considered. Sample \underline{L}_i matrices which have been calculated to evaluate the optimal receiver performance show a small correlation between coefficients which decreases as the frequency separation increases. The level of correlation is small enough that it does not warrant consideration in terms of the argument put forth that the estimation costs for individual spectral elements be considered to achieve a minimum at the true value.

CRITERION OF OPTIMALITY

With the foregoing assumption it is appropriate to consider the estimation of one spectral element $\hat{\sigma}_k^{-2}$ independent of all of the others. What follows is a short discussion of the Bayesian approach to optimal estimation showing why it cannot readily be developed into a nonBayesian criterion. An alternative criterion is introduced which is based on sufficient statistics and the theory of confidence intervals for estimating non-random parameters.

The criterion of estimation quality in a Bayesian approach to combined parameter estimation and demodulation is the expected value of the cost function $C[\sigma_k^{-2}, \hat{\sigma}_k^{-2}(\underline{z}_k)]$. The average cost or "risk" function is minimized with respect to the choice of the function $\hat{\sigma}_k^{-2}(\underline{z}_k)$ mapping the available data \underline{z}_k into the estimate. The expected value is taken with respect to the joint density of the random parameter σ_k^{-2*} and data \underline{z}_k :

$$\mathcal{R} = \int_{-\infty}^{\infty} \int_{-\infty}^{\infty} C[\sigma^{-2}, \hat{\sigma}^{-2}(\underline{z})] p(\underline{z}, \sigma^{-2}) d\underline{z} d\sigma^{-2} \quad (70)$$

This, of course, requires that a probability density be specified for σ^{-2} . Where it is not appropriate to assume a probability density for the unknown parameter one might consider a risk function similar to Equation 70 which varies with the parameter value

$$\mathcal{R}(\sigma) = \int_{-\infty}^{\infty} C[\sigma^{-2}, \hat{\sigma}^{-2}(\underline{z})] p(\underline{z}/\sigma^{-2}) d\underline{z} \quad (71)$$

* The k subscript is dropped in most of the remainder of this discussion. There should be no confusion since the entire discussion deals with the estimation of the k^{th} element of the spectrum.

but with such a formulation the estimator which minimizes this risk is inevitably

$$\widehat{\sigma^{-2}}(\underline{z}) = \sigma^{-2} \quad (72)$$

since the cost function achieves a minimum where the true parameter is used.

This result is mathematically correct but useless since it calls for an estimator which incorporates knowledge of the unknown parameter. The fundamental source of the problem seems to be that σ^{-2} appears as a constant in the right-hand side of Equation 71. In order to mathematically express the fact that σ_k^{-2} is unknown it should appear as a variable.

We propose a criterion which will allow σ^{-2} to be a variable based on the theory of confidence limits and sufficient statistics. If a sufficient statistic exists for the probability density $p(\underline{z}/\sigma^{-2})$ then it is possible to base parameter estimates of σ^{-2} on that statistic without losing any relevant information. In other words, any statistical inferences on the data \underline{z} may equivalently be made on the statistic rather than the complete data set \underline{z} . One of several criteria of the sufficiency of a statistic is that the probability density for \underline{z} conditioned on the knowledge of the statistic be independent of the parameter σ^{-2} . Here we mean functionally independent rather than statistically independent in keeping with the point of view that σ^{-2} is not specified by a probability density. This implies that the statistic incorporates all of the available information regarding the unknown parameter.

Sufficiency can be established using the functional form of the joint density for \underline{z} and the form of the sampling statistic. A discussion of the statistic

$$\bar{z}_k = \sum_{n=1}^{\infty} b_n |z_{kn}|^2 \quad (73)$$

$$E\{\bar{z}_k\} = E\{|z_{kn}|^2\} = \sigma_k^2 \quad (74)$$

which is used here to estimate the unknown parameter σ_k^{-2} is deferred to the last part of this section. \bar{z} is an approximation to a sufficient statistic for the unknown parameter.

The theory of confidence limits allows probabilistic statements to be made about the location of the parameter σ^{-2} given the value of the statistic \bar{z} . These statements are derived from analysis of the probability density $p(\bar{z}/\sigma^{-2})^*$ for a fixed parameter and are then "turned around" logically to make an inference about the value of σ^{-2} given a sample \bar{z} . With knowledge of the form of the sampling statistic $p(\bar{z}/\sigma^{-2})$ one may compute the probability, for a given ϵ , whether \bar{z} falls in the interval

$$P[(1-\epsilon)\sigma^2 < \bar{z} < (1+\epsilon)\sigma^2] = \int_{(1-\epsilon)\sigma^2}^{(1+\epsilon)\sigma^2} p(\bar{z}/\sigma^2) d\bar{z} \\ = 1 - \alpha \quad (75)$$

The probability density $p(\bar{z}/\sigma^2)$ sets up a relationship between ϵ and α such that as ϵ goes to zero α goes to 1 and as ϵ goes to infinity α goes to zero. Confidence limits are typically based on the normal density through an invocation of the central limit theorem.⁴² Such an asymptotic approximation is neither necessary or desirable in this case. We wish to consider cases where \bar{z}_k will be computed by a weighting sequence (b_n) which is too short for a normal approximation to the density $p(\bar{z}/\sigma^{-2})$.

Since the parameter σ^2 is a scale parameter for the density in the sense that

$$p_{\bar{z}/\sigma^2}(\xi\bar{z}/\xi\sigma^2) = \xi^{-1} p_{\bar{z}/\sigma^2}(\bar{z}/\sigma^2) \quad (76)$$

* Notice that $p_{\bar{z}/\sigma^2}(\bar{z}/\sigma^2) = p_{\bar{z}/\sigma^{-2}}(\bar{z}/\sigma^{-2})$ and that these notations are used interchangeably with the subscripts deleted.

the relationship between α and ϵ given by Equation 75 does not change as a function of σ^2 . This can be seen by making the change of variable from \bar{z} to $y = \sigma^{-2}\bar{z}$ in the integral:

$$\begin{aligned} \int_{(1-\epsilon)\sigma^2}^{(1+\epsilon)\sigma^2} p_{\bar{z}/\sigma^2}(\bar{z}/\sigma^2) d\bar{z} &= \int_{1-\epsilon}^{1+\epsilon} p_{\bar{z}/\sigma^2}(\sigma^2 y/\sigma^2) \sigma^2 dy \\ &= \int_{1-\epsilon}^{1+\epsilon} p_{\bar{z}/\sigma^2}(y/1) dy \end{aligned} \quad (77)$$

The confidence coefficient $1 - \alpha$ expresses the probability that a sample \bar{z} is within a factor $1 - \epsilon$ to $1 + \epsilon$ of the mean value σ^2 regardless of the magnitude of σ^2 according to this formulation.

The probabilistic statement regarding \bar{z} for a given σ^2 may be conveniently converted to a corresponding statement regarding σ^{-2} given a sample of \bar{z} . Note that \bar{z} and σ^2 are both positive.

$$(1-\epsilon)\sigma^2 < \bar{z} < (1+\epsilon)\sigma^2 \quad (78)$$

then

$$1 - \epsilon < \bar{z}\sigma^{-2} < 1 + \epsilon \quad (79)$$

or

$$\frac{1 - \epsilon}{\bar{z}} < \sigma^{-2} < \frac{1 + \epsilon}{\bar{z}} \quad (80)$$

and the confidence interval may be used to put an upper bound on the cost given a sample of the statistic \bar{z} and a confidence coefficient $1 - \alpha$.

The upper bound is derived in the following manner: Once σ^{-2} is confined to a symmetric interval about \bar{z}^{-1} the cost is upper bounded by

$$B_F(\alpha) = \max_{\sigma^{-2} \in \mathcal{B}(\alpha)} (C[\sigma^{-2}, F(\bar{z}^{-1})]) \quad (81)$$

$$\mathcal{B}(\alpha) = [\bar{z}^{-1}(1-\epsilon), \bar{z}^{-1}(1+\epsilon)] \quad (82)$$

where \mathcal{B} is the set of values for σ^{-2} prescribed by the confidence coefficient $1 - \alpha$, and $F(\cdot)$ is an instantaneous function mapping the (inverse) sufficient statistic \bar{z}^{-1} into an estimate of σ^{-2} . With this definition an equivalence is set up between the events $\{C[\sigma^{-2}, F(\bar{z}^{-1})] < B_F(\alpha)\}$ and $\{\sigma^{-2} \in \mathcal{B}(\alpha)\}$ both conditioned on \bar{z} so that the confidence limit applies equally to the event that σ^{-2} is on the interval $\mathcal{B}(\alpha)$ and the event that the cost is upper bounded by $B_F(\alpha)$ given a specific value for the statistic.

The object of optimization then is to find the function $F(\bar{z}^{-1})$ which yields the smallest upper bound $B_F(\alpha)$ for a given confidence coefficient in the equation

$$P\{C[\sigma^{-2}, F(\bar{z}^{-1})] < B_F(\alpha)\} = 1 - \alpha. \quad (85)$$

Figure 6 shows a mapping from \bar{z}^{-1} to $F(\bar{z}^{-1})$ to $C(\sigma^{-2}, F(\bar{z}^{-1}))$. The two cost curves for $\sigma^{-2} = (1-\epsilon)\bar{z}^{-1}$ and $\sigma^{-2} = (1+\epsilon)\bar{z}^{-1}$ are indicated, and the figure illustrates that an upper bounding cost $B_F(\alpha)$ will be achieved on one of the two extreme cost curves of the interval.

The conclusion that one of the two extreme curves on the interval will set the maximum cost for a given $F(\bar{z}^{-1})$ on the family of curves over the interval is justified on the assumption that the cost is monotonically increasing as a function of the distance of σ^{-2} from $F(\bar{z}^{-1})$, and that the individual cost curves in the family of curves with σ^{-2} on the interval $[(1-\epsilon)\bar{z}^{-1}, (1+\epsilon)\bar{z}^{-1}]$ are properly "nested" in the sense that

$$\begin{aligned} \frac{\partial C[\sigma^{-2}, F(\bar{z}^{-1})]}{\partial \sigma^{-2}} &> 0 \text{ for } F(\bar{z}^{-1}) > \sigma^{-2} \\ &< 0 \text{ for } F(\bar{z}^{-1}) < \sigma^{-2} \end{aligned} \quad (84)$$

for any fixed $F(\bar{z}^{-1})$. This is a fairly loose regularity condition which merely implies that the estimation cost does not reach a particularly extreme condition for some σ^{-2} on the interval.

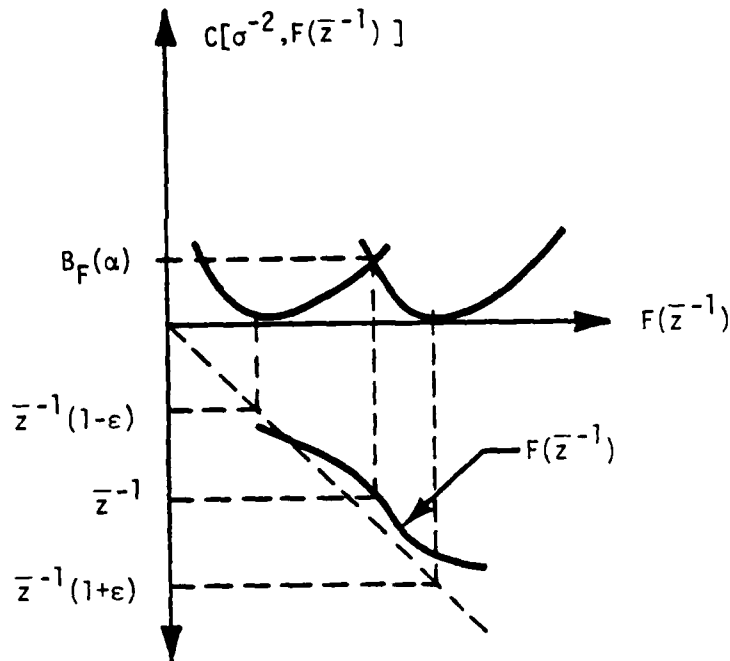


Figure 6. Mapping from \bar{z}^{-1} to $F(\bar{z}^{-1})$ to cost functions at the extremes of the confidence interval.

Under this regularity assumption the optimal function $F(\bar{z}^{-1})$ mapping the sufficient statistic would be somewhat above or below a linear function $F(\bar{z}^{-1}) = \bar{z}^{-1}$ and would occur at the crossover of the extreme curves to yield the minimum $B(\alpha)$ as illustrated in Figure 6. Furthermore, the optimal $F(\bar{z}^{-1})$ would vary with the interval used and therefore with the confidence coefficient. Therefore it is evident that in order to specify an optimal $F(\bar{z}^{-1})$ additional assumptions regarding $C[\sigma^{-2}, F(\bar{z}^{-1})]$ are required. Figure 7 illustrates the more restricted condition.

If $C[\sigma^{-2}, F(\bar{z}^{-1})]$ is a symmetric function about σ^{-2} ,

$$C[\sigma^{-2}, \sigma^{-2} + \delta] = C[\sigma^{-2}, \sigma^{-2} - \delta] \quad (85)$$

and if the cost function "translates" over the interval

$$C[\sigma^{-2}, F(\bar{z}^{-1})] = C[\sigma^{-2} + \delta, F(\bar{z}^{-1}) + \delta] \quad \text{for } \sigma^{-2} \in \mathcal{B}(\alpha) \quad (86)$$

and $\sigma^{-2} + \delta \in \mathcal{B}(\alpha)$

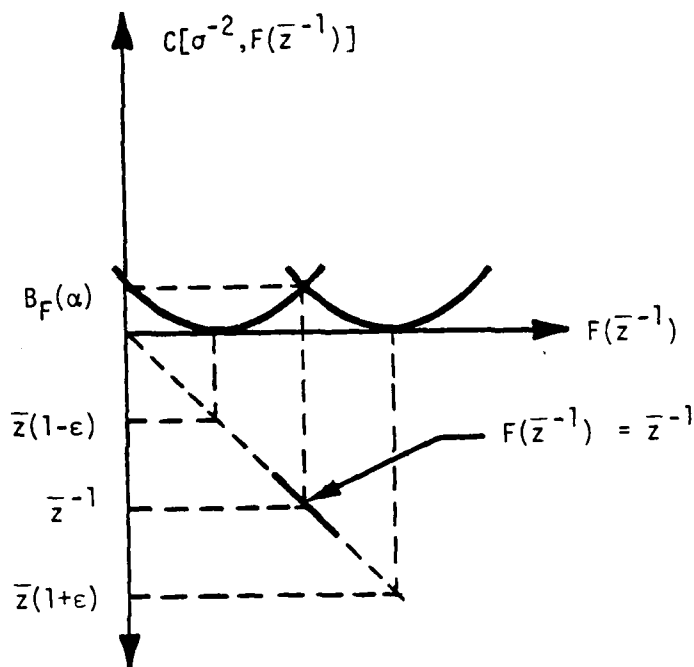


Figure 7. Mapping from (\bar{z}^{-1}) to $F(\bar{z}^{-1})$ to cost functions at the extremes of the confidence interval for symmetric, translating cost functions.

then the cost curves originating at the extremes of the interval will always cross over in the center and $F(\bar{z}^{-1}) = \bar{z}^{-1}$ is the optimal estimator of σ^{-2} for the specified criterion in that it yields the lowest bound on the estimation cost for a given confidence coefficient.

A criterion of optimality suitable for the case of an unknown but nonrandom variable has been stated and shown to apply under the following assumptions about the cost function $C(\underline{\sigma}^{-2}, \hat{\underline{\sigma}}^{-2})$:

1. The cost for estimating individual elements of the vector $\underline{\sigma}^{-2}$ achieve the minimum at the true value.
2. The cost function $C[\sigma^{-2}, F(\bar{z}^{-1})]$ for estimating individual elements of the vector are symmetric about the true value and invariant in shape, that is $C[\sigma^{-2}, F(\bar{z}^{-1})] = C[|\sigma^{-2} - F(\bar{z}^{-1})|]$ over a suitable range of possible values of σ^{-2} to apply a confidence limit criterion.

3. The cost function increases monotonically as a function of $|\sigma^{-2} - F(\bar{z}^{-1})|$.

Under these assumptions $F(\bar{z}^{-1}) = \bar{z}^{-1}$ that is, the inverse of the average of square magnitude DFT coefficients is an optimal estimator of σ^{-2} in that it yields the smallest upper bound on the cost for any confidence interval of σ^{-2} for which the above two assumptions hold.

The conditions on the cost function under which $F(\bar{z}^{-1}) = \bar{z}^{-1}$ is optimized are not precisely satisfied by $C(\sigma^{-2}, \sigma^{-2})$ but will be a good engineering approximation if a large enough DFT dimension is used and if the confidence interval is small enough.

THE STATISTIC \bar{z}

The statistic \bar{z} defined by Equation 73 is a weighted average of prior samples of magnitude squared DFT coefficients of the received signal $r_i(t)$ at a fixed frequency. It is not a sufficient statistic for the priors since it is a weighted average rather than a true average.

That an unweighted average of $|z_{kn}|^2$ terms is a sufficient statistic for a finite length sample \underline{z}_k may be determined by an application of the Neyman-Fisher factorization theorem.² The factorization theorem is a necessary and sufficient condition for the sufficiency of a statistic. The essence of the criterion is that the joint density of the data \underline{z} be factorable into two nonnegative functions, one of which does not depend on the unknown parameter, and the other which may involve the unknown parameter, but which depends on \underline{z} only through the sufficient statistic. The priors \underline{z} are distributed according to a joint complex normal distribution

$$p(\underline{z}) = \pi^{-N} |\underline{D}|^{-1} e^{-\underline{z}^T \underline{D}^{-1} \underline{z}} \quad (87)$$

where the elements of the covariance matrix \underline{D} are

$$[\underline{D}]_{ij} = E\{z_i z_j^*\} \quad (88)$$

The DFT coefficients from different sampling intervals are statistically independent if frequency band hopping is used from one observation interval to the next. They are approximately independent, depending on the signal fading rate, in a system where no hopping is used. If they are assumed to be independent and identically distributed, \underline{D} is a diagonal matrix with identical elements on the main diagonal

$$\underline{D} = d\underline{I} \quad (89)$$

and

$$p(\underline{Z}) = \prod^{-N} d^{-N} e^{-d^{-1} \sum_{n=1}^L |z_n|^2} \quad (90)$$

The statistic

$$T = \sum_{n=1}^L |z_n|^2 \quad (91)$$

is sufficient since $p(\underline{Z})$ satisfies the factorization theorem for T . It depends on the data \underline{Z} only through T . By the factorization theorem it is allowed to have two factors, one of which may depend on d but depends on \underline{Z} only through T . The other factor may depend on \underline{Z} in any way but does not depend on d . This latter factor may be taken as

$$g(\underline{Z}) = 1 \quad (92)$$

in this case.

The statistic \bar{z} is not sufficient since the weights b_n are unequal, and the factorization criterion does not hold. The reason for using unequal weights is that our confidence that the parameter d remain constant diminishes with time over the sample of priors. Thus the weighted average \bar{z} is as close as we are willing to come to a sufficient statistic.

IV. THE ADAPTIVE M-ARY FSK RECEIVER

The adaptive M-ary FSK receiver patterned after the SPLIT algorithm is discussed with emphasis on deviations from the ideal algorithm which make the receiver computationally practical. A receiver with a full dimension estimator is considered here. There is no admixture of estimates among different DFT coefficients. Data reduction techniques which further improve upon the computational efficiency of the receiver are taken up in Section 5.

ESTIMATING FILTERS

A detailed algorithm for the adaptive receiver incorporating data reduction techniques is given in Appendix F. Here is a discussion of a receiver without such data reduction with emphasis on some features that are common to receivers with and without data reduction. The receiver without data reduction has been experimentally verified to be equal or inferior in performance to those which incorporate some smoothing across DFT coefficients. The full dimensional estimation algorithm given here is significant as a step in the evolution of a practical adaptive receiver.

Figure 8 is a block diagram of the adaptive receiver which traces the flow of computations from the sample DFT coefficients

$$z_{k,m} = \sum_{n=0}^{15} (x_{n,m} + jy_{n,m}) e^{-j \frac{2\pi kn}{N}} \quad k = 0, \dots, 15 \quad (93)$$

to the receiver's decision variable $\ell_{\min}(m)$. In the double index notation (k,m) the index of frequency is k and the index of the observation interval (chip index) is m . The index of time samples within an observation

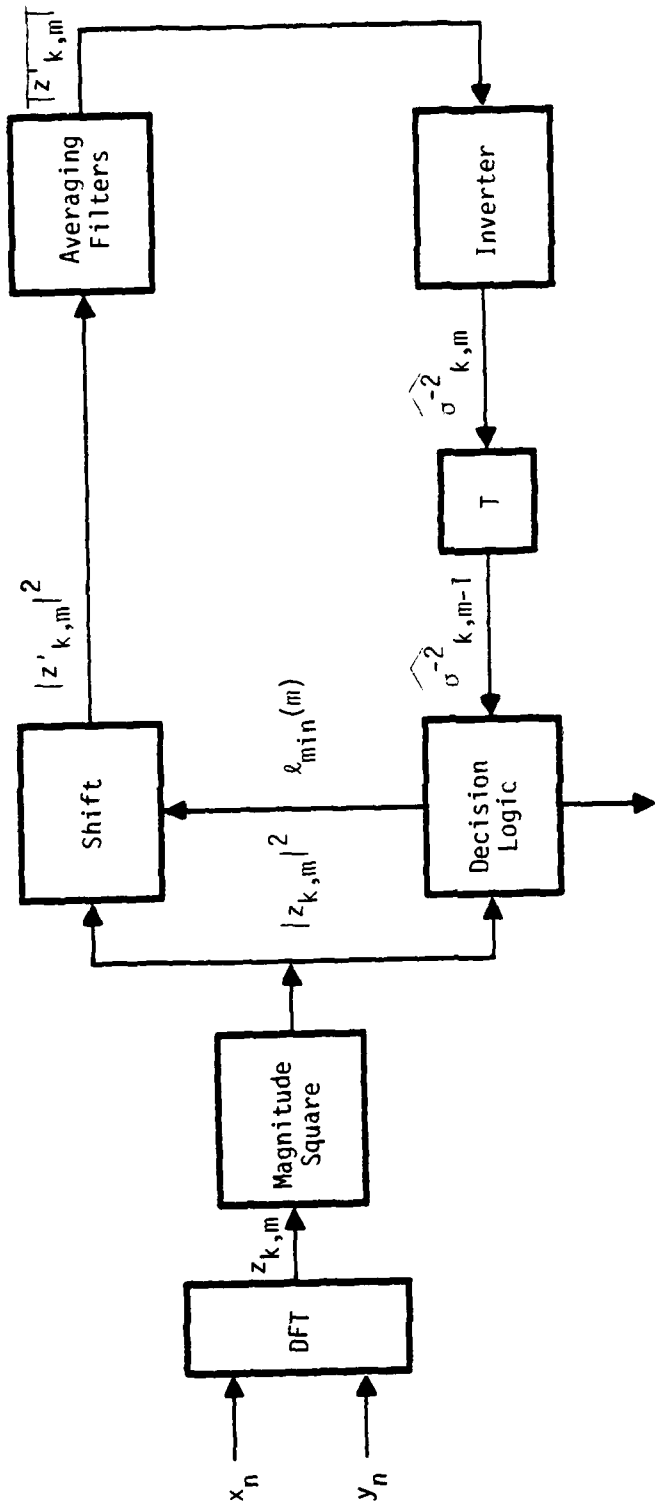


Figure 8. Block diagram of an adaptive receiver.

interval is n . The complex-valued combination of in-phase and quadrature baseband waveforms $x_{n,m} + jy_{n,m}$ are defined by Equation 45 of Section II.* A receiver with specific dimensions of $N=16$ complex samples per observation interval and $M=8$ alternative signals is used for illustration.

The first operation on the complex-valued samples $z_{k,m}$ from the m th observation interval is to convert them to magnitude-squared coefficients $|z_{k,m}|^2$. These are used in connection with the current estimate $\hat{\sigma}_{k,m-1}^{-2}$ of the inverse spectrum to determine the receiver's modulation decision by computation of M inner products

$$\rho_{\ell}(m) = \sum_{k=0}^{N-1} |z_{k,m}|^2 \hat{\sigma}_{\{k-\ell\},m-1}^{-2}, \quad \ell = \{-4, -3, \dots, 3\} \quad (94)$$

and the selection of the index of the minimum of these

$$\rho_{\ell_{\min}} \leq \rho_{\ell}(m), \quad \ell = \{-4, -3, \dots, 3\} \quad (95)$$

as the modulation decision ℓ_{\min} . The notation $\{k-\ell\}$ is a modulo addition which means that the estimates are shifted in a circular or wraparound sense to form the M different inner products. The second index is $m-1$ rather than m since the estimate must necessarily be based upon the observations leading up to but not including the current interval.

In the range of rapid signal fading for which the optimal (known statistics) receiver will operate, signal energy is effectively spread no more than three DFT coefficients from the center of the spectrum. There is a guard band of four DFT coefficients on either side of the eight possible center frequencies so that all of the signal energy is always within the baseband in the useful range of the receiver. This circumstance allows the use of circular shifts of the estimated inverse spectrum $\hat{\sigma}_{k,m-1}^{-2}$ since only the flat inverse noise level is wrapped from one end of the baseband to the other by that operation. Theoretically a 23 element estimate of the spectrum would be required, 16 elements for the signal and noise

* An impulse sampler is assumed.

spectrum at an extreme deviation frequency and 7 additional elements for spectral points shifted into the baseband as the center of the spectrum occupies the seven remaining locations. Since the additional elements required are estimates of noise levels only, these are conveniently taken from the opposite end of the spectrum by the circular shift operation.

The same circumstances allow the estimates of the signal spectrum to be based upon spectra centered by a circular shift operation. Using the modulation decision at the m th observation interval, the samples $|z_{k,m}|^2$ are realigned by the operation

$$|z'_{k,m}|^2 = |z_{\{k+\ell_{\min}\},m}|^2 \quad (96)$$

When the modulation decision is correct, the center of the signal spectrum is shifted to the first entry of the realigned set $|z'_{0,m}|^2$. The next higher frequency is shifted to the $k=1$ location and the next lower frequency to the $k=15$ location, etc. A fraction of the raw samples are incorrectly aligned when modulation level errors occur. These errors have proven to be inconsequential to the receiver performance.

At this stage, the algorithms incorporating data reduction differ with that currently being described. The aligned samples are subjected to a data reduction operation before insertion into averaging filters. For the full dimensional estimate at hand, each of the sixteen DFT coefficients is input to a single-pole recursive filter:

$$\overline{|z_{k,m}|^2} = K \overline{|z_{k,m-1}|^2} + (1-K) |z_{k,m}|^2 \quad (97)$$

where $K < 1$ is the pole location of the filter. The average coefficients $\overline{|z_{k,m}|^2}$ are inverted to form the estimate of the inverse spectrum

$$\hat{\sigma}_{k,m}^{-2} = \left[\overline{|z_{k,m}|^2} \right]^{-1} \quad (98)$$

The block diagram shows a time delay T following the inversion. This is a convention which allows a computational sequence to be represented in a block diagram. The time delay is implicit in the order of computations. Since the current demodulation decision $\hat{\ell}_{\min}(m)$ is used to realign the current samples $|z_{k,m}|^2$ the estimate of the spectrum used to demodulate the m th sample is necessarily based only on prior samples up to the $m-1$ th.

V. DATA REDUCTION

Several stages of investigation have led up to this final expository section in which a useful receiver is introduced. Let us review these briefly to put the work reported here in perspective.

The objective of all of this research is to achieve a practical receiver with near optimal performance for rapid signal fading conditions. The first object of study was the optimal receiver for demodulating an M-ary FSK signal in rapid signal fading and additive white noise. Although it cannot be practically implemented due to the incorporation of a priori knowledge of the received signal and noise spectrum, the performance of the optimal receiver, in terms of probability of misclassification error, is useful as a benchmark for the evaluation of practical adaptive receivers. The optimal performance, along with the conventional M-ary FSK receiver's performance (in rapid signal fading), provide a band of acceptable performance for the proposed receiver. Candidate adaptive receivers should significantly outperform the conventional receiver, or the simpler conventional algorithm would be preferred. On the other extreme, the proposed adaptive receiver will necessarily not perform as well as the optimal receiver but should fall near the optimal extreme of the acceptable band of performance. These two bounds are used for evaluating adaptive receiver performance in Section VI where experimental results are discussed.

As an offshoot of the optimal receiver algorithm, a more efficient suboptimal algorithm was discussed. The so called SPLOT algorithm eliminates the need for certain matrix inversions of the optimal receiver by using the

approximation that off-diagonal terms of the L_i matrix may be set to zero without noticeable effect on the receiver performance. This result has been experimentally established for the channel conditions of interest and is documented in Section VI. The SPLOT receiver is also not a practical receiver. It incorporates a priori information about the received signal and noise random processes in the same way as the optimal algorithm.

One candidate technique for an adaptive receiver was introduced in Section IV. That receiver substitutes a spectral estimate for the a priori known spectrum of the SPLOT receiver. The spectral estimate is formed by averaging the spectra over prior observation intervals with the use of single pole recursive filters. It is implemented with a decision feedback technique. The current modulation decision is used to determine which sample is averaged with the center of the spectrum, next higher and lower frequency, etc. Results in Section VI show that it performs near optimally with an averaging time constant of about 40 prior observation intervals. Some drawbacks of this first cut adaptive receiver are explained here and two improved receivers are introduced which use a reduced dimensional representation of the received spectrum.

REPARAMETERIZATION OF THE SPECTRAL ESTIMATE

The spectral estimate incorporated in the first proposed adaptive receiver (which is referred to here as a 16-parameter estimate since the dimension of the raw spectral estimate is 16 in our simulations), is cumbersome from a computational point of view. Sixteen independent estimates are formed in the receiver, and each of these requires its own storage register and associated arithmetic operations. A means of reducing this computational load while not further degrading the receiver performance is discussed here. A reduced dimensional parametric spectral representation is used, where the parameters of the representation are estimated rather than the raw spectral density itself. Depending on the signal-to-noise ratio,

experimental results have shown either an improved receiver performance or an identical performance for parametric spectral estimates of four or five dimensions versus the original 16-dimensional estimate.

Only two parameters enter the description of the received random process which is input to the simulations of receivers evaluated in Section VI. Thus, a reduction to two dimensions is the best that can be expected from reparameterization. One of these parameters describes the fading rate of the process and the other gives the signal-to-noise ratio. Although these two parameters are certainly the most efficient representation of the spectrum in terms of dimension, since they come from physically independent sources, they are not useful for the parametric spectral estimate. One of the two enters the functional description of the spectrum in a nonlinear manner. To analyze the data in terms of these parameters requires the solution of nonlinear equations (an iterative solution) which is impractical in a real-time receiver.

The original motivation to reduce the dimension of the spectral estimate was not just to improve computational efficiency but to obtain improved receiver performance from a more accurate spectral estimate. The raw spectra are made up of essentially independent random variables, and by averaging over these independent samples one expects to reduce the variability of the estimate. It is shown in this section that an improvement in receiver performance with reduced dimensional estimates versus the 16-parameter estimate is not guaranteed on an analytical basis. However, experimental results reported in Section VI show a slight improvement due to parametric spectral estimation at lower signal-to-noise ratios.

Computational savings are brought about with parametric spectral estimation when the numerical conversion from raw spectra to the reduced dimensional representation is efficient, and when the conversion can precede averaging over prior observation intervals. If the parameter conversion

is a linear operation it may be exchanged in order with the average over priors. In addition, if the data reduction process is a projection operator, it can be accomplished efficiently. The investigation of data reduction algorithms is therefore confined to linear projection operators in the following discussion.

Parametric spectral estimation implies that the spectrum will be represented in a functional form with variable parameters. The parameters of the spectrum become the object of estimation rather than the spectral density itself over frequency. If the functional form is linear in the parameters, that is if the spectral estimate is expressed as

$$\hat{\underline{\sigma}}^2 = \sum_{i=1}^P \hat{c}_i \underline{x}_i \quad (99)$$

where the set of \hat{c}_i are the estimated parameters and \underline{x}_i are a set of standard functions, the parameterization is linear. For a computationally efficient analysis, the vectors \underline{x}_i , $i=1, \dots, P$ should form an orthonormal set. When the \underline{x}_i are orthonormal, the coefficients \hat{c}_i may be computed from the raw estimate, designated $\hat{\underline{\sigma}}_s^2$, by forming P inner products

$$\hat{c}_i = \underline{x}_i^T \hat{\underline{\sigma}}_s^2, \quad i = 1, \dots, P \quad (100)$$

and then computing the estimate by Equation 99.

The composite operation of computing the \hat{c}_i 's and reconstructing a spectrum $\hat{\underline{\sigma}}^2$ is

$$\hat{\underline{\sigma}}^2 = \sum_{i=1}^P \underline{x}_i \underline{x}_i^T \hat{\underline{\sigma}}_s^2 \quad (101)$$

which may be expressed in vector-matrix notation as

$$\widehat{\underline{\sigma}}^2 = \underline{K} \widehat{\underline{\sigma}}_s^2 \quad (102)$$

where

$$\underline{K} = \sum_{i=1}^P \underline{x}_i \underline{x}_i^T \quad (103)$$

By construction, \underline{K} is a linear projection operator. The term projection derives from the fact that \underline{K} projects any N-vector into the subspace spanned by the set of \underline{x}_i . Our next concern is with the design of an appropriate set of \underline{x}_i vectors to use for data reduction.

The approach followed here to the design of this orthonormal set is necessarily less than ideal since the sensitivity function of the receiver performance to errors in the spectral estimate is an intractable integral (see Equation 43). The receiver performance is only available through a Monte Carlo integration over an N-dimensional space requiring several hundred trials per integral. To design an optimal orthonormal set of \underline{x}_i 's would require the evaluation of the second cross partial derivatives of the receiver performance as a function of deviations in the spectral estimate about the true spectrum. The number of computations involved to obtain these sensitivities to a useful degree of accuracy would be astronomical by a Monte Carlo procedure.

In lieu of obtaining an optimal solution, the analysis is carried out formally as if the sensitivity function were available and a deviation is made from the ideal approach which leads to suboptimal solutions that do not involve the unavailable sensitivity functions. In the course of the formal analysis it is found that the performance cost can be broken down into two components: one is due to the covariance of the estimate and the other is due to bias error in the reparameterization. An orthonormal set of \underline{x}_i are determined that are guaranteed to result in almost zero bias

error, with a considerably reduced dimension, and which are not a function of the unknown sensitivity. However, the resulting projection operator \underline{K} is not necessarily optimal in terms of the total covariance and modeling (bias) error. The practical advantage of this suboptimal solution is demonstrated experimentally in Section VI.

OPTIMIZATION CRITERION

The probability of error in the receiver as a function of the actual statistics and the incorrectly estimated statistics of the received random process is used as a cost function in a straightforward optimization. The problem is stated formally even though the optimal \underline{K} cannot be determined since the practical methods of data reduction are derived as an offshoot of the ideal approach. The following development flows from the definition of cost in terms of misclassification of samples using a particular spectral estimate, to the derivation of an approximate average cost or risk over an ensemble of spectral estimates. A Taylor series expansion of the cost function about the actual statistics is used in developing the risk, and terms of greater than third order are neglected.

In Section II an expression for the probability of error in terms of an arbitrary receiver matrix $\tilde{\Gamma}$ and the optimal receiver matrix $\underline{\Gamma}$ was introduced. It gives the probability of a correct decision on the i^{th} hypothesis of transmitted signal

$$\tilde{P}_{c/i} = \iint \dots \int_{\tilde{\mathcal{P}}_i} |\underline{L}_i|^{-1} |\tilde{\Gamma}|^{-1} e^{-\tilde{\Gamma}^{-1} \tilde{\Gamma} \tilde{q}_i} d\tilde{q}_1 d\tilde{q}_2 \dots d\tilde{q}_N \quad (104)$$

The reader is referred to Section II for the definitions of the various symbols in Equation 104. It suffices here to note that the expression relates both the $\underline{\Gamma}$ and $\tilde{\Gamma}$ matrices to the receiver performance.

Analysis upon this expression is only carried out formally since it is an intractable integral.

The average error over M hypotheses is

$$\tilde{P}_c(\underline{\Gamma}, \tilde{\underline{\Gamma}}) = \frac{1}{M} \sum_{i=1}^M \tilde{P}_{c/i}(\underline{\Gamma}, \tilde{\underline{\Gamma}}) \quad (105)$$

A loss function may be defined as the difference in the probability of a correct decision when using $\tilde{\underline{\Gamma}}$ versus $\underline{\Gamma}$ in the receiver

$$\mathcal{L}(\underline{\Gamma}, \tilde{\underline{\Gamma}}) = \tilde{P}_c(\underline{\Gamma}, \underline{\Gamma}) - \tilde{P}_c(\underline{\Gamma}, \tilde{\underline{\Gamma}}) \quad (106)$$

and the risk function is the expected value of the loss over the ensemble of random estimates $\tilde{\underline{\Gamma}} = \hat{\underline{\Gamma}}$.

$$\mathcal{R}(\underline{\Gamma}, \underline{K}) = E\{\mathcal{L}(\underline{\Gamma}, \hat{\underline{\Gamma}}(\underline{K}))\} \quad (107)$$

The risk function is dependent on the way that the estimate is formed. Here the risk is symbolically given as a function of \underline{K} the projection operator used, where $\hat{\underline{\Gamma}}(\underline{K})$ is the random estimate derived through a given projection \underline{K} .

The loss function $\mathcal{L}(\underline{\Gamma}, \tilde{\underline{\Gamma}})$ is expanded in a Taylor series about $\tilde{\underline{\Gamma}} = \underline{\Gamma}$ reflecting an interest in the behavior of the receiver only in the neighborhood of the optimal point $\underline{\Gamma}$. The elements of $\underline{\Gamma}$ and $\tilde{\underline{\Gamma}}$ are inverse spectra but, in the interests of linearity, the spectral estimates will be made on noninverted spectra and the resulting estimates will be inverted for use in the receiver. The partial derivatives are, accordingly,

taken with respect to the inverses of elements of $\underline{\Gamma}$ (noninverted spectral points). Expanding the loss function:

$$\begin{aligned}
 \mathcal{L}(\underline{\Gamma}, \tilde{\underline{\Gamma}}) &= \tilde{\mathcal{P}}_c(\underline{\Gamma}, \underline{\Gamma}) - \tilde{\mathcal{P}}_c(\underline{\Gamma}, \tilde{\underline{\Gamma}}) \\
 &= - \sum_{i,j} \frac{\partial \tilde{\mathcal{P}}_c}{\partial \Gamma_{i,j}^{-1}} \bigg|_{\tilde{\underline{\Gamma}} = \underline{\Gamma}} (\tilde{\Gamma}_{i,j}^{-1} - \Gamma_{i,j}^{-1}) \\
 &\quad - \sum_{i,j} \sum_{k,\ell} \frac{\partial^2 \tilde{\mathcal{P}}_c}{\partial \Gamma_{i,j}^{-1} \partial \Gamma_{k,\ell}^{-1}} \bigg|_{\tilde{\underline{\Gamma}} = \underline{\Gamma}} (\tilde{\Gamma}_{i,j}^{-1} - \Gamma_{i,j}^{-1}) (\tilde{\Gamma}_{k,\ell}^{-1} - \Gamma_{k,\ell}^{-1}) \\
 &\quad - \dots
 \end{aligned} \tag{108}$$

Since $\tilde{\underline{\Gamma}} = \underline{\Gamma}$ is optimal, the first partial terms must go to zero. Terms of third and higher order are neglected. Then the risk function is approximately equal to the expectation of the second order term with $\tilde{\underline{\Gamma}}$ replaced by $\hat{\underline{\Gamma}}$.

$$\mathcal{R}(\underline{\Gamma}, \underline{K}) \cong - \sum_{i,j} \sum_{k,\ell} \frac{\partial^2 \tilde{\mathcal{P}}_c}{\partial \Gamma_{i,j}^{-1} \partial \Gamma_{k,\ell}^{-1}} \bigg|_{\tilde{\underline{\Gamma}} = \underline{\Gamma}} E\{(\hat{\Gamma}_{i,j}^{-1} - \Gamma_{i,j}^{-1})(\hat{\Gamma}_{k,\ell}^{-1} - \Gamma_{k,\ell}^{-1})\} \tag{109}$$

With this approximation the risk is formulated as the sum of covariance terms for the estimate $\hat{\underline{\Gamma}}$ weighted by coefficients from the second partial derivative of the channel performance function $\tilde{\mathcal{P}}_c(\underline{\Gamma}, \tilde{\underline{\Gamma}})$.

There are some practical considerations related to the particulars of sample rate, number of transmitted frequencies, tone separation, and consequent degree of frequency dispersion over which the receiver can be expected to operate, which allow the spectral estimate to be made on an N-dimensional spectrum where N is the number of samples per observation interval. This is not necessarily true in general. There are, in our

simulations, $N = 16$ spectral points in each sample spectrum, but modulation of the center of the spectrum over $M = 8$ locations brings the total number of spectral points that the receiver must estimate up to 23. Only ten of these spectral points are always available to sample, the others are sometimes modulated outside the skirts of the baseband filter. It happens that the signal portion of the received spectrum is always within these ten points if the fading rate is less than the cutoff rate for the optimal receiver. These circumstances allow the receiver's internal estimate of the spectrum to be conveniently made on an $N = 16$ dimensional basis with the $M = 8$ alternative spectra generated by rotational shifts of one spectral estimate. (There is no problem of wrap-around of the signal portion of the spectrum with these dimensions. Only the flat noise portion of the spectrum is wrapped around by the rotational shift.)

In terms of the $\underline{\Gamma}$ matrix these 16 points may be considered to come from either of its two centermost rows. It is convenient to use a vector notation for the spectrum with

$$\Gamma_{\frac{N}{2} \pm 1, j}^{-1} = \sigma_j^2 \quad j = 0, 1, \dots, N-1 \quad (110)$$

and

$$\underline{\sigma}^2 \triangleq [\sigma_1^2 \sigma_2^2 \dots \sigma_N^2] \quad (111)$$

then the risk may be expressed as the trace of the product of two $N \times N$ matrices

$$\mathcal{R}(\underline{\sigma}^2, \underline{K}) = \text{tr}\{\underline{C}_{\underline{\sigma}} \underline{M}\} \quad (112)$$

where

$$[\underline{C}_{\underline{\sigma}}]_{ij} = - \frac{\partial^2 \tilde{P}_c}{\partial \tilde{\sigma}_i^2 \partial \tilde{\sigma}_j^2} \bigg|_{\tilde{\sigma}_i^2 = \sigma_i^2} \quad \begin{array}{l} i = 1, \dots, N \\ j = 1, \dots, N \end{array} \quad (113)$$

and

$$[M]_{ij} = E\{(\hat{\sigma}_i^2 - \sigma_i^2)(\hat{\sigma}_j^2 - \sigma_j^2)\} \quad \begin{matrix} i = 1, \dots, N \\ j = 1, \dots, N \end{matrix} \quad (114)$$

or, in vector notation

$$\underline{M} = E\{(\underline{\hat{\sigma}}^2 - \underline{\sigma}^2)(\underline{\hat{\sigma}}^2 - \underline{\sigma}^2)^T\}$$

where $\underline{\sigma}^2$ is the true spectrum and $\underline{\hat{\sigma}}^2$ is the spectral estimate used in the receiver. The full dimensional estimate ($K=I$) will be designated $\hat{\sigma}_s^2$ to distinguish it from reduced dimensional estimate $\hat{\sigma}^2$. $\hat{\sigma}_s^2$ results from a point-by-point single pole recursive average over prior spectra and is (to within a negligible adjustment factor) an unbiased estimate. The reduced dimensional estimates generally will introduce some bias. Notationally,

$$E(\hat{\sigma}_s^2) = \underline{\sigma}^2 \quad (115)$$

$$E(\hat{\sigma}^2) = \underline{\hat{\sigma}}^2 \quad (116)$$

$$\neq \underline{\sigma}^2$$

With these practical considerations introduced and various notations established, we proceed with the analysis.

PROJECTION OPERATOR

In a practical receiver it will be necessary to reduce the dimension of the spectral estimate (from $N=16$ in our simulations) to a much smaller number, say three to five parameters, in the interest of computational efficiency. An improved performance may also be achieved but it is not the primary objective of data reduction. A linear projection operator represented by the $N \times N$ matrix \underline{K} , such that

$$\underline{K} = \underline{X}\underline{X}^T \quad (117)$$

where \underline{X} is a $P \times N$ matrix with $P < N$, will serve this purpose. The columns of \underline{X} are orthonormal and act as a type of linear transform with only P transform coefficients computed. The projection equation is

$$\widehat{\underline{\sigma}}^2 = \underline{K} \widehat{\underline{\sigma}}_s^2 \quad (118)$$

where $\widehat{\underline{\sigma}}_s^2$ is the raw spectral estimate and $\widehat{\underline{\sigma}}^2$ is the reduced dimensional estimate.

Using the projection operator the matrix \underline{M} can be expressed in terms of the statistics of the raw spectral estimate

$$\begin{aligned} \underline{M} &= E\{(\widehat{\underline{\sigma}}^2 - \underline{\sigma}^2)(\widehat{\underline{\sigma}}^2 - \underline{\sigma}^2)^T\} \\ &= E\{(\underline{K} \widehat{\underline{\sigma}}_s^2 - \underline{\sigma}^2)(\underline{K} \widehat{\underline{\sigma}}_s^2 - \underline{\sigma}^2)^T\} \\ &= \underline{K} E\{\widehat{\underline{\sigma}}_s^2 \widehat{\underline{\sigma}}_s^2 T\} \underline{K}^T - \underline{\sigma}^2 \underline{\sigma}^{2T} \underline{K}^T - \underline{K} \underline{\sigma}^2 \underline{\sigma}^{2T} + \underline{\sigma}^2 \underline{\sigma}^{2T} \end{aligned} \quad (119)$$

The raw spectral estimate has an approximately diagonal covariance matrix

$$E\{(\widehat{\underline{\sigma}}_s^2 - \underline{\sigma}^2)(\widehat{\underline{\sigma}}_s^2 - \underline{\sigma}^2)^T\} = \underline{D} \quad , \quad \underline{D} \text{ is diagonal} \quad (120)$$

so that Equation 119 becomes

$$\underline{M} = \underline{K} \underline{D} \underline{K}^T + (\underline{K} - \underline{I}) \underline{\sigma}^2 \underline{\sigma}^{2T} (\underline{K} - \underline{I})^T \quad (121)$$

These two terms can be interpreted as covariance error and bias error. The first term is the covariance of the reduced data estimate $\widehat{\underline{\sigma}}^2$.

$$\begin{aligned} E\{(\widehat{\underline{\sigma}}^2 - E\{\widehat{\underline{\sigma}}^2\})(\widehat{\underline{\sigma}}^2 - E\{\widehat{\underline{\sigma}}^2\})^T\} &= E\{(\underline{K} \widehat{\underline{\sigma}}_s^2 - \underline{\sigma}^2)(\widehat{\underline{\sigma}}_s^2 - \underline{\sigma}^2)^T \underline{K}^T\} \\ &= \underline{K} \underline{D} \underline{K}^T \end{aligned} \quad (122)$$

and the remaining term is the contribution to the error from bias introduced in reparameterization. Note that for $\underline{K} = \underline{I}$, corresponding to no data reduction, this term goes to zero. The linearized risk can also be separated into these two terms

$$\mathcal{R}(\underline{\sigma}^2, \underline{K}) \cong \text{tr}\{\underline{C}_\sigma \underline{K} \underline{D} \underline{K}^T\} + \text{tr}\{\underline{C}_\sigma (\underline{K} - \underline{I}) \underline{\sigma}^2 \underline{\sigma}^{2T} (\underline{K} - \underline{I})\} \quad (123)$$

Note that the risk is a function of the particular fading rate and signal-to-noise ratio imbedded in $\underline{\sigma}^2$. To minimize the risk as it stands would result in a \underline{K} which is a function of the unknown statistic, a useless result. One would have to find the average risk over an ensemble of $\underline{\sigma}^2$ to obtain the optimal \underline{K} . Since \underline{C}_σ is unavailable at any $\underline{\sigma}^2$, it is not possible to carry out this optimization. However, Equation 123 is useful in delineating the two sources of degradation in receiver performance, and in showing the linear nature of the mixture to a second order approximation of the Taylor series expansion of the cost function about the actual spectrum.

As an alternative to computing the optimal \underline{K} , two approaches to derive a suboptimal \underline{K} are suggested. In each of these methods, only the modeling error term is used in the selection of \underline{K} . That is, reduced dimension estimates are found for which the spectra are very accurately represented over an ensemble of $\underline{\sigma}^2$. There is no guarantee that the reduction in the modeling term will not be compensated by increases in the covariance term, but experimental results show that the receiver performance is either improved or maintained at the same level as the $\underline{K} = \underline{I}$ case.

One of these techniques uses independent estimates of spectral points in the neighborhood of the center of the signal portion of the received spectrum. The more remote points are averaged together under the assumption that they are drawn from the same noise-only distribution. The symmetry of the spectrum about its center is also exploited by averaging

the conjugate points on each side of the center within the expected band of signal spreading. This technique does not involve any assumptions about $\underline{\sigma}^2$ other than the band-limited nature of the received signal power, symmetry about the center point, and the presence of additive white noise. It is referred to in the sequel as the band-limited-symmetric-spectrum [BLSS] data reduction algorithm.

The other technique is based upon a more analytical foundation. It makes the selection of \underline{K} through the use of a set of specific examples of $\underline{\sigma}^2$. These spectra have the particular functional forms and range of parameters over which the receiver is expected to operate. This latter technique which is called the spectral eigenvector [SEV] algorithm is developed next. Results for both methods are given in Section VI.

SPECTRAL EIGENVECTOR ALGORITHM

The BLSS algorithm is an obvious technique for accurately curve fitting the spectrum. It makes use of the most salient features of the received data, and these features are not dependent on detailed predictions of the ionospheric channel. This simple expedient is shown in Section VI to perform equally well as the $\underline{K} = \underline{I}$ case for high signal-to-noise ratio and slightly better for low ratios with a projection from sixteen to five dimensions. The success of this heuristic technique motivated further investigation of the potential of a spectral eigenvector method which involves more detailed knowledge of the received spectrum.

To this end we focus our attention on the modeling error portion of the risk

$$\mathcal{R}_m(\underline{\sigma}^2, \underline{K}) = \text{tr}\{\underline{C}_{\underline{\sigma}}(\underline{K} - \underline{I})\underline{\sigma}^2\underline{\sigma}^{2T}(\underline{K} - \underline{I})\} \quad (124)$$

A projection matrix \underline{K} is sought which is of low rank and causes $\mathcal{R}_m(\underline{\sigma}^2, \underline{K})$ to be close to zero over the predicted ensemble of $\underline{\sigma}^2$ independent of \underline{C}_σ . Then $\underline{K} - \underline{I}$ must be effectively in the null space of $\underline{\sigma}^2 \underline{\sigma}^{2T}$ over the range of $\underline{\sigma}^2$. In the following discussion it is shown that such a $\underline{K} - \underline{I}$ can be obtained by a numerical evaluation of eigenvectors and eigenvalues of the matrix

$$\underline{S} = \sum_{i=1}^J \underline{\sigma}_i^2 \underline{\sigma}_i^{2T} \quad (125)$$

which is simply a sum of dyads made up from samples of predicted $\underline{\sigma}^2$'s over the predicted operating range of the receiver. The matrix \underline{S} has been experimentally shown to have a rank of four for the conditions of interest, and that rank corresponds to the rank of \underline{K} which will drive the modeling error to zero.

These results follow from the fact that vectors in the null space of \underline{S} are necessarily also in the null space of each of the $\underline{\sigma}_i^2 \underline{\sigma}_i^{2T}$. To show this let us make the following definitions. The $N \times N$ matrix \underline{K} is symmetric since it can be written as a sum of dyads (Equation 103). If \underline{K} is of rank P it may be factored into the product

$$\underline{K} = \underline{X} \underline{X}^T \quad (126)$$

where \underline{X} is an $N \times P$ matrix. The columns of \underline{X} are the orthonormal set of \underline{x}_i referred to earlier. If the orthonormal set is augmented to a complete N -dimensional set by a set of vectors \underline{y}_i , the columns of \underline{Y} , then

$$\underline{X} \underline{X}^T + \underline{Y} \underline{Y}^T = \underline{I} \quad (127)$$

and $\underline{Y} \underline{Y}^T$ is a projection operator with a range space orthogonal to that of $\underline{X} \underline{X}^T$ and which fills out the N -dimensional space. Now the expression for the modeling error can be rewritten

$$(\underline{K} - \underline{I}) \underline{\sigma}_i^2 \underline{\sigma}_i^{2T} (\underline{K} - \underline{I})^T = \underline{Y} \underline{Y}^T \underline{\sigma}_i^2 \underline{\sigma}_i^{2T} \underline{Y} \underline{Y}^T \quad (128)$$

Consider the sum of J such terms $\underline{Y}\underline{Y}^T\underline{S}\underline{Y}\underline{Y}^T$. If the columns of \underline{Y} are in the null space of \underline{S} , the trace of this expression is zero.

$$\text{tr}\{\underline{Y}\underline{Y}^T\underline{S}\underline{Y}\underline{Y}^T\} = 0 \quad (129)$$

By the properties of the trace and the orthogonality of the columns of \underline{Y}

$$\begin{aligned} \text{tr}\{\underline{Y}\underline{Y}^T\underline{S}\underline{Y}\underline{Y}^T\} &= \text{tr}\{\underline{Y}^T\underline{S}\underline{Y}\} \\ &= \sum_{i=1}^{N-P} \underline{Y}_i^T \underline{S} \underline{Y}_i \\ &= 0 \end{aligned} \quad (130)$$

But, by expanding \underline{S} it is evident that each term is nonnegative.

$$\begin{aligned} &= \sum_{i=1}^{N-P} \sum_{j=1}^J \underline{Y}_i^T \underline{\sigma}_j^2 \underline{\sigma}_j^{2T} \underline{Y}_i \\ &= \sum_{i=1}^{N-P} \sum_{j=1}^J (\underline{Y}_i^T \underline{\sigma}_j)^2 \end{aligned} \quad (131)$$

Then each of the component terms must be zero

$$\underline{\sigma}_j^{2T} \underline{Y}_i = 0 \quad , \quad \begin{array}{l} j = 1, \dots, J \\ i = 1, \dots, N-P \end{array} \quad (132)$$

which establishes the fact that the columns of \underline{Y} are in the null space of each of the $\underline{\sigma}_j^2 \underline{\sigma}_j^{2T}$.

An expanded discussion of this data reduction technique is given in Appendix G. The relationship to principal component analysis in statistics is explored, and the case where \underline{S} is full rank is discussed.

VI. EXPERIMENTAL RESULTS

Receiver performance curves for all of the receivers under study are presented in this section. Included are the performance of the optimal receiver, the SPLOT algorithm, the conventional receiver, 16-parameter adaptive receiver, and the adaptive receivers using the BLSS and SEV data reduction techniques introduced in Section V.

CONVENTIONAL AND OPTIMAL RECEIVERS

All of the results presented here are for an uncoded 8-ary FSK system with the following parameters:

Modulation Interval	T = 5 ms
Frequency Separation	$\Delta f = 200$ Hz
Sample Rate	N/T = 3200/s
Number of Complex Samples Per T	N = 16
Baseband Width	B = 1600 Hz

The performance of a conventional 8-ary FSK receiver in rapid signal fading is given for several degrees of fading rapidity along with the corresponding optimal performance and that for the SPLOT algorithm (which are indistinguishable in all of the cases considered). Two types of functional form of the signal portion of the received random process are used. These are the Gaussian signal spectrum

$$\psi_r(f-f_c) = C_1 e^{-\left[\frac{(f+\Delta f)\tau_0}{\pi}\right]^2} \quad (133)$$

and the cubic roll-off spectrum

$$\psi_{r'}(f-f_c) = C_2 \frac{1}{[a + [(f-f_c)\tau_0]^2]^{3/2}} \quad (134)$$

$$a = \frac{2.54}{(2\pi)^2}$$

In each case, the decorrelation time τ_0 is the e^{-1} point on the autocorrelation function associated with the signal power spectral density $\psi_{r'}(f-f_c)$. The cubic roll-off spectrum is used since it is characteristic of the results obtained with multiple phase screen numerical models of a highly ionized ionosphere. The Gaussian spectrum is included primarily as an indicator of the validity of decorrelation time as a measure of the difficulty to demodulate the signal, although it also represents the ionospheric channel under some extreme conditions. Graphs of the two spectra are shown in Figures 9 and 10 to illustrate the degree of overlap expected within the useful operating range of the optimal receiver. Curves are shown for a range of decorrelation times from about twice the observation interval, where there is essentially no overlap of the spectra, to one-fifth of the observation interval where the signal spectra are spread well into the adjacent channels. Degradation in the receiver performance comes from additional errors due to the spreading of signal energy into nearby channels. Thus, the degree of overlap shown in the figures is illustrative of the difficulty in demodulating signals in a frequency dispersive channel. It is not intended, by the introduction of these curves, to embark upon a discussion of comparative performance for the two spectral shapes. Comparison of the receiver performance for the two spectra at a given decorrelation time is not justified, since decorrelation time is an arbitrary measure of dispersion for the spectrum, which does not necessarily reflect the difficulty presented to the receiver by a particular functional form. The Gaussian spectrum is somewhat more compact than the cubic roll-off spectrum at the same decorrelation time, and therefore the performance characteristics are correspondingly better; but this does not imply that a Gaussian spectrum presents less difficulty to

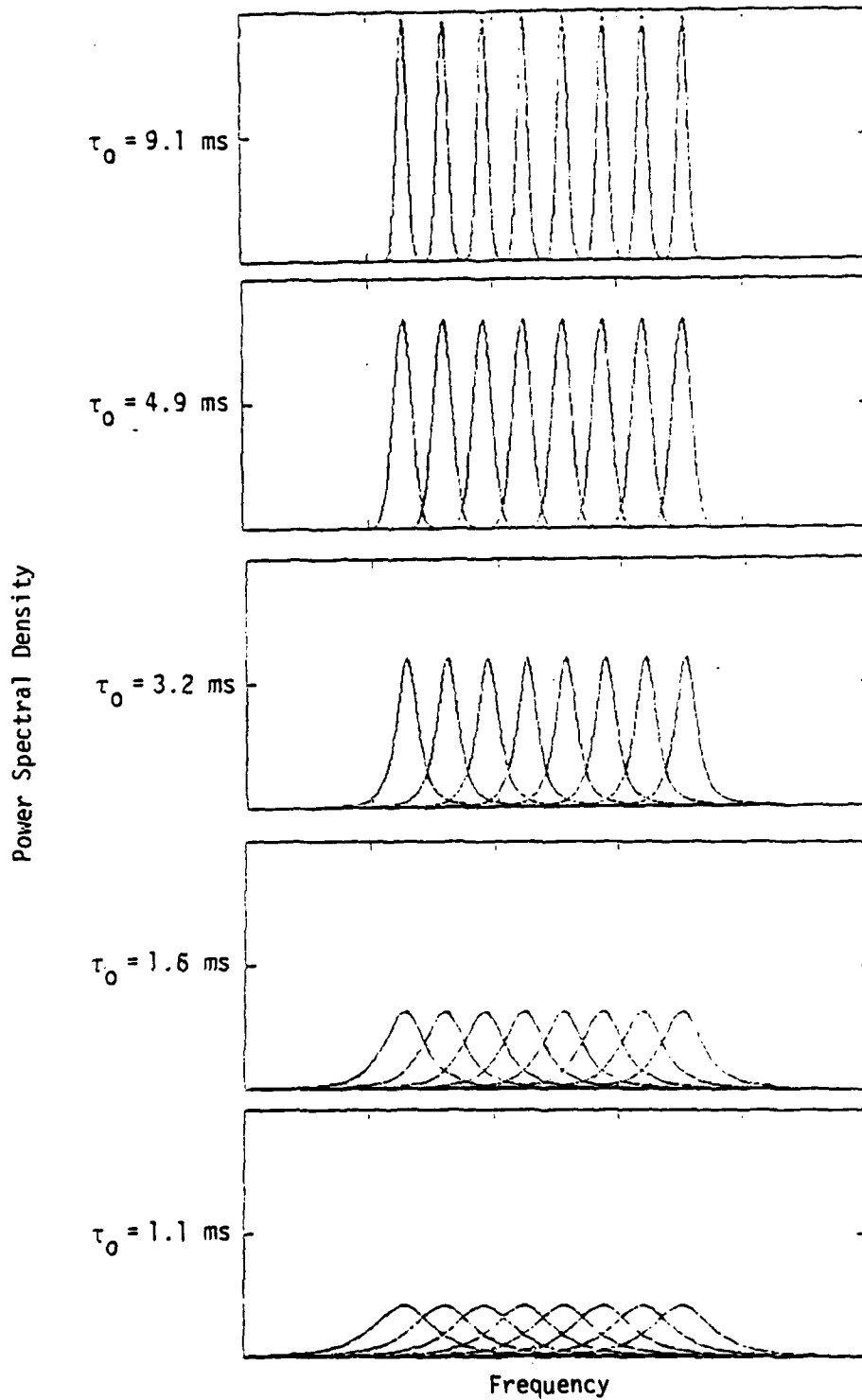


Figure 9. Gaussian signal power spectral density - various decorrelation times, normalized signal power, $\Delta f = 1/T \text{ Hz}$.

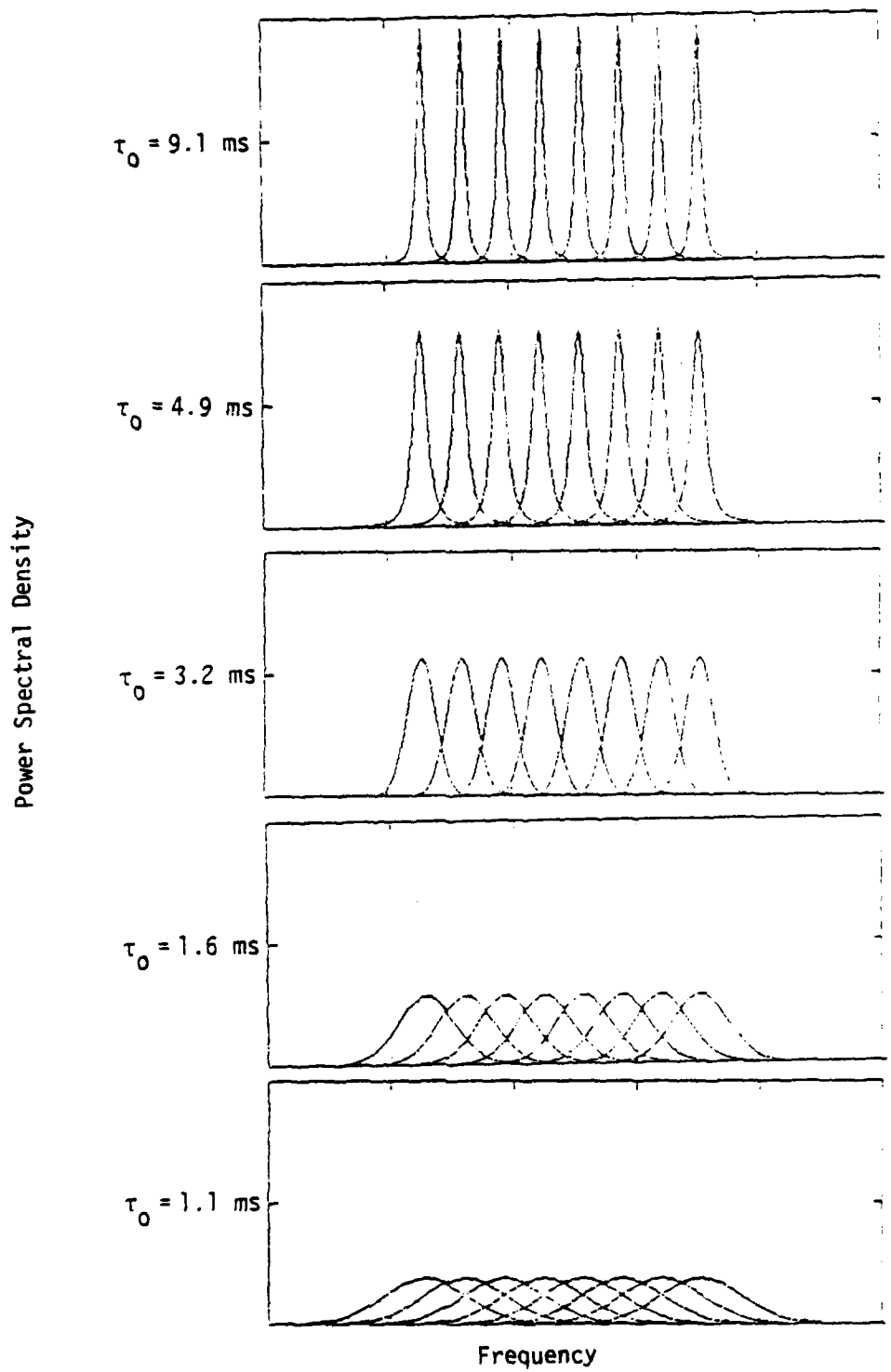


Figure 10. Cubic roll-off power spectral density - various decorrelation times, normalized signal power, $\Delta f = 1/T$ Hz.

the receiver. One should rather look at the similarity of the response curves as an indicator that decorrelation time is a useful standard measure of signal dispersion.

Figures 11 and 12 are the receiver operating characteristic curves for the conventional and optimal receivers in terms of normalized error (with 0.5 representing random performance) as a function of the mean bit energy-to-noise density. The ratio shown is 1/3 of the SNR defined by Equation 44 of Section 2 to reflect the fact that three uncoded bits are transmitted during each observation interval T .

Receiver operating characteristic curves are shown for the same five decorrelation times illustrated in Figures 9 and 10. In addition, the curve of the slow fading limit, which was determined analytically, is given as a means of comparison of rapid fading performance to the corresponding performance with independent Rayleigh fading.

The slow fading limit is derived under the assumption that the signal is constant across each observation interval with the variation from interval to interval described by a Rayleigh distribution. The signal envelopes are considered to vary independently from one observation interval to another in the slow fading derivation.

The convergence of the Monte Carlo sampling procedure, used to obtain the data points in these figures, depends upon the probability of error. To account for this more samples are used at the higher signal-to-noise ratios where the error probability is lower. For data points falling above a binary probability of error of seven percent, 800 trials were used, that is an average of 100 trials per channel with random selection of channels. To estimate lower probabilities 2400 trials were used, or an average of 300 trials per channel.

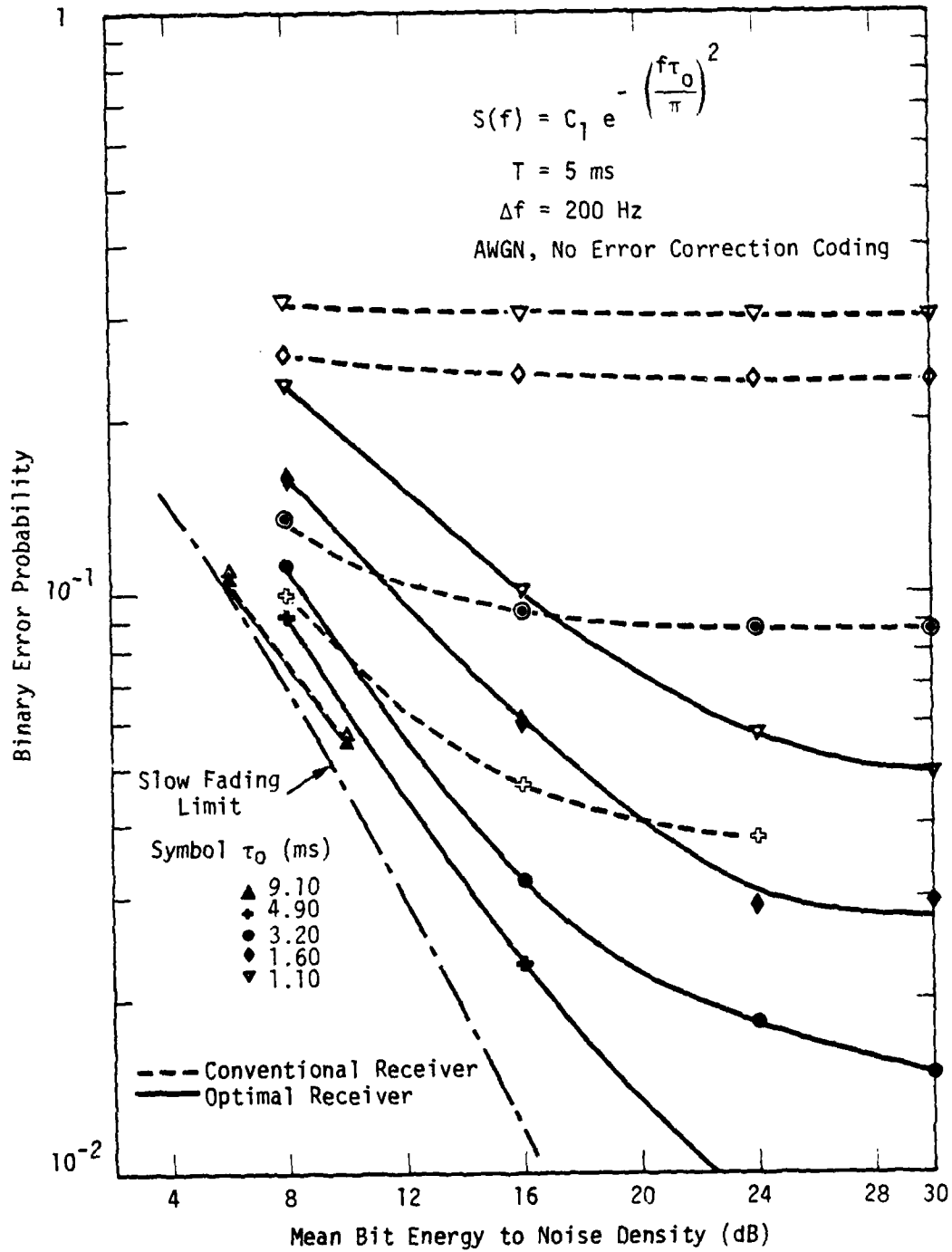


Figure 11. 8-ary frequency shift keying performance in fast Rayleigh fading channel (Gaussian signal spectrum).

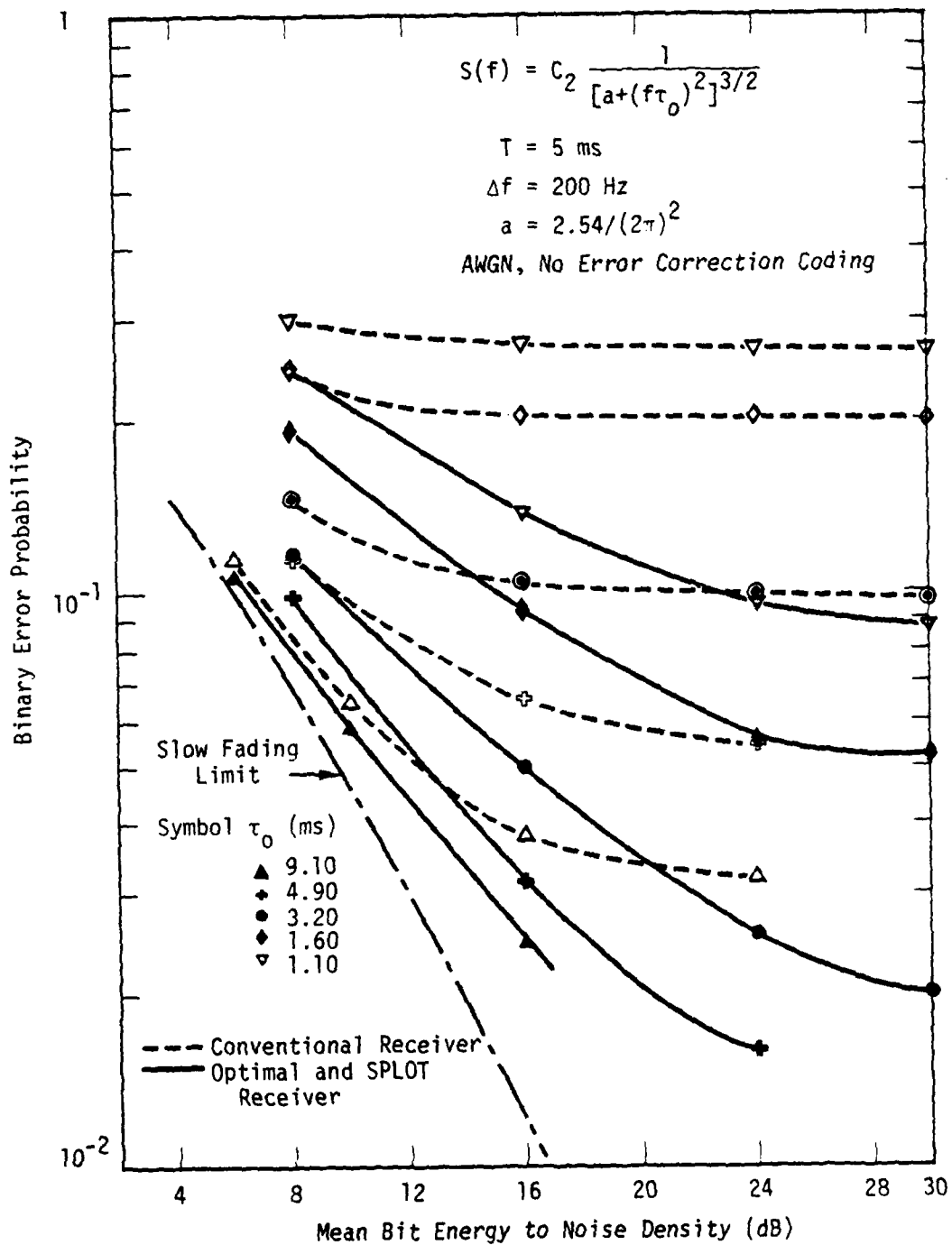


Figure 12. 8-ary frequency shift keying performance in fast Rayleigh fading channel (cubic roll-off signal spectrum).

Results show a marked improvement for the performance of the optimal receiver over the conventional receiver. At the two shorter decorrelation times $\tau_0 = 1.10$ ms and $\tau_0 = 1.60$ ms the conventional receiver makes an error in about one out of every three trials, while the optimal receiver is in error only one out of ten to twenty trials in the mid range of signal-to-noise ratio. The performance of the two receivers converges at lower signal-to-noise ratios and at longer decorrelation times.

In every case shown in these figures the SPLOT algorithm was statistically indistinguishable from the optimal performance, and is therefore not given in a separate set of curves. The significant improvement in performance of the SPLOT algorithm over the conventional receiver was the motivation to pursue the design of adaptive receivers patterned after it.

An alternative way of viewing the data which highlights the degree of operation into a rapidly fading environment is given by Figure 13.

Here the signal-to-noise ratio required to obtain a given binary probability of error is graphed as a function of τ_0 for the cubic roll-off spectrum only. At a criterion of ten percent binary errors the optimal (and SPLOT) receiver are functioning at fading rates two to three times more rapid than the conventional receiver. At three percent binary errors the cutoff fading rates are slower but the ratio remains about the same.

ADAPTIVE RECEIVERS

All of the results shown for adaptive receivers have been computed for spectral estimates using single pole recursive averaging filters and decision feedback. In Appendix F the algorithms used in these receivers are recorded and a discussion of decision feedback is given. Only the results are discussed here.

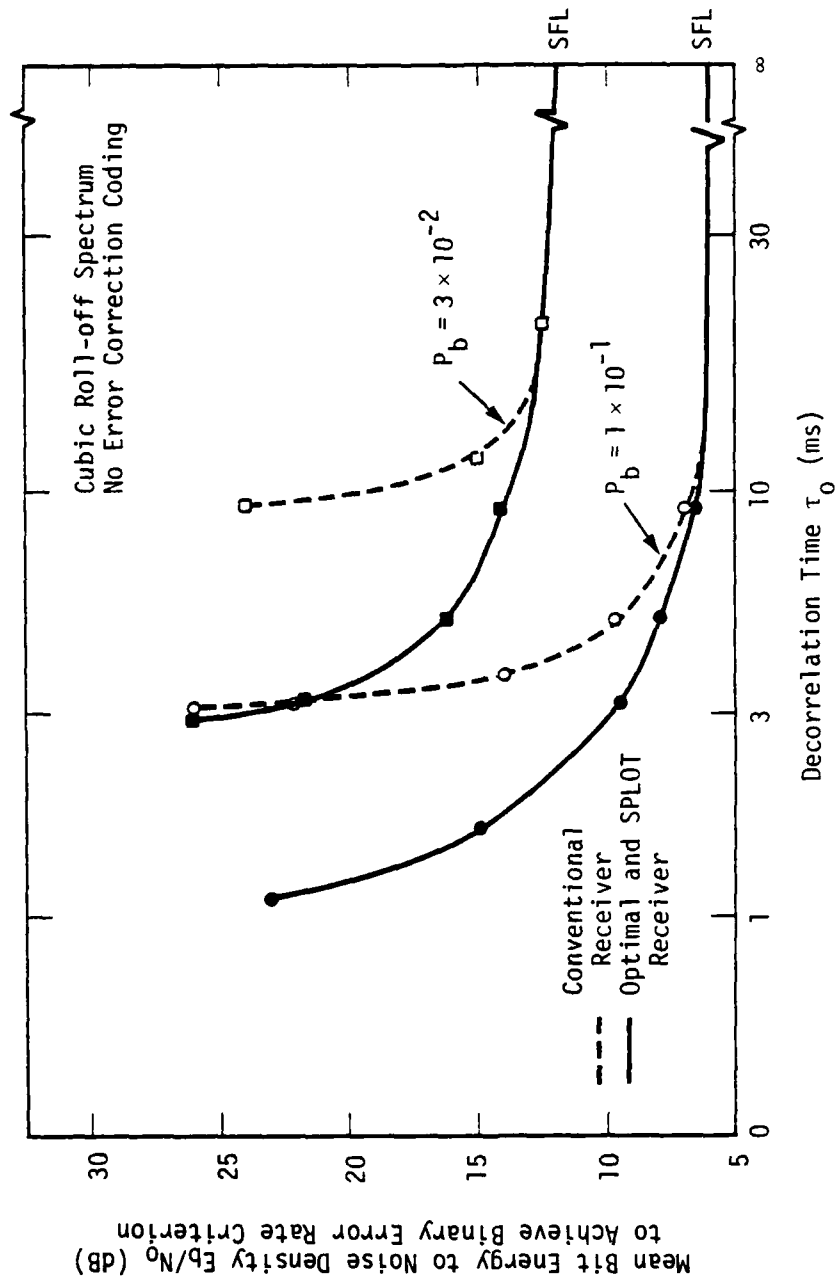


Figure 13. Signal bit energy-to-noise density required to achieve binary error rate P_b at various decorrelation times.

The first adaptive receiver to be considered is one using a full dimensional estimate—the so-called sixteen parameter adaptive receiver. Figure 14 shows the receiver operating characteristic for this receiver versus the optimal and conventional receiver at $\tau_0 = 3.20$ ms, an intermediate level of signal fading*. A time constant of 40 prior observation intervals is used in the estimator. The adaptive receiver stays within 20 percent of the optimal performance over the entire range of signal-to-noise ratio and is clearly near optimal in comparison to the conventional receiver except at the lower ratios. Results for a five-parameter BLSS algorithm operating on the same data are included. The BLSS receiver performance coincides with the sixteen parameter receiver at high signal-to-noise ratios but shows a slight improvement at lower levels. Subsequent data indicate that the coincidence at high signal levels is due to a compensation of performance degradation from modeling error and improved estimation accuracy from smoothing in the frequency dimension. It is significant that the reduced dimensional estimate maintains the performance of the raw estimate at a considerable computational savings. Improvements in the performance are slight.

Next, we consider performance of the two competing algorithms for data reduction of the spectral estimates. To put these on an equal footing, four dimensional spectral estimates are used in each case. The set of σ^2 used in computing the \underline{S} matrix for the SEV algorithm are listed in Table 1. The criterion to select these was based upon a desire to maintain the performance most carefully at higher error rates. The decorrelation times and signal-to-noise ratios are from a slice across Figure 12 at a binary probability of error of ten percent. This level of errors is considered about the greatest that may practically be handled with error correction codes for this system. The best possible fit is desired in the region of the worst tolerable case of error probability since degraded performance due to modeling error, in lower regions of the operating characteristics will presumably be well within the capabilities of the error correction code.

* Differences in conventional and optimal receiver performance curves among Figures 11 through 20 are due to statistical variation. All curves on each figure are based on the same statistical sample.

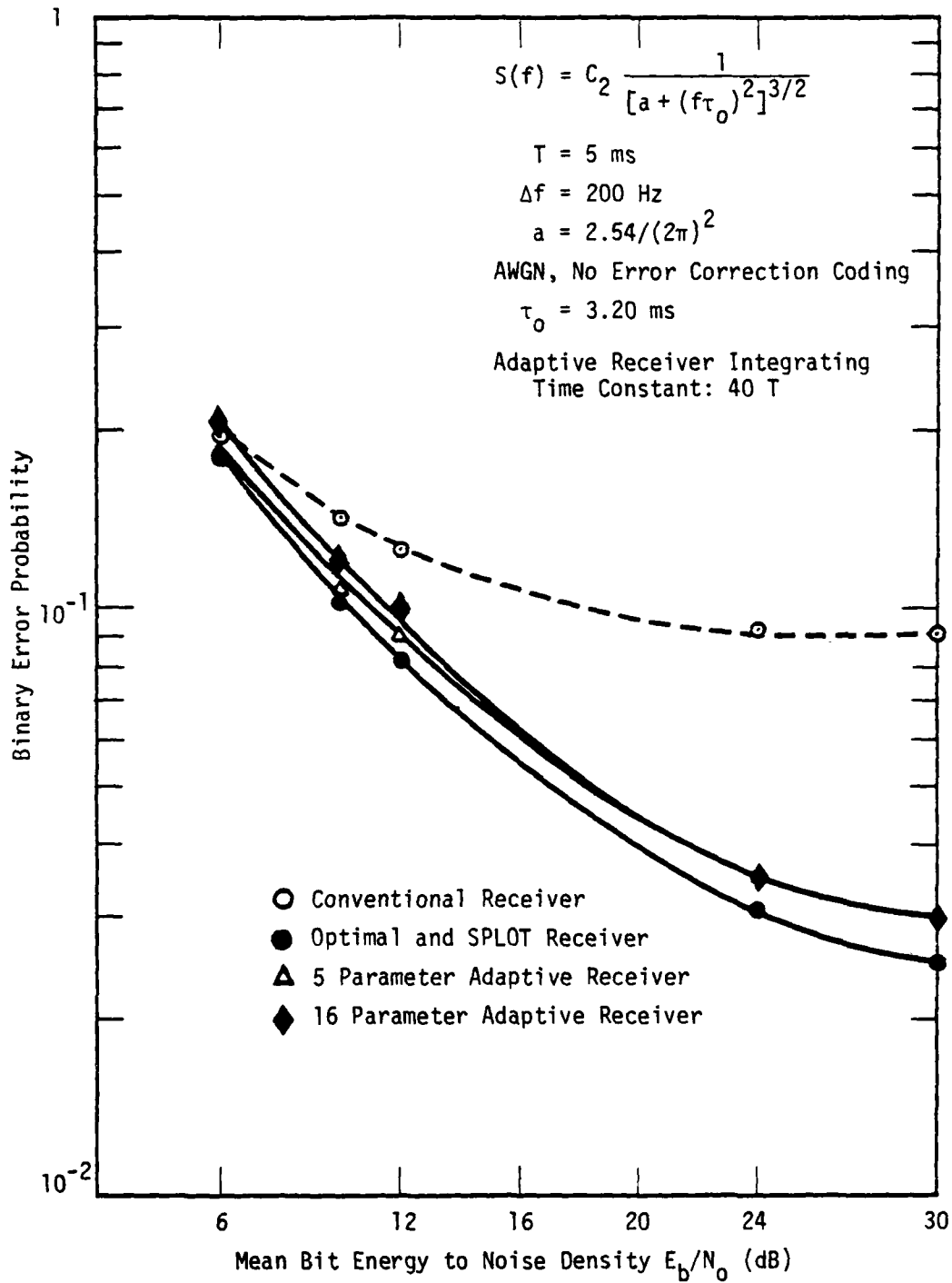


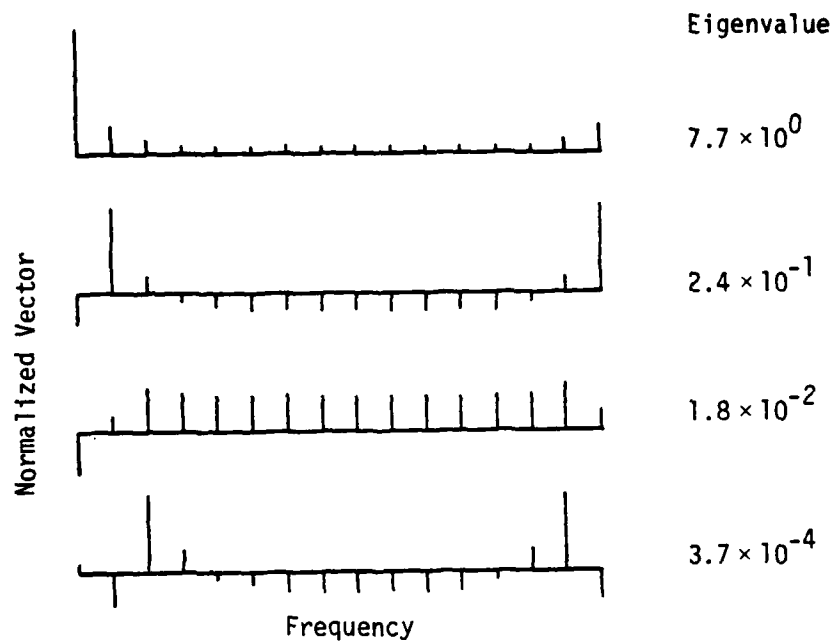
Figure 14. 8-ary FSK receiver performance. Adaptive vs. optimal and conventional receivers.

Table 1. Parameters of σ^2 used in constructing the matrix \underline{S} .

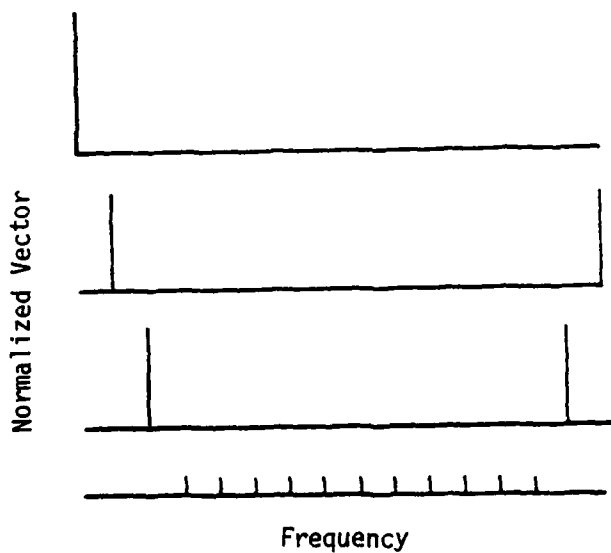
τ_o (ms)	E_b/N_o (dB)
9.1	5
7.5	6
6.0	7
4.9	8
4.0	9
3.2	10
1.6	15
1.1	23

Figure 15 shows the four eigenvectors of \underline{S} with nonzero eigenvalues arranged in the order of descending eigenvalue. For comparison, the four basic functions of a four-dimensional BLSS algorithm are also shown. Note that the SEV eigenvectors seem to mimic the BLSS vectors. One vector accentuates the center of the spectrum. Two others focus on the next to center and second from center values, and one is evidently arranged to compute the noise level. The performance associated with the two algorithms is, however, remarkably different.

Figure 16 gives the receiver operating characteristic for the four-dimensional BLSS and SEV algorithms along with the conventional and SPLOT receiver. The integrating time constant for averaging over priors is 40 observation intervals for each of the adaptive receivers. The performance of the SEV algorithm is right at the optimal level, but the BLSS receiver has about 20 percent more errors in the mid range of signal-to-noise ratio. Notice that even though the \underline{S} matrix was made up from spectra along the ten percent error line, performance of the SEV algorithm is on the optimal characteristic throughout the range of signal-to-noise ratio including much lower error probabilities.



(a) Four-parameter SEV data reduction algorithm.



(b) Four-parameter BLSS data reduction algorithm.

Figure 15. Normalized basis vectors for four-parameter SEV and BLSS data reduction algorithms.

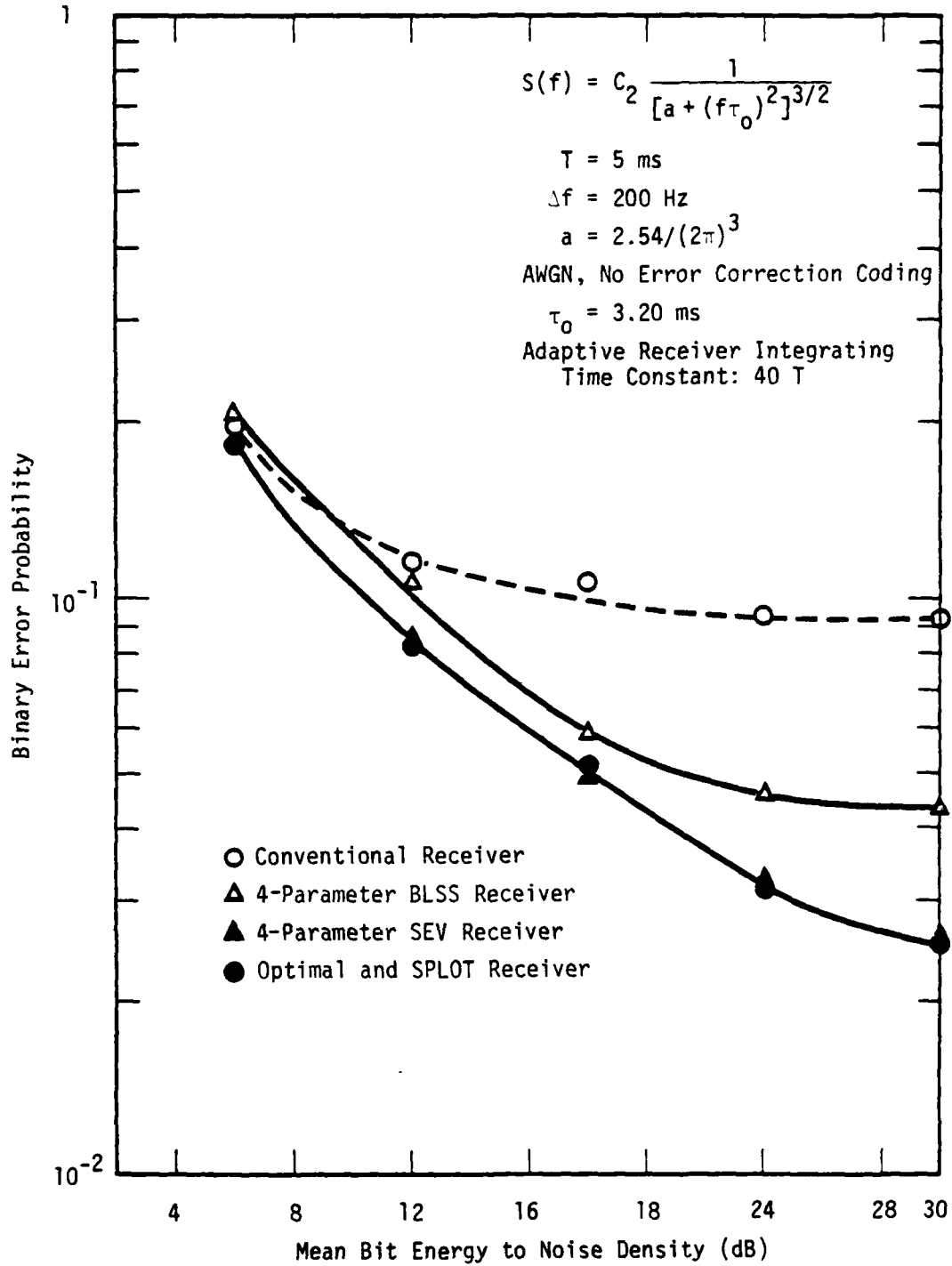


Figure 16. 8-ary frequency shift keying performance in fast Rayleigh fading channel (cubic roll-off signal spectrum). Four-parameter SEV receiver vs. four-parameter BLSS receiver at $\tau_0 = 3.2 \text{ ms}$.

With the addition of one more parameter the BLSS algorithm can be made to perform almost as well as the SEV algorithm. Figure 17 shows a comparison of a five-parameter BLSS algorithm with a four-parameter SEV algorithm under the same conditions of Figure 16. Figures 18 and 19 show that there is no problem with curve fitting at longer decorrelation times which might be suspected due to poor curve fitting there. The performance of both adaptive receivers converges, along with the SPLOT receiver, to the slow fading limit of the conventional 8-ary FSK receiver.

The integrating time constant of 40 prior observation intervals was selected arbitrarily, but it is evidently sufficient for convergence in terms of receiver performance. The excellent results obtained with the SEV algorithm, at that time constant, is ample evidence of this. To see how short an observation interval could be used, several runs were made with successively shorter intervals until the performance curve started to break upwards. Figure 20 is a graph of the BLSS performance at integrating time constants of $40 T$ and $4T$. There were only about ten percent more errors for an order of magnitude less smoothing. Without introducing any further channel disturbances such as jamming interference, it would be possible to use quite short integrating times in the spectral estimate. However, jamming considerations are likely to prohibit the use of very short prior averaging times, or otherwise to dictate the dynamics of the spectral estimator.

CONCLUSIONS

Adaptive M-ary FSK demodulation with nearly optimal performance is feasible for rapid signal fading conditions. Spectral estimates which use decision feedback and single pole averaging filters with time constants of less than 40 prior observation intervals have been demonstrated to achieve optimal or nearly optimal performance. The advantage over the conventional 8-ary FSK receiver is that the adaptive receiver can operate at a factor of two to three more rapid signal fading.

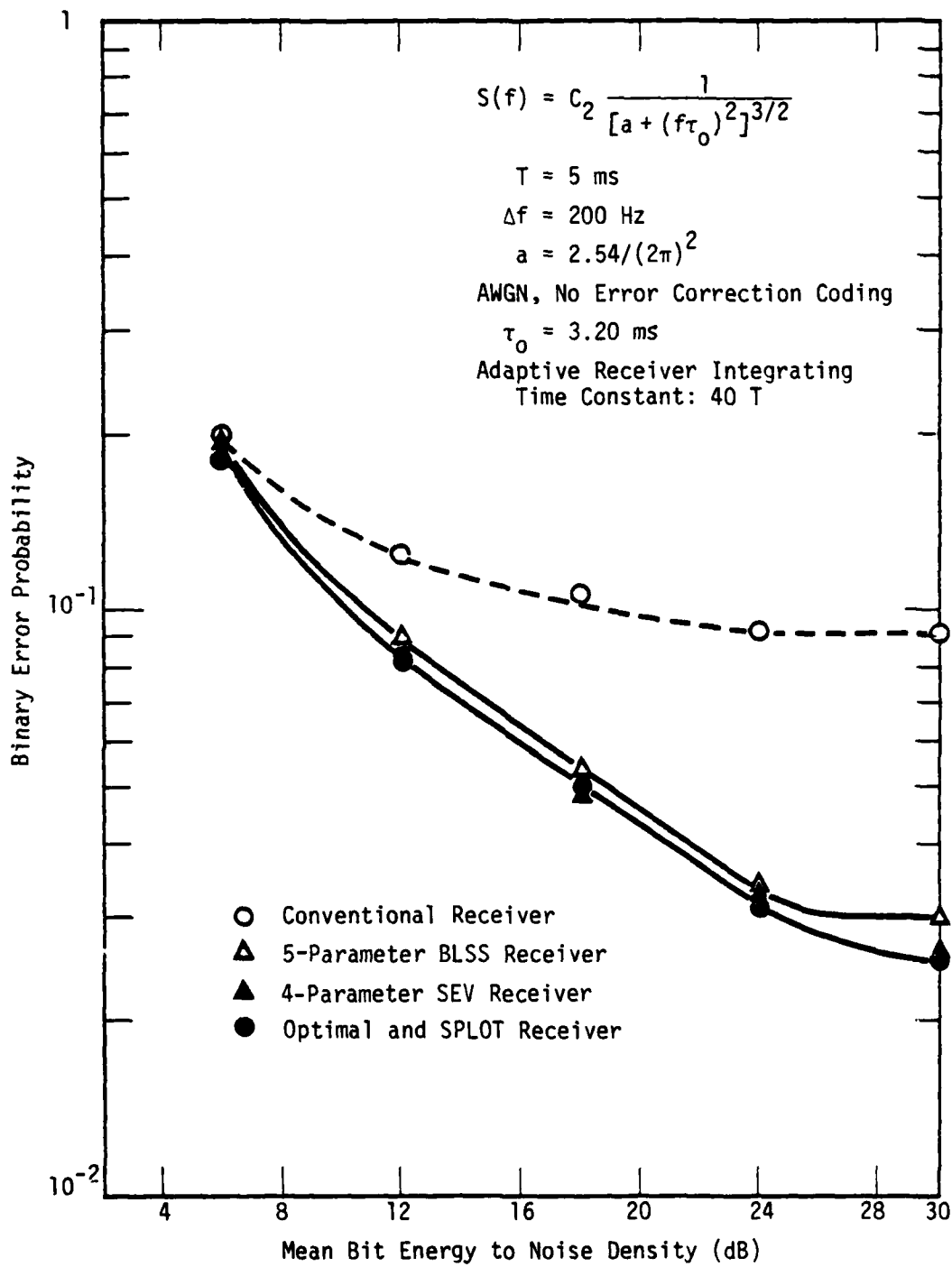


Figure 17. 8-ary frequency shift keying performance in fast Rayleigh fading channel (cubic roll-off signal spectrum). Four-parameter SEV receiver vs. five-parameter BLSS receiver at $\tau_0 = 3.2 \text{ ms}$.

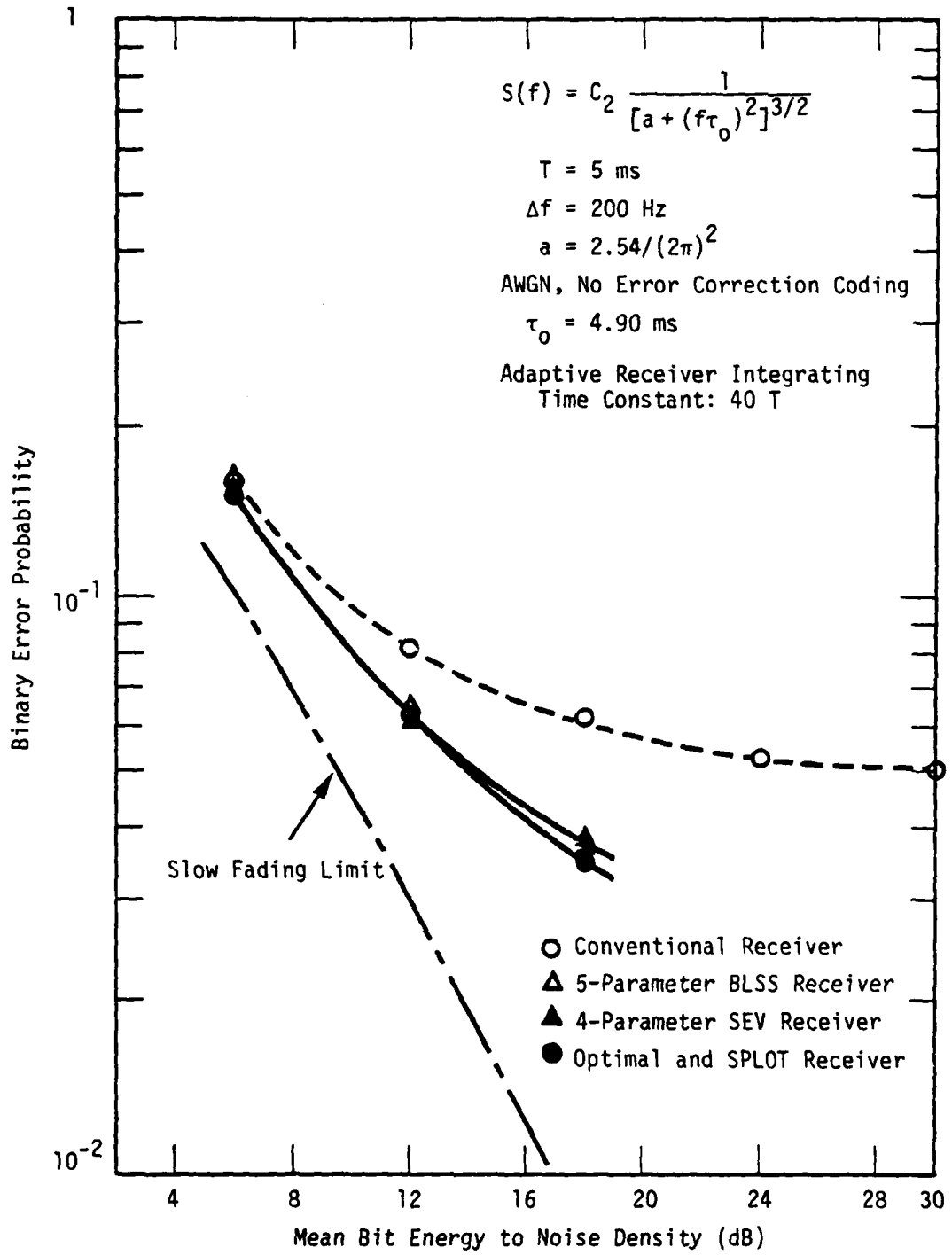


Figure 18. 8-ary FSK frequency shift keying performance in fast Raleigh fading channel (cubic roll-off signal spectrum). Four-parameter SEV receiver vs. five-parameter BLSS receiver at $\tau_0 = 4.90 \text{ ms}$.

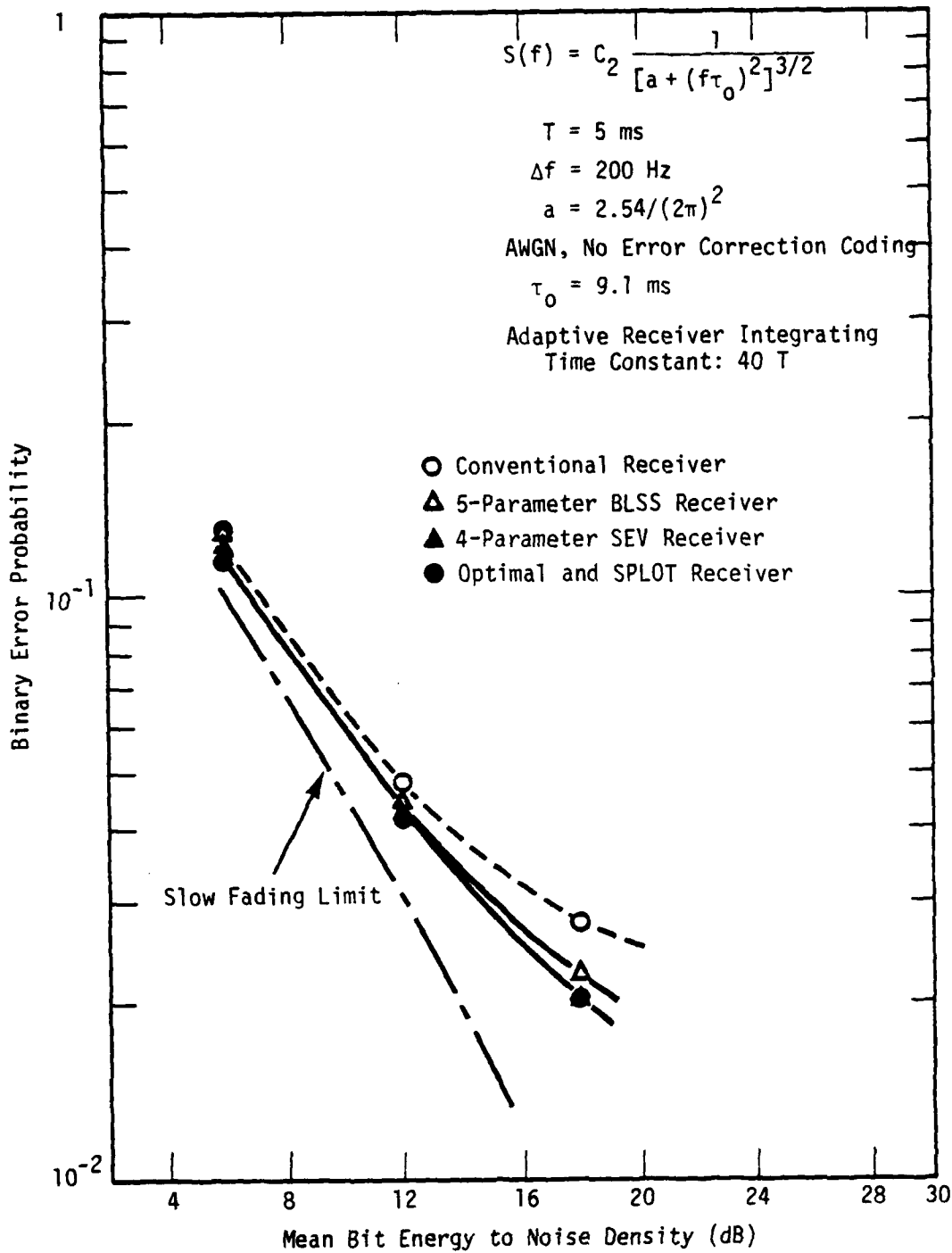


Figure 19. 8-ary FSK frequency shift keying performance in fast Rayleigh fading channel (cubic roll-off signal spectrum). Four-parameter SEV receiver vs. five-parameter BLSS receiver at $\tau_0 = 9.10 \text{ ms}$.

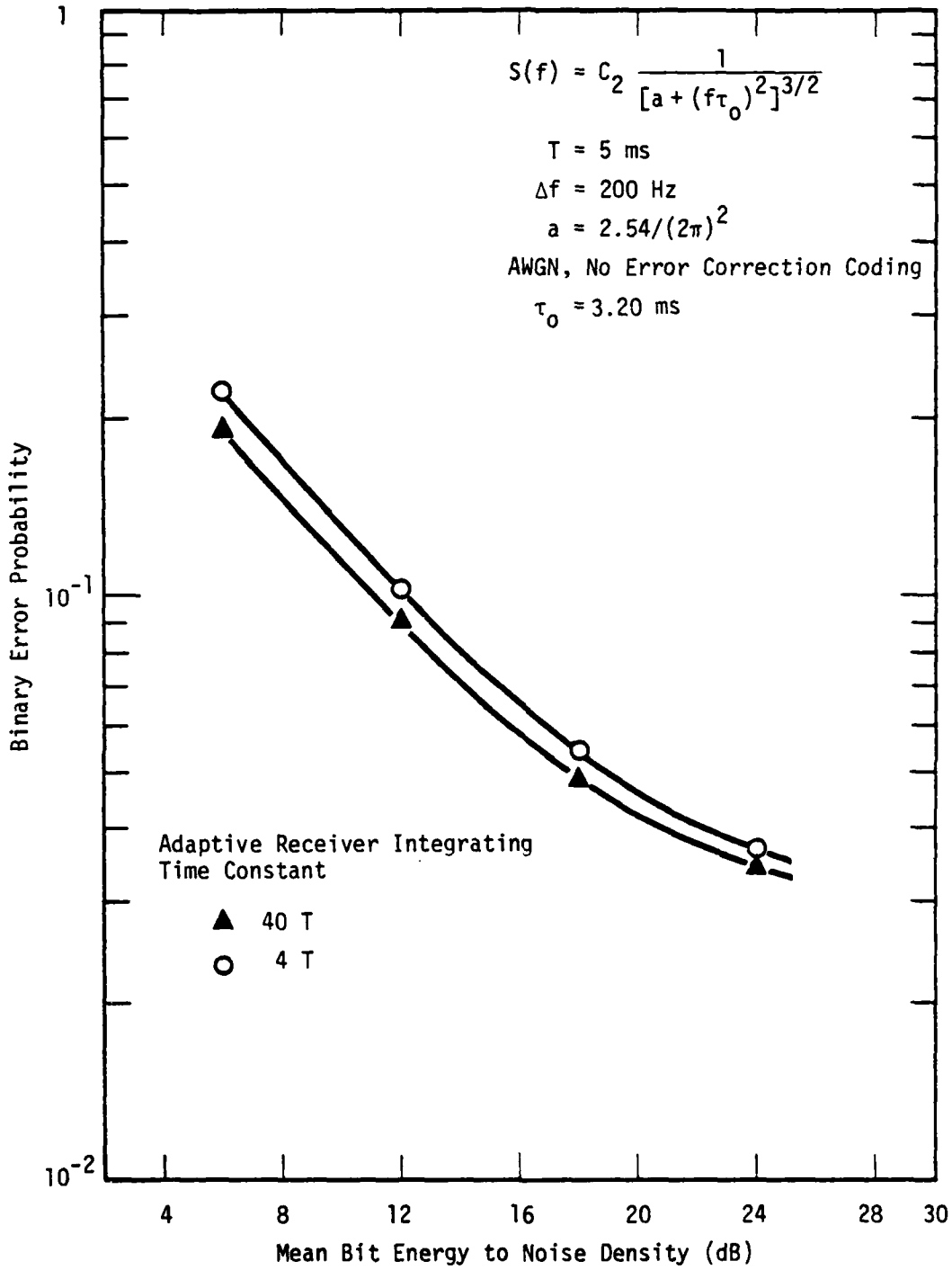


Figure 20. Comparative performance of BLSS algorithm at long and short prior integrating times.

The spectral estimate can be linearly parameterized to four or five parameters without any significant degradation in performance. Two techniques of data reduction were investigated. One of these, the band limited symmetric spectrum (BLSS) algorithm uses no detailed knowledge of the signal portion of the spectrum except that it is limited to a few DFT coefficients and is symmetric. The other technique, which is called the spectral eigenvector (SEV) algorithm, uses an ensemble of predicted spectra for the received random process to derive basis vectors for the spectral estimate. The SEV algorithm with four basis vectors and the BLSS algorithm with five basis vectors achieve nearly optimal performance. If the spectral functional form can be reliably predicted, the SEV algorithm would be preferred, whereas the BLSS method is applicable to a larger family of spectra which do not have to be predicted in detail.

The introduction of a spectral estimator to the receiver may make it more vulnerable to other sources of channel disturbance. For instance, an intentional jamming signal may be directed toward upsetting the spectral estimate as well as the demodulation decision. Incorporation of deliberate jamming threats in the channel is a primary direction for further research in this area. The jamming source should be considered a part of the channel as is the scintillation source, and the fundamental receiver algorithm for minimum probability of error should be rederived for a channel with rapid signal fading and deliberate interference. If the combined threat problem could be put on as firm a theoretical foundation as the rapid signal fading case, the adaptive receiver would be firmly established as the preferred system for the rapidly fading channel. As it is today, there remains a need to evaluate the performance of the adaptive receiver against the combined scintillation and jamming threat.

REFERENCES

1. Van Trees, H. L., Detection, Estimation, and Modulation Theory, Part I, John Wiley and Sons, Inc., New York, 1968, p. 86, p. 46.
2. Rao, C. R., Linear Statistical Inference and Its Application, Second Edition, John Wiley and Sons, Inc., New York, 1973, p. 443, p. 131.
3. Davenport, W. B., Jr., and W. L. Root, An Introduction to the Theory of Random Signal and Noise, McGraw-Hill Book Company, New York, 1958, p. 347.
4. Ratcliffe, J. A., "Some Aspects of Diffraction Theory and Their Application to the Ionosphere," Report on Progress in Physics, Vol. 19, pp. 188-256, 1956.
5. Tartarski, V. I., Wave Propagation in a Turbulent Medium, Dover, New York, 1967, pp. 208-210.
6. Knepp, D. L., and G. C. Valley, "Properties of Joint Gaussian Statistics," Radio Science, Vol. 13, No. 1, pp. 59-68, January 1978.
7. Wittwer, L. A., The Propagation of Satellite Signals Through Turbulent Media, AFWL-TR-77-183, Air Force Weapons Laboratory, Kirtland AFB, New Mexico, January 1978.
8. Price, R., "The Detection of Signals Perturbed by Scatter and Noise," IRE Transactions on Information Theory, Vol. PGIT-4, pp. 163-170, September, 1954.
9. Price, R., "Optimum Detection of Random Signals in Noise, With Applications to Scatter-Multipath Communicators, I," IRE Transactions on Information Theory, Vol. PGIT-6, pp. 125-135, December 1956.
10. Middleton, D., "On the Detection of Stochastic Signal in Additive Normal Noise, I," IRE Transactions on Information Theory, Vol. IT-3, pp. 86-121, June 1957.
11. Kailath, T., "Correlation Detection of Signals Perturbed by a Random Channel," IRE Transactions on Information Theory, Vol. IT-6, pp. 361-366, June 1960.

12. Stratonovich, R. L., and Y. G. Sosulin, "Optimal Detection of a Markov Process in Noise," Engineering Cybernetics, Vol. 6, pp. 7-19, October 1964.
13. Schweppe, F., "Evaluation of Likelihood Functions for Gaussian Signals," IEEE Transactions on Information Theory, Vol. IT-11, pp 61-70, January 1965.
14. Kennedy, R. S., Fading Dispersive Communication Channels, John Wiley and Sons, New York, 1969.
15. Van trees, H. L., Detection Estimation and Modulation Theory, Part III, John Wiley and Sons, New York, 1971.
16. Helstrom, C. W., Statistical Theory of Signal Detection, Pergamon Press, London, 1968, Chapter 11.
17. Whalen, A. D., Detection of Signals in Noise, Academic Press, 1971, p. 380-382.
18. Hancock, J. C., and P. A. Wintz, Signal Detection Theory, McGraw Hill Publishing Company, New York, 1966, Chapters 7 and 8.
19. Esposito, R., "A Class of Estimators for Optimum Adaptive Detection," Information and Control, Vol. 10, pp. 137-148, 1967.
20. Esposito, R., "On a Relation Between Detection and Estimation in Decision Theory," Information and Control, Vol. 12, pp. 116-120, 1968.
21. Kailath, T., "A General Likelihood Ratio Formula for Random Signals in Gaussian Noise," IEEE Transactions on Information Theory, Vol. IT-15, pp. 350-361, May 1969.
22. Schwartz, S. C., "Conditional Mean Estimates and Bayesian Hypothesis Testing," IEEE Transactions On Information Theory, Vol. IT-21, November 1975.
23. Schwartz, S. C., "The Estimator-Correlator for Discrete-Time Problems," IEEE Transactions on Information Theory, Vol. IT-23, January 1977.
24. Birdsall, T. G., and J. O. Gobien, "Sufficient Statistics and Reproducing Densities in Simultaneous Sequential Detection and Estimation," IEEE Transactions on Information Theory, Vol. IT-19, No. 6, pp. 760-768, November 1973
25. Gobien, J. O., "On Detecting a Signal While Estimating the Spectrum of Gauss-Markov Noise," IEEE Transactions on Information Theory, March 1977.

26. Lee, S. C., L. W. Nolte, and C. P. Hatsell, "A Generalized Likelihood Ratio Formula: Arbitrary Noise Statistics for Doubly Composite Hypotheses," IEEE Transactions on Information Theory, Vol. IT-23, No. 5, September 1977.
27. Keehn, D. G., "A Note on Learning for Gaussian Properties," IEEE Transactions on Information Theory, January 1965.
28. Spragins, J., "A Note on the Iterative Application of Bayes' Rule," IEEE Transactions on Information Theory, October 1965.
29. Chien, Y. T., and K. S. Fu, "On Bayesian Learning and Stochastic Approximation," IEEE Transactions on Systems Science and Cybernetics, Vol. SSC-3, No. 1, June 1967.
30. Patrick, E. A., and J. P. Costello, Unsupervised Estimation and Processing of Unknown Signals, Management Information Services, Detroit, Michigan, 1970.
31. Miller, K. S., and M. M. Rochwager, "Estimation of Spectral Moments of Time Series," Biometrika, Vol. 57, No. 3, pp. 513-517, 1970.
32. Miller, K. S., and M. M. Rochwager, "On Estimating Spectral Moments in the Presence of Colored Noise," IEEE Transactions on Information Theory, Vol. IT-16, No. 3, pp. 303-308, May 1970.
33. Miller, K. S., and M. M. Rochwager, "A Covariance Approach to Spectral Moment Estimation," IEEE Transactions on Information Theory, Vol. IT-18, No. 5, pp. 588-596, September 1972.
34. Miller, K. S., and M. M. Rochwager, "Hypothesis Testing of Complex Covariance Matrices," IEEE Transactions on Information Theory, Vol. IT-22, No. 1, pp. 26-33, January 1976.
35. Weaver, C. S., "Adaptive Communication Filtering," IEEE Transactions on Information Theory, Vol. IT-8, pp. S169-S178, September 1962.
36. Balkrishnan, A. V., "An Adaptive Non-Linear Data Predictor," 1962 National Telemetering Conference Proceedings.
37. Davisson, L. D., "A Theory of Adaptive Filtering," IEEE Transactions on Information Theory, Vol. IT-12, No. 2, pp. 97-102, April 1966.
38. Mehra, R. K., "On the Identification of Variances and Adaptive Kalman Filtering," IEEE Transactions on Automatic Control, Vol. AC-15, No. 2, pp. 175-184, April 1970.

AD-A099 512 MISSION RESEARCH CORP SANTA BARBARA CA F/G 17/2.
OPTIMAL/ADAPTIVE DEMODULATION FOR M-ARY FSK IN FAST FADING.(U)
MAR 81 M J BARRETT F29601-78-C-0033

UNCLASSIFIED MRC-R-453

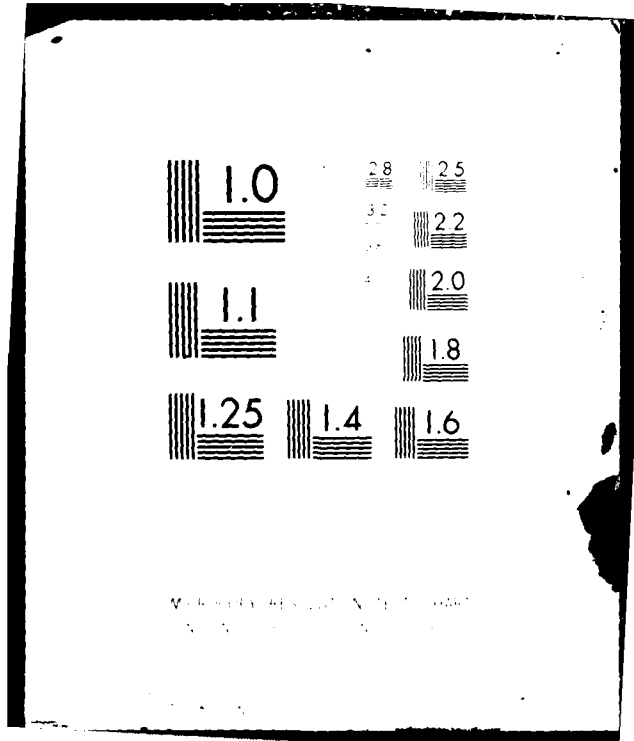
AFWL-TR-80-69

N/1

2 of 2
ADA
393 57

[REDACTED]	[REDACTED]	[REDACTED]	[REDACTED]	[REDACTED]	[REDACTED]	[REDACTED]	[REDACTED]	[REDACTED]	[REDACTED]	[REDACTED]	[REDACTED]	[REDACTED]
[REDACTED]	[REDACTED]	[REDACTED]	[REDACTED]	[REDACTED]	[REDACTED]	[REDACTED]	[REDACTED]	[REDACTED]	[REDACTED]	[REDACTED]	[REDACTED]	[REDACTED]
[REDACTED]	[REDACTED]	[REDACTED]	[REDACTED]	[REDACTED]	[REDACTED]	[REDACTED]	[REDACTED]	[REDACTED]	[REDACTED]	[REDACTED]	[REDACTED]	[REDACTED]

END
DATE
FILMED
104-82
DEIC



Resolution Test Chart

39. Magill, P. T., "Optimal Adaptive Estimation of Sampled Stochastic Processes," Ph.D. Dissertation, Department of Electrical Engineering, Stanford University, Stanford, California.
40. Lainiotis, D. G., "Sequential Structure and Parameter Adaptive Pattern Recognition—Part I: Supervised Learning," IEEE Transactions on Information Theory, Vol. IT-16, No. 5, September 1970.
41. Cullen, C. G., Matrices and Linear Transformation, Addison-Wesley Publishing Company, 1967, p. 72.
42. Bendat, J. S., and A. G. Piersol, Random Data: Analysis and Measurement Procedures, Wiley-Interscience, New York, 1971, p. 113.
43. Wooding, R. A., "The Multivariate Distribution of Complex Normal Variables," Biometrika, Vol. 43, pp. 212-215, 1956.
44. Hotelling, H., "Analysis of a Complex of Statistical Variables Into Principal Components," J. Educational Psychology, Vol. 24, pp. 417-444, 498-520, 1933.
45. Good, I. J., "Some Applications of the Singular Decomposition of a Matrix," Technometrics, Vol. 11, No. 4, 1969.

APPENDIX A
PROPERTIES OF THE IN-PHASE AND QUADRATURE
COMPONENTS OF A NARROWBAND GAUSSIAN PROCESS

The received signal-plus-noise may be expressed as a narrow-band random process referred to the carrier frequency ω_c :

$$\begin{aligned} r(t) &= s(t) + n(t) \\ &= x(t) \cos \omega_c t - y(t) \sin \omega_c t \end{aligned} \quad \text{A.1}$$

In Section II it is shown how the in-phase and quadrature signals $x(t)$ and $y(t)$ may be extracted from $r(t)$ through a combination of mixing and filtering. In order that there be an efficient representation of the probability density of the DFT components of the sampled version of the pre-envelope signal $x(t) + jy(t)$, the following two properties must hold for $x(t)$ and $y(t)$

$$E\{x(t)x(t-\tau)\} = E\{y(t)y(t-\tau)\} \quad \text{A.2}$$

$$E\{x(t)y(t-\tau)\} = -E\{y(t)x(t-\tau)\} \quad \text{A.3}$$

That these properties hold for the narrowband Gaussian Process $r(t)$ is a standard result in communication theory, which is repeated here for the convenience of the reader. The derivation shown here follows that in Whalen¹⁷ rather closely.

The Hilbert Transform of $r(t)$ is

$$\hat{r}(t) = x(t) \sin \omega_c t + y(t) \cos \omega_c t \quad \text{A.4}$$

Solving Equations A.1 and A.4 for $x(t)$ and $y(t)$ results in

$$x(t) = r(t) \cos \omega_c t + \hat{f}(t) \sin \omega_c t$$

$$y(t) = \hat{f}(t) \cos \omega_c t - r(t) \sin \omega_c t$$

Using the properties of the Hilbert Transform:*

$$R_{r\hat{f}}(\tau) = -\hat{R}_r(\tau) \quad \text{A.5}$$

$$R_{\hat{f}r}(\tau) = \hat{R}_r(\tau) \quad \text{A.6}$$

$$R_{\hat{f}\hat{f}}(\tau) = R_r(\tau) \quad \text{A.7}$$

the autocorrelation of $x(t)$ may be expressed

$$\begin{aligned} R_x(\tau) &= E\{x(t)x(t-\tau)\} = E\{r(t)r(t-\tau)\} \cos \omega_c t \cos \omega_c(t-\tau) \\ &\quad + E\{\hat{f}(t)r(t-\tau)\} \sin \omega_c t \sin \omega_c(t-\tau) \\ &\quad + E\{r(t)\hat{f}(t-\tau)\} \cos \omega_c t \sin \omega_c(t-\tau) \\ &\quad + E\{\hat{f}(t)\hat{f}(t-\tau)\} \sin \omega_c t \sin \omega_c(t-\tau) \end{aligned}$$

$$\begin{aligned} &= R_r(\tau) \cos \omega_c t \cos \omega_c(t-\tau) + R_{\hat{f}r}(\tau) \sin \omega_c t \cos \omega_c(t-\tau) \\ &\quad + R_{r\hat{f}}(\tau) \cos \omega_c t \sin \omega_c(t-\tau) + R_{\hat{f}\hat{f}}(\tau) \sin \omega_c t \sin \omega_c(t-\tau) \end{aligned}$$

Using Equations A.5, A.6, and A.7,

$$\begin{aligned} R_x(\tau) &= R_r(\tau) \cos \omega_c t \cos \omega_c(t-\tau) + \hat{R}_r(\tau) \sin \omega_c t \cos \omega_c(t-\tau) \\ &\quad - \hat{R}_r(\tau) \cos \omega_c t \sin \omega_c(t-\tau) + R_r(\tau) \sin \omega_c t \sin \omega_c(t-\tau) \\ &= R_r(\tau) [\cos \omega_c t \cos \omega_c(t-\tau) + \sin \omega_c t \sin \omega_c(t-\tau)] \\ &\quad - \hat{R}_r(\tau) [\cos \omega_c t \sin \omega_c(t-\tau) - \sin \omega_c t \cos \omega_c(t-\tau)] \end{aligned}$$

$$R_x(\tau) = R_r(\tau) \cos \omega_c \tau + \hat{R}_r(\tau) \sin \omega_c \tau \quad \text{A.8}$$

* The Hilbert transform is $\hat{g}(t) = \pi^{-1} \int_{-\infty}^{\infty} g(t-\tau) \tau^{-1} d\tau$. Note that it exists for sample functions of a stationary random process unlike the Fourier transform, and is also well defined for auto- and cross correlation functions.

It may be shown by a similar development that

$$R_y(\tau) = R_r(\tau) \cos \omega_c \tau + \hat{R}_r(\tau) \sin \omega_c \tau \quad A.9$$

so that

$$R_x(\tau) = R_y(\tau) \quad A.10$$

which is the property stated in Equation A.2.

Next

$$\begin{aligned} R_{xy}(\tau) &= E\{x(t) y(t-\tau)\} \\ &= E\{r(t) \hat{r}(t-\tau)\} \cos \omega_c t \cos \omega_c (t-\tau) \\ &\quad + E\{\hat{r}(t) r(t-\tau)\} \sin \omega_c t \cos \omega_c (t-\tau) \\ &\quad - E\{r(t) r(t-\tau)\} \cos \omega_c t \sin \omega_c (t-\tau) \\ &\quad - E\{\hat{r}(t) r(t-\tau)\} \sin \omega_c t \sin \omega_c (t-\tau) \\ &= R_{rr}(\tau) \cos \omega_c t \cos \omega_c (t-\tau) \\ &\quad + R_{\hat{r}r}(\tau) \sin \omega_c t \cos \omega_c (t-\tau) \\ &\quad - R_r(\tau) \cos \omega_c t \sin \omega_c (t-\tau) \\ &\quad - R_{r\hat{r}}(\tau) \sin \omega_c t \sin \omega_c (t-\tau) \end{aligned}$$

Using Equations A.5, A.6, and A.7

$$\begin{aligned} R_{xy}(\tau) &= R_r(\tau) [\sin \omega_c t \cos \omega_c (t-\tau) - \cos \omega_c t \sin \omega_c (t-\tau)] \\ &\quad - \hat{R}_r(\tau) [\cos \omega_c t \cos \omega_c (t-\tau) + \sin \omega_c t \sin \omega_c (t-\tau)] \end{aligned}$$

or

$$R_{xy}(\tau) = R_r(\tau) \sin \omega_c \tau - \hat{R}_r(\tau) \cos \omega_c \tau \quad A.11$$

A parallel analysis results in

$$R_{xy}(\tau) = -R_{yx}(\tau) \quad A.12$$

which is the property stated in Equation A.3.

If the noise term $n(t)$ in Equation A.1 is white (uncorrelated) then Equation A.8 may be rewritten

$$\begin{aligned} R_x(\tau) &= R_s(\tau) \cos \omega_c \tau + \hat{R}_s(\tau) \sin \omega_c \tau + \frac{N_0 B}{2} \delta(\tau) \\ &= R_{x_s}(\tau) + \frac{N_0 B}{2} \delta(\tau) \end{aligned} \quad \text{A.13}$$

where N_0 is the noise power spectral density of $n(t)$ in watts/Hz, B is the noise bandwidth of the baseband analog filter, and $R_{x_s}(\tau)$ is the signal component of the baseband autocorrelation $R_x(\tau)$. Also from A.11

$$R_{xy}(\tau) = R_s(\tau) \sin \omega_c \tau - \hat{R}_s(\tau) \cos \omega_c \tau \quad \text{A.14}$$

The white noise does not contribute to the crosscorrelation of the baseband waveforms $x(t)$ and $y(t)$.

APPENDIX B
THE PROBABILITY DISTRIBUTION OF THE DFT
OF A SAMPLED COMPLEX GAUSSIAN PROCESS

The development of Appendix A shows that the baseband in-phase and quadrature waveforms have certain statistical regularities given by Equations A.2 and A.3. If an impulse sampler is assumed, the corresponding properties of the sampled waveforms are

$$E \{ x_n x_m \} = E \{ y_n y_m \} \quad \text{B.1}$$

$$E \{ x_n y_m \} = -E \{ y_n x_m \} \quad \text{B.2}$$

In order to express the probability distribution of the DFT coefficients of $x_n + jy_n$ in an efficient manner, it is necessary that a similar property hold in the frequency domain. Let

$$z_k = \alpha_k + jy_k = \frac{1}{N} \sum_{n=0}^{N-1} (x_n + jy_n) e^{-j \frac{2\pi kn}{N}} \quad k=0, \dots, N-1 \quad \text{B.3}$$

with α_k and γ_k real valued, be the set of DFT coefficients of the sequence

$$x_n + jy_n \quad n = 0, 1, 2, \dots, N-1$$

Then the desired properties are

$$E \{ \alpha_k \alpha_l \} = E \{ \gamma_k \gamma_l \} \quad \text{B.4}$$

$$E \{ \alpha_k \gamma_l \} = -E \{ \gamma_k \alpha_l \} \quad \text{B.5}$$

Proceeding directly from Equation B.3,

$$\begin{aligned}\alpha_k &= \operatorname{Re} \left\{ \frac{1}{N} \sum_{n=0}^{N-1} (x_n + jy_n) e^{-j \frac{2\pi kn}{N}} \right\} \\ &= \sum_{n=0}^{N-1} \left[x_n \cos\left(\frac{2\pi kn}{N}\right) + y_n \sin\left(\frac{2\pi kn}{N}\right) \right]\end{aligned}\quad \text{B.6}$$

$$\begin{aligned}\gamma_k &= \operatorname{Im} \left\{ \frac{1}{N} \sum_{n=0}^{N-1} (x_n + jy_n) e^{-j \frac{2\pi kn}{N}} \right\} \\ &= \sum_{n=0}^{N-1} \left[-x_n \sin \frac{2\pi kn}{N} + y_n \cos \frac{2\pi kn}{N} \right]\end{aligned}\quad \text{B.7}$$

$$\begin{aligned}E \{ \alpha_k \alpha_\ell \} &= \sum_{n=0}^{N-1} \sum_{m=0}^{N-1} \left[E \{ x_n x_\ell \} \cos\left(\frac{2\pi kn}{N}\right) \cos\left(\frac{2\pi \ell m}{N}\right) \right. \\ &\quad + E \{ y_n y_\ell \} \sin\left(\frac{2\pi kn}{N}\right) \sin\left(\frac{2\pi \ell m}{N}\right) \\ &\quad + E \{ y_n x_\ell \} \sin\left(\frac{2\pi kn}{N}\right) \cos\left(\frac{2\pi \ell m}{N}\right) \\ &\quad \left. + E \{ x_n y_\ell \} \cos\left(\frac{2\pi kn}{N}\right) \sin\left(\frac{2\pi \ell m}{N}\right) \right] \\ &= \sum_{n=0}^{N-1} \sum_{m=0}^{N-1} \left[E \{ x_n x_\ell \} \cos\left(\frac{2\pi (kn - \ell m)}{N}\right) \right. \\ &\quad \left. + E \{ y_n x_\ell \} \sin\left(\frac{2 (kn - \ell m)}{N}\right) \right]\end{aligned}\quad \text{B.8}$$

$$\begin{aligned}
E \{ \gamma_k \gamma_\ell \} &= \sum_{n=0}^{N-1} \sum_{m=0}^{N-1} \left[E \{ x_n x_\ell \} \sin\left(\frac{2\pi kn}{N}\right) \sin\left(\frac{2\pi \ell m}{N}\right) \right. \\
&\quad + E \{ y_n y_\ell \} \cos\left(\frac{2\pi kn}{N}\right) \cos\left(\frac{2\pi \ell m}{N}\right) \\
&\quad - E \{ y_n x_\ell \} \cos\left(\frac{2\pi kn}{N}\right) \sin\left(\frac{2\pi \ell m}{N}\right) \\
&\quad \left. - E \{ x_n y_\ell \} \sin\left(\frac{2\pi kn}{N}\right) \cos\left(\frac{2\pi \ell m}{N}\right) \right]
\end{aligned}$$

$$\begin{aligned}
&= \sum_{n=0}^{N-1} \sum_{m=0}^{N-1} \left[E \{ x_n x_\ell \} \cos\left(\frac{2\pi(kn-\ell m)}{N}\right) \right. \\
&\quad \left. + E \{ y_n x_\ell \} \sin\left(\frac{2\pi(kn-\ell m)}{N}\right) \right]
\end{aligned}$$

B.9

which proves Equation B.4, and

$$\begin{aligned}
E \{ \alpha_k \gamma_\ell \} &= \sum_{n=0}^{N-1} \sum_{m=0}^{N-1} \left[- E \{ x_n x_m \} \cos \frac{2\pi kn}{N} \sin \frac{2\pi \ell m}{N} \right. \\
&\quad + E \{ y_n y_m \} \sin \frac{2\pi kn}{N} \cos \frac{2\pi \ell m}{N} \\
&\quad - E \{ y_n x_m \} \sin \frac{2\pi kn}{N} \sin \frac{2\pi \ell m}{N} \\
&\quad \left. + E \{ x_n y_m \} \cos \frac{2\pi kn}{N} \cos \frac{2\pi \ell m}{N} \right]
\end{aligned}$$

$$\begin{aligned}
&= \sum_{n=0}^{N-1} \sum_{m=0}^{N-1} \left[E \left\{ x_n x_m \right\} \sin\left(\frac{2\pi(kn-\ell m)}{N}\right) \right. \\
&\quad \left. - E \left\{ y_n x_m \right\} \cos\left(\frac{2\pi(kn-\ell m)}{N}\right) \right] \quad \text{B.10}
\end{aligned}$$

$$\begin{aligned}
E \left\{ \gamma_k \alpha_\ell \right\} &= \sum_{n=0}^{N-1} \sum_{m=0}^{N-1} \left[- E \left\{ x_n x_m \right\} \sin\left(\frac{2\pi kn}{N}\right) \cos\left(\frac{2\pi \ell m}{N}\right) \right. \\
&\quad \left. + E \left\{ y_n y_m \right\} \cos\left(\frac{2\pi kn}{N}\right) \sin\left(\frac{2\pi \ell m}{N}\right) \right] \\
&\quad + E \left\{ y_n x_m \right\} \cos\left(\frac{2\pi kn}{N}\right) \cos\left(\frac{2\pi \ell m}{N}\right) \\
&\quad - E \left\{ x_n y_m \right\} \sin\left(\frac{2\pi kn}{N}\right) \sin\left(\frac{2\pi \ell m}{N}\right)
\end{aligned}$$

$$\begin{aligned}
&= \sum_{n=0}^{N-1} \sum_{m=0}^{N-1} \left[- E \left\{ x_n x_m \right\} \sin\left(\frac{2\pi(kn-\ell m)}{N}\right) \right. \\
&\quad \left. + E \left\{ y_n x_m \right\} \cos\left(\frac{2\pi(kn-\ell m)}{N}\right) \right] \quad \text{B.11}
\end{aligned}$$

which proves Equation B.5.

These properties allow the covariance matrix of combined real and imaginary parts of the DFT coefficients to be written in the form

$$\underline{A} = \underline{E} \left\{ \begin{pmatrix} \underline{\alpha} \\ \underline{\gamma} \end{pmatrix} \begin{pmatrix} \underline{\alpha}^T & \underline{\gamma}^T \end{pmatrix} \right\} = \begin{bmatrix} \underline{A} & \underline{B} \\ \underline{B}^T & \underline{A} \end{bmatrix} \quad \text{B.12}$$

where

$$\begin{pmatrix} \underline{\alpha}^T & \underline{\gamma}^T \end{pmatrix} = (\alpha_0, \alpha_1, \dots, \alpha_{N-1}, \gamma_0, \dots, \gamma_{N-1}) \quad \text{B.13}$$

and

$$\underline{A} = \underline{A}^T \quad \text{B.14a}$$

$$\underline{B} = -\underline{B}^T \quad \text{B.14b}$$

Wooding⁴³ has shown that if the covariance matrix of a collection of zero mean Gaussian random variables $\underline{\alpha}$ and $\underline{\gamma}$ can be written in this form, then the probability density of the complex variates $\underline{z} = \underline{\alpha} + j\underline{\gamma}$ may be expressed as

$$p(\underline{z}) = \pi^{-N} |\underline{L}|^{-1} e^{-\underline{z}^T \underline{L}^{-1} \underline{z}} \quad \text{B.15}$$

where \underline{L} is a Hermetian covariance matrix for \underline{z} .

His development follows from the decomposition

$$\begin{bmatrix} \underline{A} & \underline{B} \\ \underline{B}^T & \underline{A} \end{bmatrix}^{-1} = \begin{bmatrix} (\underline{A} + \underline{B}\underline{A}^{-1}\underline{B})^{-1} & 0 \\ 0 & (\underline{A} + \underline{B}\underline{A}^{-1}\underline{B})^{-1} \end{bmatrix} \begin{bmatrix} \underline{A} & -\underline{B} \\ -\underline{B}^T & \underline{A} \end{bmatrix} \begin{bmatrix} \underline{A}^{-1} & 0 \\ 0 & \underline{A}^{-1} \end{bmatrix} \quad \text{B.16}$$

$$= \begin{bmatrix} (\underline{A} + \underline{B}\underline{A}^{-1}\underline{B})^{-1} & -(\underline{A} + \underline{B}\underline{A}^{-1}\underline{B})^{-1} \underline{B}\underline{A}^{-1} \\ -(\underline{A} + \underline{B}\underline{A}^{-1}\underline{B})^{-1} \underline{B}^T \underline{A}^{-1} & (\underline{A} + \underline{B}\underline{A}^{-1}\underline{B})^{-1} \end{bmatrix} \quad \text{B.17}$$

which is of the same form as Equation B.12 since

$$\begin{aligned} (\underline{A} + \underline{BA}^{-1}\underline{B})^{-1T} &= (\underline{A}^T + \underline{B}^T \underline{A}^{-1T} \underline{B}^T)^{-1} \\ &= (\underline{A} + \underline{BA}^{-1}\underline{B})^{-1} \end{aligned} \quad \text{B.18}$$

and

$$\begin{aligned} \left[(\underline{A} + \underline{BA}^{-1}\underline{B})^{-1} \underline{BA}^{-1} \right]^T &= \underline{A}^{-1T} \underline{B}^T (\underline{A} + \underline{BA}^{-1}\underline{B})^{-1T} \\ &= \underline{A}^{-1} \underline{B} (\underline{A} + \underline{BA}^{-1}\underline{B})^{-1} \\ &= - \left[(\underline{A} + \underline{BA}^{-1}\underline{B}) \underline{B}^{-1} \underline{A} \right]^{-1} \\ &= - \left[\underline{AB}^{-1} \underline{A} + \underline{B} \right]^{-1} \\ &= - \left[\underline{AB}^{-1} (\underline{A} + \underline{BA}^{-1}\underline{B}) \right]^{-1} \\ &= - (\underline{A} + \underline{BA}^{-1}\underline{B})^{-1} \underline{BA}^{-1} \end{aligned} \quad \text{B.19}$$

Then one may write

$$\begin{bmatrix} \underline{A} & \underline{B} \\ \underline{B}^T & \underline{A} \end{bmatrix}^{-1} = \begin{bmatrix} \underline{P} & \underline{Q} \\ \underline{Q}^T & \underline{P} \end{bmatrix} \quad \text{B.20}$$

where

$$\underline{P} = (\underline{A} + \underline{BA}^{-1}\underline{B})^{-1} \quad \text{B.21a}$$

$$\underline{Q} = - (\underline{A} + \underline{BA}^{-1}\underline{B})^{-1} \underline{BA}^{-1} \quad \text{B.21b}$$

with

$$\begin{aligned}\underline{P} &= \underline{P}^T \\ \underline{Q} &= -\underline{Q}^T\end{aligned}\quad . \quad \text{B.22}$$

It may be readily demonstrated that

$$\underline{P} \pm j\underline{Q} = (\underline{A} \pm j\underline{B})^{-1} \quad . \quad \text{B.23}$$

The combination of Equations B.21a, B.21b, and B.23 will result in a simple expression for the probability density of the complex variates \underline{z} .

The probability density for the real and imaginary parts of \underline{z} is

$$f(\underline{x}, \underline{y}) = (2\pi)^{-N} |\underline{\Lambda}|^{-1/2} e^{-1/2(\underline{x}^T \ \underline{y}^T) \underline{\Lambda}^{-1} \begin{pmatrix} \underline{x} \\ \underline{y} \end{pmatrix}} \quad . \quad \text{B.24}$$

The exponent may be rewritten

$$-\frac{1}{2} (\underline{x}^T \ \underline{y}^T) \underline{\Lambda}^{-1} \begin{pmatrix} \underline{x} \\ \underline{y} \end{pmatrix} = -\frac{1}{2} (\underline{x} - j\underline{y})^T (\underline{P} - j\underline{Q}) (\underline{x} + j\underline{y}) \quad \text{B.25}$$

and the determinant of $\underline{\Lambda}$ may be expressed in terms of $|\underline{A} - j\underline{B}|$ through the decomposition

$$\begin{bmatrix} \underline{P} & \underline{Q} \\ \underline{Q}^T & \underline{P} \end{bmatrix} = \begin{bmatrix} \underline{I} & -j\underline{I} \\ \underline{0} & \underline{I} \end{bmatrix} \begin{bmatrix} \underline{P}-j\underline{Q} & \underline{0} \\ -\underline{Q} & \underline{I} \end{bmatrix} \begin{bmatrix} \underline{I} & j\underline{I} \\ \underline{0} & \underline{P}+j\underline{Q} \end{bmatrix} \quad \text{B.26}$$

$$\begin{aligned}|\underline{\Lambda}|^{-1} &= |\underline{P} - j\underline{Q}| |\underline{P} + j\underline{Q}| \\ &= |\underline{P} - j\underline{Q}| |(P - jQ)^T| \\ &= |\underline{P} \pm j\underline{Q}|^2 = |\underline{A} \pm j\underline{B}|^{-2}\end{aligned} \quad \text{B.27}$$

or

$$|\underline{\Lambda}|^{-1/2} = |\underline{A} + j\underline{B}|^{-1} \quad . \quad \text{B.28}$$

Then the distribution of Equation B.24 may be rewritten

$$f(\underline{z}) = (2\pi)^{-N} |\underline{A} - j\underline{B}|^{-1} e^{-1/2 (\underline{\alpha} - j\underline{\gamma})^T (\underline{A} - j\underline{B})^{-1} (\underline{\alpha} + j\underline{\gamma})}$$

but

B.29

$$\begin{aligned} E \{ \underline{z} \underline{z}^{T*} \} &= E \{ \underline{\alpha} \underline{\alpha}^T + j \underline{\gamma} \underline{\alpha}^T - j \underline{\alpha} \underline{\gamma}^T + \underline{\gamma} \underline{\gamma}^T \} \\ &= 2 [E \{ \underline{\alpha} \underline{\alpha}^T - j \underline{\alpha} \underline{\gamma}^T \}] \\ &= 2 [\underline{A} - j\underline{B}] \end{aligned} \quad \text{B.30}$$

then

$$|\underline{L}| \stackrel{\Delta}{=} |E \{ \underline{z} \underline{z}^{T*} \}| = 2^N |\underline{A} - j\underline{B}| \quad \text{B.31}$$

and the probability density becomes

$$f(\underline{z}) = \pi^{-N} |\underline{L}|^{-1} e^{-\underline{z}^T \underline{L}^{-1} \underline{z}} \quad \text{B.32}$$

or equivalently as

$$f(\underline{z}) = \pi^{-N} |\underline{L}|^{-1} e^{-\underline{z}^T \underline{L}^{-1*} \underline{z}^*}$$

which is occasionally used in this report.

APPENDIX C
COMPUTATION OF THE COVARIANCE MATRICES L_j FROM THE
SIGNAL AUTOCORRELATION FUNCTION AND WHITE NOISE DENSITY

The covariance of the complex variates z_k and z_ℓ is

$$E \{ z_k z_\ell^* \} = E \left\{ \frac{1}{N^2} \sum_{n=0}^{N-1} \sum_{m=0}^{N-1} (x_n + jy_n)(x_m - jy_m) e^{-j \frac{2\pi kn}{N}} e^{j \frac{2\pi \ell m}{N}} \right\} \quad \text{C.1}$$

$$= \frac{1}{N^2} \sum_{n=0}^{N-1} \sum_{m=0}^{N-1} E \left\{ x_n x_m + y_m y_n + jy_n x_m - jx_n y_m \right\} e^{-j \frac{2\pi kn}{N}} e^{j \frac{2\pi \ell m}{N}} \quad \text{C.2}$$

Using Equations A.10 and A.12 in sampled versions,

$$E \{ z_k z_\ell^* \} = \frac{1}{N^2} \sum_{n=0}^{N-1} \sum_{m=0}^{N-1} 2 \left(R_x(n-m) + jR_{yx}(n-m) \right) e^{-j \frac{2\pi kn}{N}} e^{j \frac{2\pi \ell m}{N}} \quad \text{C.3}$$

and by Equation A.13

$$= \frac{1}{N^2} \sum_{n=0}^{N-1} \sum_{m=0}^{N-1} 2 \left(R_{x_s}(n-m) + jR_{yx}(n-m) \right) e^{-j \frac{2\pi kn}{N}} e^{j \frac{2\pi \ell m}{N}} + \frac{N_B}{N} \delta(k, \ell) \quad \text{C.3b}$$

where B is the noise bandwidth of the baseband analog filter preceding the sampler. (It is assumed here that the white noise term $n(t)$ affects only the zero-lag point of the discrete-time autocorrelation.)

Equation C.3 may be implemented using a two dimensional DFT with a rearrangement of terms to accommodate the two different signs on the exponents. The two dimensional DFT has the form

$$X(k, \ell) = \frac{1}{N^2} \sum_{n=0}^{N-1} \sum_{m=0}^{N-1} x(n, m) e^{-j \frac{2\pi k n}{N}} e^{-j \frac{2\pi \ell m}{N}} \quad C.4$$

To obtain Equation C.3 the columns of $X(k, \ell)$ between $\ell = 1$ and $\ell = N-1$ are reversed in order, giving

$$X(k, N-\ell) = \frac{1}{N^2} \sum_{n=0}^{N-1} \sum_{m=0}^{N-1} x(n, m) e^{-j \frac{2\pi k n}{N}} e^{-j \frac{2\pi (N-\ell) m}{N}} \quad C.5$$

The integer rotation $j2\pi N/N$ may be dropped from the expression and Equation C.3 results.

Under the assumption that the signal autocorrelation function has the same envelope for any hypothesis of signal transmitted, or equivalently that the signal PSD's are simple translations of one another

$$R_{r_i}(\tau) = f(\tau) \cos \omega_i \tau + \frac{N_0}{2} \delta(\tau) \quad , \quad C.6$$

where ω_i is the transmitted frequency on the i th hypothesis, the various ω_i are closely related and may be calculated with one operation of the two dimensional DFT. It is equivalent to assume that the spectrum of $n(t)$ is symmetric about the frequency $\omega_i(t)$, and that the baseband lowpass filter is wide enough to pass the entire signal spectrum. The

assumption C.6 is highly restrictive and does not hold where the signal doppler spreading is a significant portion of the width of the baseband analog filter. The technique described here to obtain all of the covariance matrices \underline{L}_i as a rotationally related set is not actually used in performance calculations for the receiver, but is merely recorded here for its theoretical value as an aid to understanding the relationships among the covariance matrices.

With the signal autocorrelation of the form C.6, using Equation A.9,

$$R_x(\tau) = f(\tau) \cos\omega_i\tau \cos\omega_c\tau + f(\tau) \sin\omega_i(\tau) \sin\omega_c\tau + \frac{N_o}{4} \delta(\tau) \quad C.7$$

where $f(\tau) \sin\omega_i(\tau)$ is the Hilbert transform of $f(\tau) \cos\omega_i(\tau)$. Similarly, using Equation A.12

$$R_{yx}(\tau) = -f(\tau) \cos\omega_i\tau \sin\omega_c\tau + f(\tau) \sin\omega_i\tau \cos\omega_c\tau \quad C.8$$

and the autocorrelation required in Equation C.3 is

$$\begin{aligned} 2(R_x(\tau) + jR_{yx}(\tau)) &= 2[f(\tau) \cos(\omega_i - \omega_c)\tau + jf(\tau) \sin(\omega_i - \omega_c)\tau \\ &= 2f(\tau) e^{j(\omega_i - \omega_c)\tau} + \frac{N_o}{2} \delta(\tau) \end{aligned} \quad C.9$$

with the corresponding sampled version

$$2(R_x(n) + jR_{yx}(n)) = 2f(n) e^{j \frac{2\pi\delta n}{n}} + \frac{N_o B}{2} \delta(n) \quad C.10$$

where δ is the frequency deviation assumed to be a multiple of the sampling frequency

$$\delta = \frac{(\omega_i - \omega_\delta)}{2\pi} \Delta t \quad \delta = 0, \pm 1, \pm 2, \dots \quad . \quad C.11$$

Then Equation C.3 may be rewritten

$$E \left\{ z_k z_\ell^* \right\}_\delta = \frac{1}{N^2} \sum_{n=0}^{N-1} \sum_{m=0}^{N-1} 2f(n-m) e^{j \frac{2\pi\delta(n-m)}{N}} e^{-j \frac{2\pi kn}{N}} e^{j \frac{2\pi \ell m}{N}} + \frac{N_0 B}{2} \delta(k, \ell) \quad C.12$$

$$= \frac{1}{N^2} \sum_{n=0}^{N-1} \sum_{m=0}^{N-1} 2f(n-m) e^{-j \frac{2\pi(k-\delta)n}{N}} e^{j \frac{2\pi(\ell-\delta)m}{N}} + \frac{N_0 B}{2} \delta(k, \ell) ,$$

so that

$$E \left\{ z_{k-j} z_{\ell-\delta}^* \right\}_\delta = \frac{1}{N^2} \sum_{n=0}^{N-1} \sum_{m=0}^{N-1} 2f(n-m) e^{-j \frac{2\pi kn}{N}} e^{j \frac{2\pi \ell m}{N}} + \frac{N_0 B}{2} \delta(k, \ell) \quad C.13$$

and all of the \underline{L}_i may be obtained from one DFT operation which uses only the envelope $f(n)$ of the autocorrelation of the signal $s(t)$ and the noise spectral density. The alternate \underline{L} 's are obtained by a rotating shift along the main diagonal.

APPENDIX D
 THE GENERATION OF COMPLEX RANDOM VARIATES
 WITH THE CORRELATION MATRIX \underline{L}

Starting with a set of independent Complex Normal Variates \underline{S} with the distribution,

$$f(\underline{S}) = \pi^{-N} e^{-\underline{S}^T \underline{I} \underline{S}} \quad \text{D.1}$$

it will be straightforward to obtain a set of variates with the desired covariance \underline{L} . \underline{L} may be factored

$$\underline{L} = 1/2(\underline{A} - j\underline{B}) = 1/2(\underline{C} - j\underline{D})(\underline{C} + j\underline{D}) \quad , \quad \text{D.2}$$

and that \underline{C} and \underline{D} matrices exist to satisfy D.2 follows from the relationship

$$\underline{A} = \underline{C}^2 + \underline{D}^2 \quad \text{D.3}$$

$$\underline{B} = \underline{D}\underline{C} - \underline{C}\underline{D} \quad \text{D.4}$$

which may be expressed in the form

$$\begin{bmatrix} \underline{D} & \underline{C} \\ \underline{C} & -\underline{D} \end{bmatrix} \begin{bmatrix} \underline{D} & \underline{C} \\ \underline{C} & -\underline{D} \end{bmatrix} = \begin{bmatrix} \underline{A} & \underline{B} \\ \underline{B}^T & \underline{A} \end{bmatrix} \quad \text{D.5}$$

or

$$\begin{bmatrix} \underline{D} & \underline{C} \\ \underline{C} & -\underline{D} \end{bmatrix} = \underline{\Delta}^{1/2} \quad . \quad \text{D.6}$$

The square root of $\underline{\Lambda}$ exists since, as the covariance matrix of Gaussian real variables it is positive definite. Then, given a set of variables \underline{S} , they are transformed by

$$\underline{z} = [\underline{C} - j\underline{D}]\underline{S} \quad . \quad \text{D.7}$$

The resulting variables \underline{z} have the density

$$\begin{aligned} p(\underline{z}) &= \pi^{-N} |\underline{C} - j\underline{D}|^{-1} e^{\underline{z}^{T*} [\underline{C} + j\underline{D}]^{-1} [\underline{C} - j\underline{D}]^{-1} \underline{z}} \\ &= \pi^{-N} |\underline{L}|^{-1} e^{\underline{z}^{T*} \underline{L}^{-1} \underline{z}} \end{aligned} \quad \text{D.8}$$

where $|\underline{L}|$ is the Jacobian of the transformation from \underline{S} to \underline{z} .

APPENDIX E

PROPERTIES OF THE COVARIANCE MATRIX WHICH ARE USEFUL IN OBTAINING INVERSES AND SQUARE ROOTS

The covariance matrices \underline{L}_i are complex valued in general and Hermetian. To obtain the optimal receiver's statistics it is necessary to invert these matrices, and to obtain sample variates it is necessary to square root one of them. The phase angles of the elements of these matrices are unrelated to the received signal spectrum and are an artifact of the sampling process. They occur in an orderly fashion that enables a simple procedure to compute inverses and square roots based upon the corresponding inverses and square roots of the magnitude matrices. The phase property is obtained via the complex conjugate of Equation C.3b (the noise term is deleted here since it is always real and affects only the main diagonal of the covariance matrix)

$$E^*\{z_k z_\ell^*\} = \frac{1}{N^2} \sum_{n=0}^{N-1} \sum_{m=0}^{N-1} R_{zz_s}^*(n-m) e^{j \frac{2\pi kn}{N} - j \frac{2\pi \ell m}{N}} \quad E.1$$

$$R_{zz_s}^*(n-m) = 2(R_{x_s}(n-m) + jR_{zx}(n-m)) \quad E.2$$

Since R_{zz_s} is an autocorrelation function of a complex Gaussian baseband signal, it is Hermetian, so that the argument $(n-m)$ may be reversed and the conjugate sign removed:

$$E^*\{z_k z_\ell^*\} = \frac{1}{N^2} \sum_{n=0}^{N-1} \sum_{m=0}^{N-1} R_{zz_s}(m-n) e^{j \frac{2\pi kn}{N} - j \frac{2\pi \ell m}{N}} \quad E.3$$

Now by changing variables to

$$\begin{aligned} n' &= N - 1 - n \\ m' &= N - 1 - m \end{aligned} \quad \text{E.4}$$

the expression may be rewritten as

$$= \frac{1}{N_2} \sum_{n'=0}^{N-1} \sum_{m'=0}^{N-1} R_{zz^*}^{(n'-m')} e^{j \frac{2\pi k(N-1-n')}{N}} e^{-j \frac{2\pi \ell(N-1-m')}{N}} \quad \text{E.5}$$

$$E^*\{z_k z_\ell^*\} = e^{j \frac{2\pi(\ell-k)}{N}} E\{z_k z_\ell^*\}$$

This is a simple relationship between the elements of the covariance matrix and the corresponding complex conjugates. From this expression one may obtain the result that the phase angle of each element of the covariance matrix is

$$\begin{aligned} \theta_{k,\ell} &= \frac{\pi(k-\ell)}{N} \pm \pi & \ell &= 0, \dots, N-1 \\ & & k &= 0, \dots, N-1 \end{aligned} \quad \text{E.6}$$

which prescribes the phase angle structure of any of the covariance matrices \underline{L}_i . The angles are zero on the main diagonal, and the matrix can be arranged in polar form so that angles decrease in steps of $2\pi/N$ for elements to the right of the main diagonal and increase by the same increments for elements to the left of the main diagonal. In this form, the phase angles in any row or column range over a phase difference of π .

Then for matrices of the form

$$[\underline{L}]_{k,\ell} = \alpha_{k,\ell} e^{j \frac{\pi(k-\ell)}{N}} \quad \text{E.7}$$

where $\alpha_{k,\ell}$ may be a positive or negative real number, if the inverse of the matrix of elements $\alpha_{k,\ell}$ is known and has elements $\gamma_{k,\ell}$ such that

$$\sum_{n=0}^{N-1} \alpha_{kn} \gamma_{nl} = \delta_{k,l} \quad \text{E.8}$$

Then the inverse of \underline{L} has elements

$$\gamma_{kl} e^{j \frac{\pi(k-l)}{N}}$$

since

$$\begin{aligned} \sum_{n=0}^{N-1} \alpha_{k,n} e^{j \frac{\pi(k-n)}{N}} \gamma_{nl} e^{j \frac{\pi(n-l)}{N}} & \quad \text{E.9} \\ = e^{j - \frac{\pi(k-l)}{N}} \sum_{n=0}^{N-1} \alpha_{kn} \gamma_{nl} \\ = \delta_{k,l} \end{aligned}$$

A similar result holds for the square root. If the square root of matrix of elements $\alpha_{k,l}$ is known, with elements $\beta_{k,l}$ such that

$$\sum_n \beta_{kn} \beta_{nl} = \gamma_{kl} \quad \text{E.10}$$

then the square root of \underline{L} (if it exists) is a matrix of elements

$$\beta_{kl} e^{j \frac{\pi(k-l)}{N}}$$

since

$$\begin{aligned} \sum_n \beta_{kn} e^{j \frac{\pi(k-n)}{N}} \beta_{nl} e^{j \frac{\pi(n-l)}{N}} & \quad \text{E.11} \\ = e^{j \frac{\pi(k-l)}{N}} \sum_n \beta_{kn} \beta_{nl} \end{aligned}$$

$$= \gamma_{k,l} e^{j \frac{\pi(k-l)}{N}} \quad \text{E.12}$$

APPENDIX F
ALGORITHM FOR THE ADAPTIVE RECEIVER
WITH DATA REDUCTION

The adaptive receiver algorithm is presented here in detail for the reader who is interested in constructing a simulation or a real-time receiver. To avoid the notational complexity that may occur with arbitrary receiver dimensions, the equations are given in terms of an 8-ary system with $N=16$ complex samples per observation interval.

A double index notation is used to keep track of the observation intervals and functions of frequency within each observation interval. The index of observation intervals is m and the frequency index is k . Where a time sample index is required, for time samples within an observation interval, the variable n is the index of time samples.

Figure F-1 is a block diagram of an adaptive M-ary FSK receiver. It illustrates the flow of computations from the time samples to the modulation decision. The following equations give the explicit operations represented by each block of the diagram. Scalar notation, as opposed to matrix-vector notation is used wherever it is possible, for the convenience of the programmer.

During each observation interval $N=16$ complex valued DFT coefficients are computed from time samples of the in-phase and quadrature waveforms x_n and y_n . These are formed into the complex valued function:

$$x_{n,m} + jy_{n,m} \quad n = 0, \dots, 15 \quad \text{F.1}$$

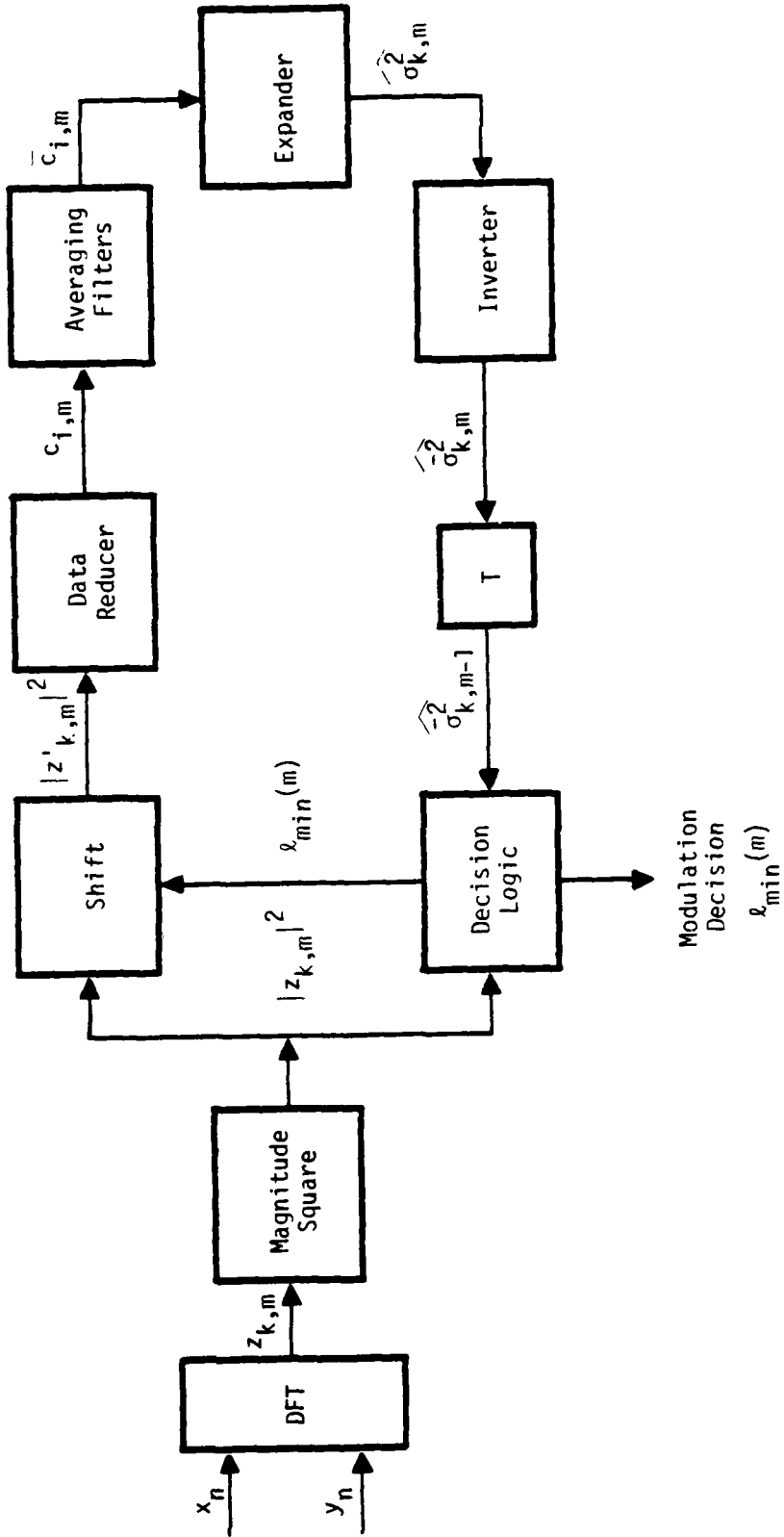


Figure F-1. Block diagram of an adaptive receiver with data reduction.

for a given observation interval m and transformed to DFT coefficients:

$$z_{k,m} = \sum_{n=0}^{15} (x_{n,m} + jy_{n,m}) e^{-\frac{j2\pi kn}{16}} \quad k = 0, \dots, 15 \quad \text{F.2}$$

The first operation on these coefficients is to compute the square of the magnitude of each $|z_{k,m}|^2$, $k = 0, \dots, 15$. These values are tested against $M = 8$ different inverse spectra derived from the estimates $\hat{\sigma}_{k,m-1}^{-2}$ in the operation labeled "decision logic" in the block diagram. The estimates $\hat{\sigma}_{k,m-1}^{-2}$ are arranged so that $k = 0$ corresponds to the center of the signal portion of the spectrum. $k = 1$ is the next higher frequency estimate; $k = 15$ is the next to center on the lower frequency side, and so forth. (The index $m-1$ indicates that the estimate is based on modulation intervals prior to the m^{th} and not including the m^{th} interval.) The modulation decision is the index $\ell_{\min}(m)$ of the smallest inner product of the two vectors whose elements are $|z_{k,m}|^2$ and circularly shifted versions of $\hat{\sigma}_{k,m}^{-2}$. These inner products are:

$$\rho_{\ell}(m) = \sum_{k=0}^{N-1} |z_{k,m}|^2 \hat{\sigma}_{\{k-\ell\},m-1}^{-2}, \quad \ell = \{-4, -3, \dots, 3\} \quad \text{F.3}$$

and ℓ_{\min} is given by

$$\rho_{\ell_{\min}}(m) \leq \rho_{\ell}(m), \quad \ell = \{-4, -3, \dots, 3\} \quad \text{F.4}$$

where $\{k-\ell\}$ is a modulo 16 addition, indicating that the inverse spectrum is wrapped around by the shift operation. The range of ℓ indicated will shift the center point of the spectrum into the eight possible locations where the center frequency of $|z_{k,m}|^2$ is expected.

The modulation decision ℓ_{\min} is used to align the $|z_{k,m}|^2$ for insertion into the estimator of the signal spectrum. This operation is

labeled "shift" on the block diagram. The realigned version of the spectrum is designated $|z'_{k,m}|^2$ where

F.5

$$|z'_{k,m}|^2 = |z_{\{k+\ell_{\min}\},m}|^2$$

When the modulation decision is correct, the center of the signal spectrum is shifted to the first entry of the realigned set $|z'_{0,m}|^2$. The next higher frequency is shifted to the $k=1$ location; the next lower frequency is shifted to the $k=15$ location etc. A certain fraction of the spectra will be incorrectly aligned when demodulation errors occur. These errors have proven to be inconsequential to the receiver performance in the useful operating region of the receiver operating characteristic curves.

The realigned data $|z'_{k,m}|$ are subjected to the data reduction algorithm which allows the average over prior observation intervals to be made with only a few storage registers—four or five for the receiver dimensions and conditions of interest here. Some discussion of the coefficients of the data reduction algorithm precedes the introduction of the data reduction equations.

The two techniques for data reduction which were investigated in Sections V and VI do not differ in terms of the algorithm, but only in a certain set of coefficients. These are $16 \times P$ in number and are most naturally organized as the coordinates of P 16 dimensional vectors, where $P=4$ or $P=5$. A set of four vectors for the BLSS algorithm is

$$\left. \begin{aligned} x_1 &= [100\dots 0]^T \\ x_2 &= 2^{-\frac{1}{2}} [0100\dots 01]^T \\ x_3 &= 2^{-\frac{1}{2}} [00100\dots 010]^T \\ x_4 &= 11^{-\frac{1}{2}} [000111\dots 1100]^T \end{aligned} \right\} \quad \text{F.6}$$

They are normalized so that

$$\sum_{k=0}^{15} x_k^2 = 1 \quad \text{F.7}$$

The first three vectors are arranged to make independent estimates of the center of the spectrum, the pair of adjacent points, and the pair of next-to-adjacent points. The fourth vector is structured to obtain a noise level estimate by averaging over the remaining points.

A similar set of vectors are used in the SEV algorithm. These are computed through an eigenvector-eigenvalue numerical analysis of a 16×16 matrix \underline{S} . The eigenvector of \underline{S} corresponding to nonzero eigenvalues are the \underline{x}_i vectors in the algorithm. The matrix \underline{S} is a sum of dyads of spectra from the predicted operating range of the receiver. In matrix-vector notation:

$$\underline{S} = \sum_{i=1}^J \sigma_i^2 \underline{\sigma}_i \underline{\sigma}_i^T \quad \text{F.8}$$

where the vectors $\underline{\sigma}_i^2$ are defined by Equation 67 of Section III. In scalar notation, the elements of \underline{S} are

$$[\underline{S}]_{n,\ell} = \sum_{i=1}^J \widehat{\sigma}_{i,n}^2 \widehat{\sigma}_{i,\ell}^2 \quad \begin{array}{l} n = 0, \dots, 15 \\ \ell = 0, \dots, 15 \end{array} \quad \text{F.9}$$

Since \underline{S} is symmetric, n may be considered the index of rows and ℓ the index of columns or vice versa. Each of the vectors $\underline{\sigma}_i^2$ is a sixteen-dimensional discrete power spectral density (expectation or mean value of the magnitude-square DFT coefficients of the received signal-plus-noise random process). For the results given in Section 6, eight $\underline{\sigma}_i^2$ were selected along the line of 10 percent error probability from the receiver operating characteristic curve of the optimal receiver (Figure 12). This

set gave excellent performance, very close to optimal, throughout the useful operating range of the (optimal) receiver. The data reduction equation is

$$c_{i,m} = \sum_{n=0}^{15} x_{i,n} |z'_{n,m}|^2 \quad i = 1, \dots, P \quad \text{F.10}$$

The $c_{i,m}$ are averaged over prior observation intervals by a set of single pole digital filters

$$\bar{c}_{i,m} = K \bar{c}_{i,m-1} + (1-K)c_{i,m} \quad \text{F.11}$$

where $K < 1$ is the pole location of each of the filters. The appropriate value of K for a given time constant of Q observation intervals is given by

$$K = e^{-1/Q} \quad \text{F.12}$$

The averaged coefficients $\bar{c}_{i,m}$ are expanded into a sixteen dimensional spectral estimate by the expression

$$\hat{\sigma}_{k,m}^2 = \sum_{i=1}^P \bar{c}_{i,m} x_{i,k} \quad k = 0, \dots, 15 \quad \text{F.13}$$

This operation is referred to as an expander in the block diagram. These estimates are subsequently inverted

$$\hat{\sigma}_{k,m}^{-2} = [\hat{\sigma}_{k,m}^2]^{-1} \quad k = 0, \dots, 15 \quad \text{F.14}$$

to obtain the inverse spectrum required by the receiver.

The time delay T shown in the diagram does not actually occur as a final step in the sequence of operations. It is inserted to show that the estimate used in the decision logic at the m^{th} modulation interval will not include data from the m^{th} step which is not available until the m^{th} decision has been made.

APPENDIX G
PRINCIPAL COMPONENTS AND THE REDUCED
DIMENSION SPECTRAL ESTIMATE

The connection between the data reduction technique incorporated in the SEV algorithm and principal component analysis in statistics is explored. It is shown that whereas principal components are designed to retain as much as possible of the covariance structure of a random vector in a reduced dimensional representation, the coefficients of the SEV algorithm are designed to minimize the combined covariance and squared bias of the reduced dimension spectral estimate.

PRINCIPAL COMPONENT ANALYSIS

Principal component analysis was introduced by H. Hotelling⁴⁴ in 1933. It is a technique of deriving a linear transformation of a random vector which results in a lower dimension vector while preserving as much of the variance of the original vector as possible. Given a random N -vector \underline{x} with covariance matrix $\underline{\Sigma}$, it is desired to construct a P -vector

$$\underline{y} = \underline{H}^T \underline{x} \qquad \text{G.1}$$

where \underline{H} is an $N \times P$ matrix with orthonormal columns ($\underline{H}^T \underline{H} = \underline{I}$) so that the total variation of \underline{y} , defined as the sum of variances of the components, is maximized. The solution is given by a matrix \underline{H} whose columns are the eigenvectors of $\underline{\Sigma}$ associated with the P greatest eigenvalues.

The optimality of principal components may also be viewed in terms of maximizing the trace of the covariance matrix (maximizing the total variation) of an approximation to \underline{x} in its same coordinates. Consider reconstructing an N-dimensional variable $\hat{\underline{x}}$ from the principal component vector \underline{y}

$$\begin{aligned}\hat{\underline{x}} &= \underline{H}\underline{y} \\ &= \underline{H}^T \underline{H} \underline{x}\end{aligned}\tag{G.2}$$

The covariance matrix of $\hat{\underline{x}}$ is

$$E\{\hat{\underline{x}}\hat{\underline{x}}^T\} = \underline{H} \underline{H}^T \underline{\Sigma} \underline{H} \underline{H}^T\tag{G.3}$$

which has rank $P < N$. The vector $\hat{\underline{x}}$ has a singular covariance matrix since it has less than N degrees of freedom. If the columns of \underline{H} are taken as the eigenvectors of $\underline{\Sigma}$ associated with the largest eigenvalues then the

$$\text{tr}\{\underline{H}\underline{H}^T \underline{\Sigma} \underline{H} \underline{H}^T\} = \text{tr}\{\underline{H}^T \underline{\Sigma} \underline{H}\}\tag{G.4}$$

is maximized over the class of $N \times P$ matrices \underline{H} for which $\underline{H}^T \underline{H} = \underline{I}$. It may also be demonstrated^{4,5} that the

$$\text{Norm}\{\underline{\Sigma} - \underline{H}\underline{H}^T \underline{\Sigma} \underline{H} \underline{H}^T\}\tag{G.5}$$

is minimized by the same \underline{H} where the Euclidean norm

$$\text{Norm}\{\underline{A}\} = \sum_{ij} [A]_{ij}^2 \quad 1/2\tag{G.6}$$

is used. Thus the covariance matrix of $\hat{\underline{x}}$ is the best approximation to $\underline{\Sigma}$ in a mean square sense, by a rank P matrix.

DATA REDUCED SPECTRAL ESTIMATE

In reducing the dimension of the power spectrum estimate used in the adaptive FSK receiver we are confronted with a similar problem to that

of principal components. Here it is desired to derive an $N \times N$ linear projection operator $\underline{K} = \underline{X} \underline{X}^T$ of rank $P < N$ so that the raw spectral estimate $\hat{\underline{\sigma}}_s^2$ may be replaced with a reduced estimate

$$\hat{\underline{\sigma}}^2 = \underline{K} \hat{\underline{\sigma}}_s^2 \quad \text{G.7}$$

in such a way that the least additional cost, in terms of increased probability of misclassification, is incurred. In Section V it is shown that a formal Taylor expansion of the cost, about its value at the correct spectrum, with truncation at the quadratic term yields the risk function

$$\mathcal{R}(\underline{\sigma}^2, \underline{K}) = \text{tr} \{ \underline{C}_\sigma E \{ \underline{K} \hat{\underline{\sigma}}_s^2 \hat{\underline{\sigma}}_s^{2T} \underline{K}^T \} \} \quad \text{G.8}$$

The expansion is referred to as formal since the weight matrix \underline{C}_σ cannot be practically evaluated. Each component of the matrix

$$\underline{M}_\sigma \triangleq E \{ \underline{K} \hat{\underline{\sigma}}_s^2 \hat{\underline{\sigma}}_s^{2T} \underline{K}^T \} \quad \text{G.9}$$

which may be referred to as the total squared deviation, is weighted by the corresponding entry of \underline{C}_σ to assign the relative importance of deviations of the estimate $\hat{\underline{\sigma}}$ from the true spectrum $\underline{\sigma}^2$. Equation G.9 can be broken down into two terms

$$\underline{M}_\sigma = \underline{K} \underline{D} \underline{K}^T + (\underline{K} - \underline{I}) \underline{\sigma}^2 \underline{\sigma}^{2T} (\underline{K} - \underline{I})^T \quad \text{G.10}$$

which represent the covariance of the reduced spectral estimate and squared bias respectively. This breakdown of the error, from which the term "total squared deviation" derives, is familiar from the literature of power spectral density estimation as a measure of the quality of window functions.

It is necessary to average the risk function over an ensemble of power spectra $\underline{\sigma}^2$ that are predicted for the receiver. Otherwise the optimal \underline{K} would depend on the particular spectrum $\underline{\sigma}^2$ and would change

with the spectrum rather than be fixed for the entire range of fading rates and signal-to-noise ratios. In performing this average it is desired to retain the form of the risk function as the trace of the product of two matrices.

$$\begin{aligned} \bar{\mathcal{R}}(\underline{K}) &= \frac{1}{L} \sum_{i=1}^L \text{tr} \left\{ \underline{C}_{-\sigma_i} \underline{M}_{\sigma_i} \right\} \\ &= \text{tr} \left\{ \underline{C} \frac{1}{L} \sum_{i=1}^L \underline{M}_{-\sigma_i} \right\} \end{aligned} \quad \text{G.11}$$

A weighted average \underline{C} as indicated by Equation G.11 will exist as long as $\sum_{i=1}^L \underline{M}_{\sigma_i}$ is nonsingular

$$\underline{C} = \left[\sum_{i=1}^L \underline{C}_{-\sigma_i} \underline{M}_{\sigma_i} \right] \left[\sum_{i=1}^L \underline{M}_{-\sigma_i} \right]^{-1} \quad \text{G.12}$$

It is expected that the desired inverse will exist since each component in the sum is invertible and there is no reason to believe that the terms will combine in such a way that the rank of the total will be reduced. It is therefore possible to consider the cost function

$$\text{tr} \{ \underline{C} \underline{M} \} = \text{tr} \{ \underline{C} [\underline{K} \underline{D} \underline{K}^T + (\underline{K} - \underline{I}) \underline{S} (\underline{K} - \underline{I})^T] \} \quad \text{G.13}$$

where

$$\underline{D} = \frac{1}{L} \sum_{i=1}^L \underline{D}_i \quad \text{G.14}$$

and

$$\underline{S} = \frac{1}{L} \sum_{i=1}^L \underline{\sigma}_i^2 \underline{\sigma}_i^{2T} \quad \text{G.15}$$

In Section V, the approach taken to deriving the best projection operator \underline{K} was to minimize the second term in Equation G.13, that corresponding to squared bias, while ignoring the covariance term. It was discovered experimentally that the matrix \underline{S} was of considerably low rank compared to its dimension and therefore $(\underline{K} - \underline{I})^T$ was chosen so that

$$(\underline{K} - \underline{I}) = \underline{Y} \underline{Y}^T \quad \text{G.16}$$

where the $N \times (N-P)$ matrix \underline{Y} is made up of orthogonal columns which lie in the null space of \underline{S} . The particular circumstances of the problem allowed the spectrum estimate to be reduced in dimension without paying for the data reduction in the bias term of the cost. Here we have used essentially the same approach to deriving a projection operator as that given by principal components. The problem is to minimize $\text{tr}\{\underline{C} \underline{Y} \underline{Y}^T \underline{S} \underline{Y} \underline{Y}^T\}$ rather than maximize an unweighted $\text{tr}\{\underline{H} \underline{H} \underline{\Sigma} \underline{H} \underline{H}^T\}$. The eigenvectors of \underline{S} associated with the minimum eigenvalues (all approximately zero) were selected. In both cases the extreme values of the criterion function are achieved by using a set of eigenvectors (though the null space eigenvectors of \underline{S} are not unique). Furthermore, \underline{S} is not a covariance matrix like $\underline{\Sigma}$ in the principal component analysis, but rather a squared mean of the raw statistic $\underline{\sigma}_s^2$. The fact that \underline{S} is not full rank is fortunate, since otherwise the solution would depend on \underline{C} which is practically unavailable. This leaves open the question of the minimization of Equation G.13 where \underline{S} may not be of sufficiently reduced rank and \underline{C} is available or an appropriate \underline{C} could be hypothesized. In the remainder of this appendix the equations are given for for the general case.

OPTIMAL PROJECTION OPERATOR

Equation G.13 may be expanded to

$$\begin{aligned} \text{tr}\{\underline{C} \underline{M}\} &= \text{tr}\{\underline{C} \underline{K} \underline{D} \underline{K} + \underline{C} \underline{K} \underline{S} \underline{K} - \underline{C} \underline{S} \underline{K} - \underline{C} \underline{K} \underline{S} + \underline{C} \underline{S}\} \\ &= \text{tr}\{\underline{C} \underline{K} (\underline{D} + \underline{S}) \underline{K} - (\underline{C} \underline{S} + \underline{S} \underline{C}) \underline{K} + \underline{C} \underline{S}\} \end{aligned} \quad \text{G.17}$$

Here, the property of the trace that

$$\text{tr}\{\underline{A} \underline{B}\} = \text{tr}\{\underline{B} \underline{A}\} \quad \text{G.18}$$

along with the additional assumption $\underline{K} = \underline{K}^T$ have been used. Now substituting $\underline{K} = \underline{X} \underline{X}^T$ and making further use of the trace property and the assumption that $\underline{X}^T \underline{X} = \underline{I}$ yields

$$\text{tr}\{\underline{C} \underline{M}\} = \text{tr}\{\underline{X}^T \underline{C} \underline{X} \underline{X}^T (\underline{D} + \underline{S}) \underline{X} - \underline{X}^T (\underline{C} \underline{S} + \underline{S} \underline{C}) \underline{X}\} + \text{tr}\{\underline{C} \underline{S}\} \quad \text{G.19}$$

Now the object is to find the $N \times P$ matrix \underline{X} of orthonormal columns which minimizes $\text{tr}\{\underline{C} \underline{M}\}$. The extreme points of this function may be found by the usual gradient techniques with the addition of Lagrange multipliers. The equations describing the column vectors of \underline{X} at these extreme points are

$$\frac{\partial}{\partial \underline{x}_a} \left[\text{tr}\{\underline{C} \underline{M}\} + \sum_{j=1}^P \lambda_j (\underline{x}_j^T \underline{x}_j - 1) \right] = 0 \quad \text{G.20}$$

$a = 1, \dots, P$

$$\frac{\partial}{\partial \lambda_b} \left[\text{tr}\{\underline{C} \underline{M}\} + \sum_{j=1}^P \lambda_j (\underline{x}_j^T \underline{x}_j - 1) \right] = 0 \quad \text{G.21}$$

$b = 1, \dots, P$

where the λ_b are Lagrange multipliers arranged to constrain the lengths of the column vectors of \underline{X} to unity length. It is not necessary to constrain these column vectors to be orthogonal since any rank P solution to Equation G.20 is an \underline{X} with orthogonal columns without such a constraint. In carrying out the first of these partial derivatives it is convenient to write out

$$\begin{aligned} \text{tr}\{\underline{C} \underline{M}\} &= \sum_{i=1}^P \underline{x}_i^T \underline{C} \sum_{j=1}^P \underline{x}_j \underline{x}_j^T (\underline{D} + \underline{S}) \underline{x}_i \quad \text{G.22} \\ &\quad - \sum_{k=1}^P \underline{x}_k^T (\underline{C} \underline{S} + \underline{S} \underline{C}) \underline{x}_k + \text{tr}\{\underline{C} \underline{S}\} \\ &= \sum_{\substack{i=1 \\ i \neq a}}^P \underline{x}_i^T \underline{C} \sum_{\substack{j=1 \\ j \neq a}}^P \underline{x}_j \underline{x}_j^T (\underline{D} + \underline{S}) \underline{x}_i \\ &\quad + \sum_{\substack{i=1 \\ i \neq a}}^P \underline{x}_i^T \underline{C} \underline{x}_a \underline{x}_a^T (\underline{D} + \underline{S}) \underline{x}_i \\ &\quad + \underline{x}_a^T \underline{C} \sum_{\substack{j=1 \\ j \neq a}}^P \underline{x}_j \underline{x}_j^T (\underline{D} + \underline{S}) \underline{x}_a \\ &\quad + \underline{x}_a^T \underline{C} \underline{x}_a \underline{x}_a^T (\underline{D} + \underline{S}) \underline{x}_a \\ &\quad - \sum_{k=1}^P \underline{x}_k^T (\underline{C} \underline{S} + \underline{S} \underline{C}) \underline{x}_k + \text{tr}\{\underline{C} \underline{S}\} \end{aligned}$$

The second and third terms of this expression are equal. The first term does not enter the partial derivative since it is not a function of \underline{x}_a , nor does the last term, proceeding:

$$\frac{\partial}{\partial \underline{x}_a} \left[\text{tr}(\underline{C} \underline{M}) + \lambda_a \underline{x}_a^T \underline{x}_a \right] \quad \text{G.23}$$

$$\begin{aligned} &= \frac{\partial}{\partial \underline{x}_a} \left[2 \underline{x}_a^T \underline{C} \sum_{\substack{j=1 \\ j \neq a}}^P \underline{x}_j \underline{x}_j^T (\underline{D} + \underline{S}) \underline{x}_a \right. \\ &\quad \left. + \underline{x}_a^T \underline{C} \underline{x}_a \underline{x}_a^T (\underline{D} + \underline{S}) \underline{x}_a \right] \\ &\quad - \underline{x}_a^T (\underline{C} \underline{S} + \underline{S} \underline{C}) \underline{x}_a + \lambda_a \underline{x}_a^T \underline{x}_a \\ &= 2 \underline{C} \sum_{\substack{i=1 \\ i \neq a}}^P \underline{x}_i \underline{x}_i^T (\underline{D} + \underline{S}) \underline{x}_a + 2 (\underline{D} + \underline{S}) \sum_{\substack{j=1 \\ j \neq a}}^P \underline{x}_j \underline{x}_j^T \underline{C} \underline{x}_a \\ &\quad + 2 \underline{C} \underline{x}_a \underline{x}_a^T (\underline{D} + \underline{S}) \underline{x}_a + 2 (\underline{D} + \underline{S}) \underline{x}_a \underline{x}_a^T \underline{C} \underline{x}_a \\ &\quad - 2 (\underline{C} \underline{S} + \underline{S} \underline{C}) \underline{x}_a + 2 \lambda_a \underline{x}_a = 0 \\ &= 2 \underline{C} \underline{X} \underline{X}^T (\underline{D} + \underline{S}) \underline{x}_a + 2 (\underline{D} + \underline{S}) \underline{X} \underline{X}^T \underline{C} \underline{x}_a \\ &\quad - 2 (\underline{C} \underline{S} + \underline{S} \underline{C}) \underline{x}_a + 2 \lambda_a \underline{x}_a = 0 \end{aligned} \quad \text{G.24}$$

$a = 1, \dots, P$

From Equation G.24 one may deduce that, if P linearly independent solutions exist, they will form an orthogonal set (or can be arranged to do so) since they are eigenvectors of a real symmetric matrix. Each of the matrices \underline{D} , \underline{S} , and \underline{C} are themselves symmetric and $\underline{X} \underline{X}^T$ is symmetric regardless of whether the columns of \underline{X} are orthogonal. The matrix operating on \underline{x}_a is in the form of one matrix plus its transpose which sum is always symmetric. The fact that the variable matrix \underline{X} is imbedded in the symmetric matrix does not alter the conclusion about the orthogonality of a given set of P vectors \underline{x}_a which satisfy the equation. It is convenient to arrange all of the P equations into one matrix equation

$$[\underline{C} \underline{X} \underline{X}^T (\underline{D} + \underline{S}) + (\underline{D} + \underline{S}) \underline{X} \underline{X}^T \underline{C} - \underline{C} \underline{S} - \underline{S} \underline{C}] \underline{X} = \underline{X} \underline{\Lambda} \quad \text{G.25}$$

where $\underline{\Lambda}$ is a diagonal matrix with diagonal elements consisting of the Lagrange multipliers λ_b along the diagonal. The second of the two partial derivative equations, Equation G.21, yields the constraint

$$\underline{x}_i^T \underline{x}_i = 1 \quad , \quad i = 1, \dots, P \quad \text{G.26}$$

These two equations do not generally have a solution of rank P, although there is always a rank one solution. If \underline{X} is of rank one then $\underline{X} \underline{X}^T = P \underline{x}_a \underline{x}_a^T$ and Equation G.24 becomes

$$[P \underline{C} \underline{x}_a \underline{x}_a^T (\underline{D} + \underline{S}) + P (\underline{D} + \underline{S}) \underline{x}_a \underline{x}_a^T \underline{C} - (\underline{C} \underline{S} + \underline{S} \underline{C})] \underline{x}_a = \underline{x}_a \lambda_a$$

then if \underline{x}_a is an eigenvector of

$$\alpha_1 \underline{C} + \alpha_2 (\underline{D} + \underline{S}) - \underline{C} \underline{S} + \underline{S} \underline{C}$$

where

$$\alpha_1 = P \underline{x}_a^T (\underline{D} + \underline{S}) \underline{x}_a$$

$$\alpha_2 = P \underline{x}_a^T \underline{C} \underline{x}_a$$

The matrix \underline{X} made up of P columns all equal to \underline{x}_a will satisfy the extremal equations.

Placing additional constraints that the columns of \underline{X} be orthogonal yields the same Equation G.25 with the exception that the $P \times P$ matrix $\underline{\Lambda}$ be a general real symmetric matrix rather than a diagonal matrix. Such a matrix may be written in the form $\underline{G} \underline{\Lambda}' \underline{G}^T$ where \underline{G} is an orthogonal matrix and $\underline{\Lambda}'$ is diagonal:

$$[\underline{C} \underline{X} \underline{X}^T (\underline{D} + \underline{S}) + (\underline{D} + \underline{S}) \underline{X} \underline{X}^T \underline{C} - \underline{C} \underline{S} - \underline{S} \underline{C}] \underline{X} = \underline{X} \underline{G} \underline{\Lambda}' \underline{G}^T$$

This equation still requires that the columns of \underline{X} define an invariant subspace of the matrix in brackets—a condition which is evidently not possible to satisfy. It also indicates that $\underline{X} \underline{G}$ is a solution to the original equation.

One may conclude tentatively from this result that the appropriate partial derivatives of the trace (Equation G.17) do not go to zero at any points $\underline{X} \underline{X}^T$ of rank $P > 1$, for which $\underline{X} \underline{X}^T$ is a linear projection operator. Thus it is possible that the Lagrangian techniques will not be useful to determine the minimizing linear projection operator.

The means to minimize Equation G.24 by either analytical or numerical methods are still under investigation. The difficulty with this problem seems to arise from the fact that one is searching for a subspace — that spanned by the columns of \underline{X} — rather than for a unique vector as in the usual problem of the minimization of a functional. The solution appears to be of fundamental interest as a means to improve multidimensional estimators by data reduction.

ATE
LMED
-8